CZECH UNIVERSITY OF LIFE SCIENCES PRAGUE

Faculty of Tropical AgriSciences

INFLUENCE OF TEXTURE OF BRIQUETTES FROM BIOMASS TO THEIR MECHANICAL PROPERTIES

Dissertation Thesis

Author: Ing. Iva Černá

Department of Sustainable Technologies

Thesis supervisor: doc. Ing. Josef Pecen, CSc.

In Prague, 2016

Declaration

I hereby certify that the thesis I am submitting is entirely my own original work except where otherwise indicated. I am aware of regulations concerning disciplinary actions that may result from plagiarism. I have elaborated this thesis independently and quoted only sources listed in 'References'.

In Prague ……..

……

Iva Černá

Content

List of Figures

List of Charts

List of Acronyms and Nomenclature

A	aspect ratio
app.	approximately
AR	abrasion rate
B	width
BGP	biogas plant
CO	carbon monoxide
CO_2	carbon dioxide
D	particle size ratio
D1	digestate particles
D2	digestate particles
D3-I	digestate briquettes
D3-II-A	digestate briquettes
D3-II-C	digestate briquettes
D3-II-D	digestate briquettes
D4-0	digestate briquettes
DAP	di-ammonium phosphate
DG	digestate
DM	dry matter
DU test	durability test
ER	exponential regression
H_2	hydrogen
H_2S	hydrogen sulphide
IA	image analysis
IG	ingestate
K	potassium
L	length
M	mass
MAX	maximal value
MEAN	geometrical mean
MG	*Miscanthus Giganteus* L.
MIN	minimal value
N	nitrogen

NFE	nitrogen free extracts
NH_3	ammonia
NPK	three-component fertilisers providing nitrogen, phosphorus, and potassium
O_2	oxygen
OFMSW	organic fraction of municipal solid wastes
OM	organic matter
P	phosphorus
PSD	particle size distribution
PVC	polyvinyl chloride
S	area
S_{Index}	shattering index
STD	standard deviation
V	volume
WCH	woodchip particles
Y	height

Acknowledgments

I would like to express my deepest gratitude to doc. Ing. Josef Pecen, CSc. my dissertation thesis supervisor. I am grateful to him for giving me the chance to carry out this project, for his sincere engagements and help with the topic.

I also would like to thank my family for believing in me and encouraging me during my whole studies, not only during the Ph.D. program.

Very importantly, I would like to thank Ing. Tomáš Hřebíček and his family for giving me the motivation and inspiration being patient and encouraging me all the time.

Thank to Ing. Tatiana Ivanova, Ph.D. for help with scientific articles, very useful advices, inspiration and support and to Zdeněk Piksa and Ing. Martin Lexa for help in laboratory and with NIS elements program.

I would like to thank my all schoolmates, namely Ing. Zuzana Polívková, Ing. Iva Nádvorníková, Ing. Petra Brtníková and Ing. Veronika Chaloupková, for their helpfulness and good advices.

Abstract

Hand in hand with the rising number of AD technology users, the issue of liquid digestate storage has emerged. In recent time, there are some other ways to utilize the digestate besides fertilizing with the 'liquor'- the liquid part of the digestate. The digestate can be dried and pressed into a briquette or a pelleted form. In the briquette form it is important to understand relations between properties of individual components (particles) because one property can influence another one, constituting the texture of the material, and its reprocessing into the final form of the product. Thus this study was conducted, to find and/or quantify the relation between the texture of biomass briquettes and their durability and hardness of shape during manipulation, storage and use. Basic hypothesis of this work is based on the presumption that the briquette texture is influenced by many parameters. Some of those parameters were tested, namely the composition of matter, physical properties of the digestate briquettes, their durability and hardness, size analysis of particles and others. Digestate has been found a good material for compression containing high content of nutrients. The rate of abrasion has varied from 7 – 12%, at the beginning decreasing to 3 – 5%, and toughness of 99%. The Shore hardness test showed results indicating a relation between particle size and hardness. The sieve and image analysis then revealed a range of particle of sizes 1.00 – 2.50 mm with the most frequent average length of 7.30 mm and width 1.00 mm, most of them having a needle-like shape confirmed by the aspect ratio of 7.90. This study proposes a method that allows analysing particle size distribution in samples and describes other briquette properties, which can be useful for future research and commercial purposes.

Keywords*: digestate, durability, hardness, image analysis, sieve analysis.*

Abstrakt

S rostoucím množstvím uživatelů technologie AD roste problematika, jak skladovat takový tekutý materiál, kterým je digestát. V současné době existují i jiné způsoby, jak jej využívat, kromě hnojení tekutou částí digestátu. Digestát lze sušit a lisovat do formy briket nebo pelet. Ve formě brikety je důležité si uvědomovat důležitost vztahů mezi vlastnostmi jednotlivých složek (částic), protože jedna vlastnost může ovlivnit další - a tvořit tak strukturu materiálu -a jeho opětovné zpracování do podoby finálního výrobku. Tato studie byla provedena za účelem najít a/nebo kvantifikovat vztah mezi strukturou briket z biomasy a jejich odolností a pevností tvaru při manipulaci, skladování a používání. Základní hypotéza této práce je založena na předpokladu, že textura briket je závislá na mnoha parametrech. Některé z těchto parametrů byly testovány. Jmenovitě, látkové složení, fyzikální vlastnosti brikety z digestátu, pevnost a tvrdost, analýza velikosti částic a další. Digestát se ukázal být dobrým materiálem pro kompresi, navíc s vysokým obsahem živin. Množství odrolu se měnilo mezi 7 – 12% na začátku, postupně klesající na 3 – 5% s pevností kolem 99%. Zkoušky tvrdosti podle Shoreho testu prokázaly výsledky vypovídající o vztahu mezi velikostí částic a tvrdostí. Sítová a obrazová analýza pak ukázala řadu částic v rozmezí velikosti 1,00 – 2,50 mm, s nejfrekventovanější délkou 7,30 mm a šířkou 1,00 mm, většina z nich s jehlám-podobným tvarem potvrzeným hodnotou poměru stran 7,90. Tato studie navrhuje metodu, která umožňuje analýzu velikostního rozdělení částic ve vzorku, a popisuje další vlastnosti briket, které mohou být užitečné pro budoucí výzkum a pro komerční účely.

Klíčová slova: *digestát, obrazová analýza, pevnost, sítová analýza, tvrdost.*

1. Introduction

The digestate is a very complex material and its utilization, mainly its liquid fraction, has effect on wide range of physical, chemical and biological properties of the soil depending on the soil types (Makádi et al, 2008). Anaerobic digestion process, by which the digestate is produced, became a very popular technology mainly among agri-business companies and farmers; that is why the number of biogas plants is still rising. In the Czech Republic, the number of biogas plants was approximately 554 BGPs in year 2014 (Amon et al, 2007; EBTP, 2013). As the number of the BGPs keeps growing the issue of storing and disposal of such a liquid material will gain significance.

In current crop management, farmers use the digestate as a liquid fertiliser or as a soil conditioner (Pulvirenti et al, 2015; Schleiss & Barth, 2008). However, due to possible run off, leaching and eutrophication of waterways, restrictions apply on the liquor application (WRAP, 2012). Restrictions in combination with intensive livestock farming imply that BGPs in nutrients rich regions should not or only sparingly return digestate in its crude, slurry form. As well the cost of transportation and spreading makes the digestate value zero or less. However, digestate is indeed a nutrient rich fertiliser. Nutrient recycling and treatment make it costly and unsustainable alternative of energy recovery and fertilizing (Mangwandi et al, 2013).

To improve transport, handling, storing and application, it is desirable to compress the biomass to much higher densities and less volume, because it is less appropriate or inappropriate for direct use due to the high moisture content, irregular shape and sizes, (Zhang & Guo, 2014; Miao et al, 2015) and thus enhancement techniques have been developed to improve the digestate ‘product’ (Mangwandi et al, 2013).

Digestate fibre can be well dried and pressed. Pellets from the digestate have mechanical durability compliant with the standards for pellets (Černá, 2015). Using digestate for energy purposes is not too convenient. The digestate use as a combustion fuel is not too frequent, because it tends to be primarily long fibre material. The most useful application is as a soil conditioner (ADBA, 2012). Another drawback is a substantial content of nutrients in matter and ashes, which are more useful as fertilisers than an energy source (Kratzeisen et al, 2010). In other reutilizing techniques, the digestate pellets are commonly used in stables as bedding for animals or as a fertiliser after enriched with additives (Alghren et al, 2010). Another reason to use the digestate as a fertiliser in compressed form is the possibility to mix improvement

additives into briquettes without changing the compatibility of the briquette having good sorption properties (Černá, 2015).

Thus the point of this work is to find and understand the relation between properties of the digestate briquettes and its structural composition. We were investigating how such kind of matter will behave under compressed conditions. We firstly needed to assess the particle distribution and particle properties in general.

Particles of the biomass, which is to be densified, are a basic filling and construction material; and thanks to the information gained, we are able to predict, at least to some extent, how this material will form the final briquette or the pellet.

The issue of porosity and sorption by solid materials is closely related to this topic. The topic of sorption has been solved in diploma thesis and thanks to deeper knowledge of inner briquette structure; it could be further exploited and understood.

To understand this issue, the summary of literature review of this thesis has been compiled to meet all basic findings about the links between the structures of both compressed and uncompressed biomass material and possible influences (such as changes of physical properties) on the final product. Regarding the production and briquette properties, it is mostly mechanical (physical) characteristics of individual texture components and the distribution of these components in the mass of the briquette.

As regards the rough description of texture properties, it is enough to know the mechanical properties of the texture material components versus the final compressed product. Attempts have been made to find the relationship between the texture of the processed material and the final product properties. Because the research involved only certain properties of the entire sample group, and the methods applied were often very laborious and approximate, therefore, as a basic method of determining the material texture the image analysis method was used that is universal allowing an easy comparison and quantification of certain characteristics in different materials and thus determine some connections between different elements of the texture.

Basic hypothesis of this work is based on the presumption that the briquette texture is dependent on many parameters the value of which was possible to quantify (type of material, moisture content, eventually chemical composition, size of particles, porosity of material, way and conditions of briquette processing, storage conditions and expiration time c etc.). While for the same type of material of briquettes we can reach a significantly high variability of briquette properties, as the whole.

2. Literature Review

The need for better and more comprehensive knowledge of the biomass material properties is generally evident. With the development of biomass utilization, this need is stressed, because the result of successful biomass use in many views depends precisely on respecting its properties. Therefore, the research looks for methods and ways to obtain this information.

As an introduction to this issue, basic definitions and terminology should be described. Because the material used in this research is basically a biomass matter, the literature review of this paper will start with biomass terminology.

2.1. Biomass

Biomass is an organic, carbon based matter, which derives from both animal and plant, (living or recently dead) materials (GTOS, 2009). Nowadays, biomass, in the attempt to replace or partially substitute fossil fuels, is studied as a potential source of energy. Biomass of plants can be basically and simply burnt in order to produce heat and electricity or/and according to prevalent compound contents, such as sugars, starches or oil compounds, the biomass is processed to fuels in the final liquid/solid/gas form, as shown in Figure 1 (Naik et al, 2010). Biomass utilization has the following advantages: it is widely available, the technology for its conversion and production is well understood, associated with low or negligible pollution, it is suitable for both small and large applications requiring only little energy and low temperature

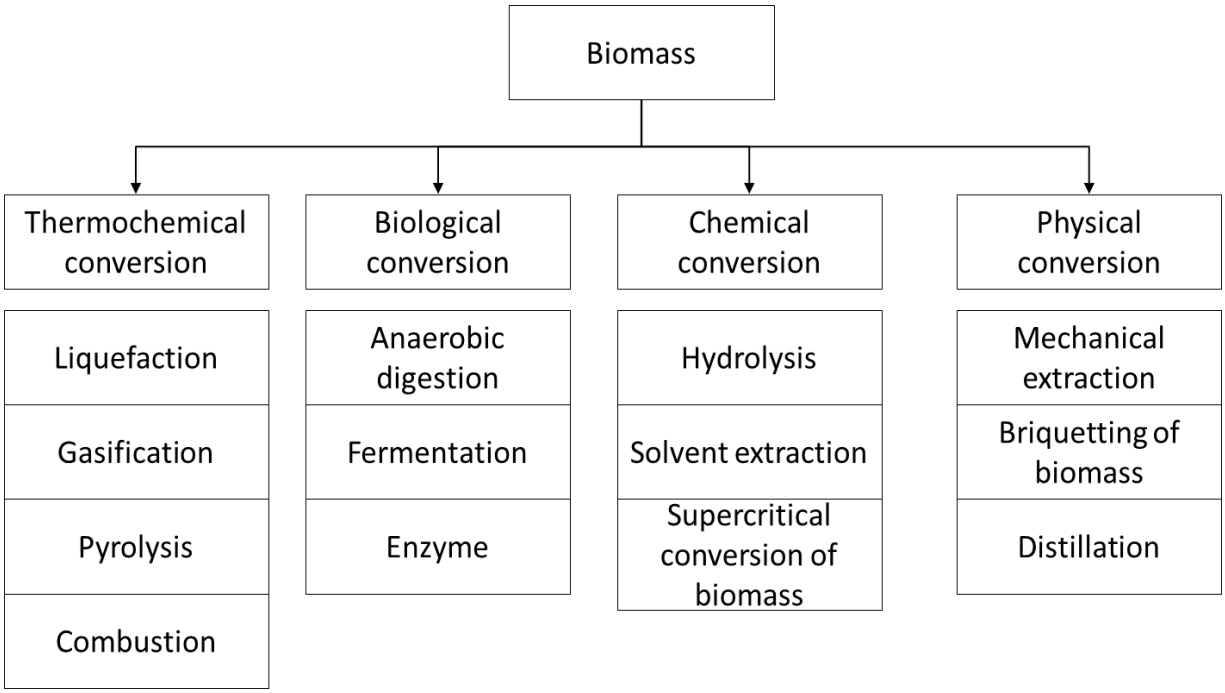

Figure 1: Biomass conversion processes (Naik et al, 2010).

(535˚C) and finally there are storage and transportation advantages regardless of geographical location (Vandenbossche et al, 2014).

The key limiting factors of conversion processes are: cost, the pre-treatment and the enzymatic hydrolysis efficiency and the C5–C6 co-fermentation. Lignocellulosic biomass transformation processes producing second generation 'biofuels' are studied worldwide, although the biomass is resistant to the enzyme action (Himmel et al, 2007) and in most cases requires pre-treatment.

2.1.1. Biomass characteristics, types

The biomass in general can be used by many different ways, from food production, timber, fibre, fertiliser, chemicals to energy production. In most cases biomass is perceived as plant-based, but it can be both animal-, vegetable- and waste- derived material. Cheap source of biomass are waste products and farming methods however this supply has its limitations. To overcome these limitations, the matter reprocessed to pellets and briquettes of consistent quality (high density, low moisture content, homogenous size and shape). Biomass has a variety of forms including food crops, energy crops, herbaceous plants/grasses including weeds, Napier grass and woody plants, and residues from timber processing, agriculture or forestry including silviculture, natural forests and plantations, home gardens and agricultural lands, aquatic and marine biomass. This category includes algae, water hyacinth, aquatic weeds, plants; sea grass beds, kelp and coral reaps, etc.; also various waste products such as municipal solid waste, municipal sewage sludge, animal waste and industrial waste, etc. (Hakeem, Jawaid & Alothman, 2015). General classification of the biomass is presented in Chart 1 and Figure 2.

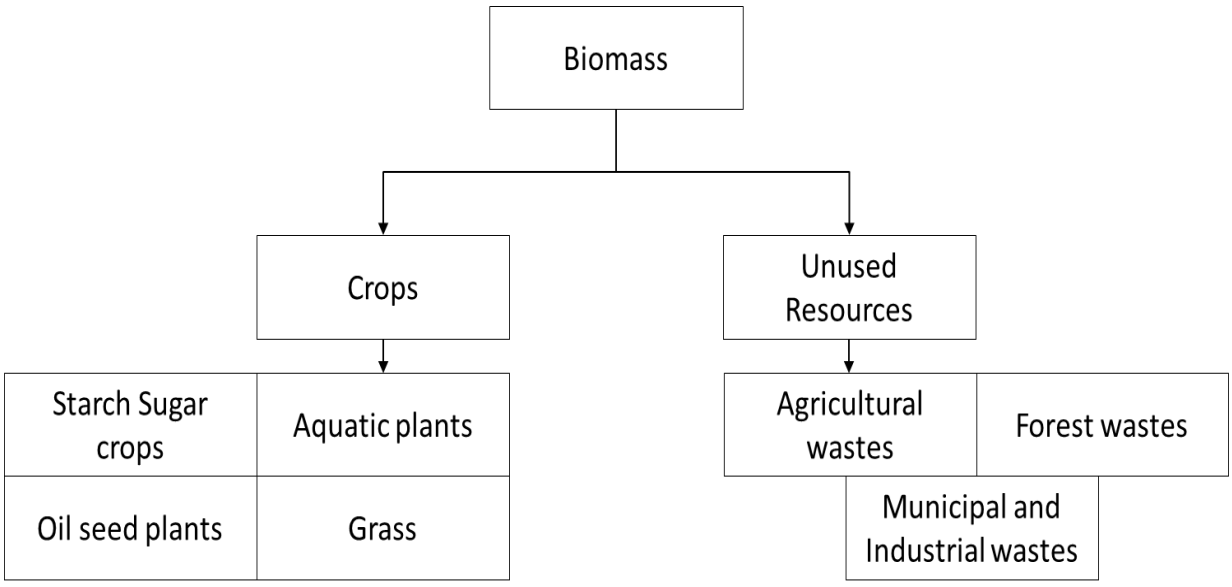

Figure 2: General biomass classifiaction (Naik et al, 2010)

Chart 1: Biomass classification v (Hakeem, Jawaid & Alothman, 2015).

Biomass group	Biomass subgroup, varieties and species
Wood and woody biomass	Coniferous or deciduous; soft or hard; stems branches, foliage, bark, chips, lumps, pellet, briquettes, sawdust, sawmill and others from various wood species
Herbaceous and agricultural biomass	Annual or perennial and field based or processed based such as: grasses and flowers (alfalfa, *Arundo*, bamboo, banana, *Brassica*, cane, *Miscanthus*, switchgrass, timothy, etc.); straws (barley, rice, wheat, sunflower, oat, rape, rye, bean, etc.); other residues (fruits, shells, husks, hulls, pits, grains, seeds, coir, stalks, cobs, kernels, bagasse, food, fodder, pulps, etc.)
Aquatic biomass	Marine or fresh water algae, macro algae or microalgae; blue, green, blue-green, brown, red, seaweed, kelp, lake weed, water hyacinth
Animal and human biomass wastes	Various manures, bones, meat-bone meal, chicken litter, etc.
Contaminated biomass and industrial biomass waste (semi/biomass)	Municipal solid waste, demolition wood, refuse-derived fuel (RDF), sewage sludge, hospital waste, paper-pulp sludge and liquors, waste paper, paperboard waste, tannery waste etc.
Biomass mixtures	Blends from the above varieties

2.1.2. Biomass structure, lignocelluloses

Focusing on plant biomass, plant organs are formed by myriads of cells with different functions in the plant's economy. Each organ has its own particular type of cell wall and its composition is related directly to the function, e.g. support (fibres), protection (epidermis) and transport (xylem, phloem). In tissues, cells are closely associated at their cell-wall interfaces to give a compact structure. This structure has to be broken by milling, and even milled plan stems limit liquid penetration by their nature (DoE, U.S., 2006).

The most of biomass supposed to be used for energy purposes consists of three major biopolymers – cellulose, hemicelluloses and lignin. Whole these compounds (polymers) are represented in plant body and create tightly interconnected molecule called lignocellulose (see Figure 3).

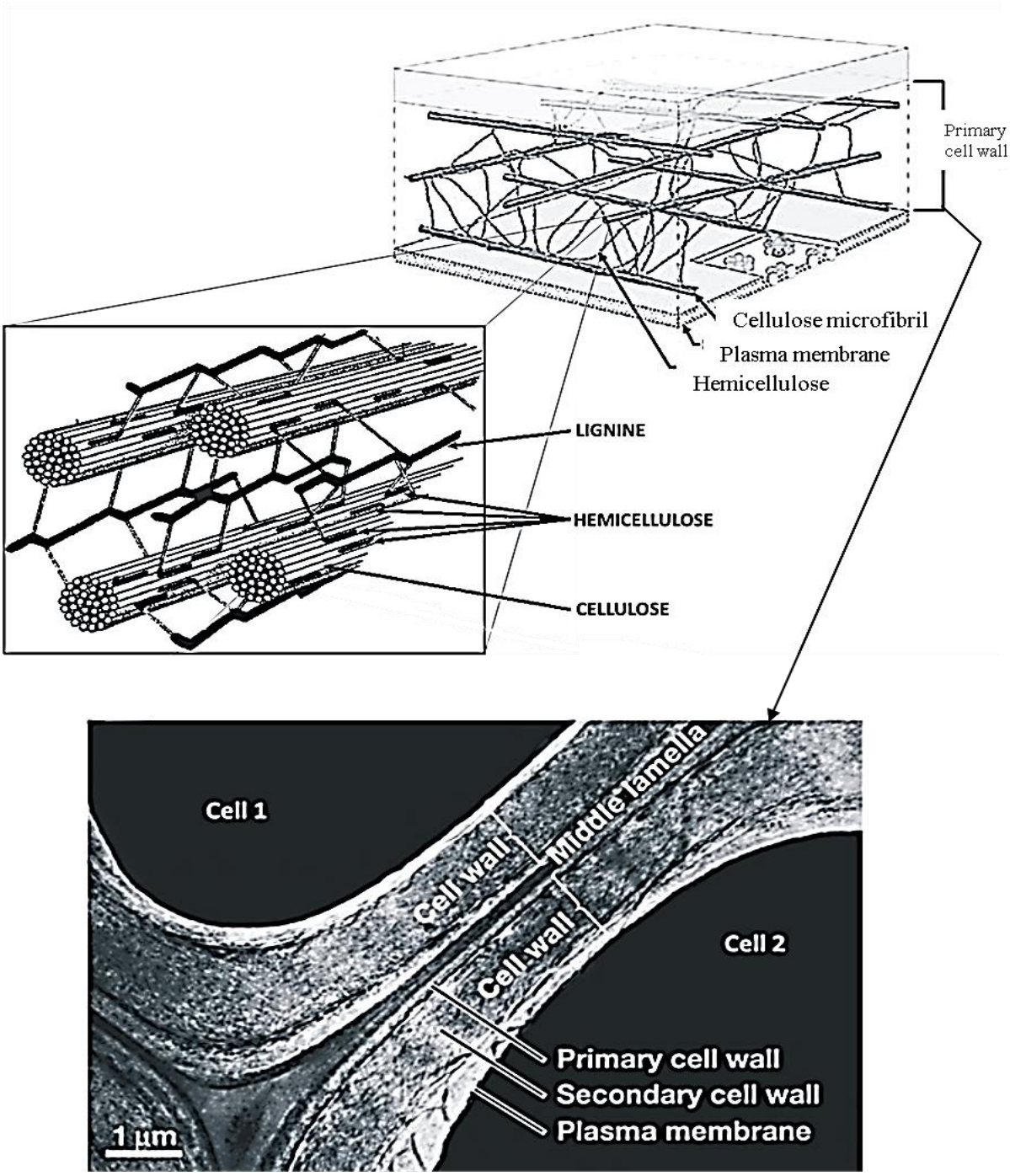

Figure 3: Plant body construction of lignocellulosic structure in cell walls, microscopic view of distribution in plant cell (Gnansounou & Dauriat, 2016, Michael G., 2013, Tabil, et al, 2011, DoE, U.S., 2006)

Primary cell wall contains mainly cellulose and hemicellulose and together with pectin and proteins from a reticular structure; aging cell walls contain lignin precipitates. By loosening the cellulose structure in primary cell wall, concentration of lignin is higher than in secondary wall (Chen, 2015).

2.1.3. Lignocelluloses compounds

Because materials used for this research is a digestate gained from biogas station, followed paragraphs refer to the main typical plant component structure of these biomass matters, lignocelluloses.

2.1.3.1. Cellulose

Cellulose is a linear chain of several hundreds to over nine thousand β (1→4) linked D-glucose $(C_6H_{10}O_5)_n$ units. Cellulose is fibrous, tough, water-insoluble substance, found particularly in stalks, stems, trunks and all woody portions of plant body. It comprises 40 – 60% of the plant's dry weight. Cellulose cannot be easily dissolved in conventional solvents, due to semi-crystalline structure and hydrogen bonds. It cannot be melted before it burns. Cellulose itself is not suitable adhesive agent. Cellulose molecule becomes more flexible after breaking the hydrogen bonds. It demands temperatures of 320˚C and pressure of 25MPa to become amorphous in water. Cellulose, followed by lignin is the main combustible compounds of lignocellulosic material.

2.1.3.2. Hemicellulose

Hemicellulose consists of heteropolymers; short-chained branches of carbohydrate 5- and 6- carbon sugars, almost all plant cells contain it along cellulose. It has a random, amorphous structure with less strength. Hemicellulose is related to cellulose and it comprises 20 – 40% of the biomass of most plants. The hemicellulose forms an amorphous structure that is more easily hydrolysed than cellulose; it is soluble in strong alkali solutions. The hemicellulose provides structural integrity to the cell.

2.1.3.3. Lignin

Lignin is a complex aromatic polymer consisting of not repeating covalently linked unit of coniferyl, sinapyl and coumaryl alcohols. Lignin has several unusual properties as a biopolymer, such as heterogeneity, lacking a defined primary structure. It fills empty space in cell walls between cellulose and hemicellulose. Lignin is covalently linked to hemicellulose and cross-linked with different plant polysaccharides providing the mechanical strength to the whole plant body (Tabil, et al, 2011) thus making the plant resistant to moisture and biological attacks. Unfortunately, in case of energetic applications, lignin inhibits the enzymatic conversion of polysaccharide components (DoE, U.S., 2006). It works as a barrier to the enzyme and microbial penetration, thereby greatly decreases the yields of fermentable sugars and affects negatively the energy production (Canam, et al, 2013). It is a bonding agent for the

cellulose fibres. At temperatures higher than 140°C it can be used as an inner resin because lignin melts and shows thermosetting properties. Lignin also permits adhesion and is firming and bulking agent. Water content in pellets (8 – 15%) can reduce the softening temperature of lignin to 100 – 135°C, then the adhesive properties of thermally softened lignin are able to contribute to the strength characteristics of briquettes made of lignocellulosic materials (Tabil, et al, 2011).

2.1.4. Used material – digestate, production and properties

In the attempt to use agro-biological material more efficiently, many disposing technologies are invented or restored. One of them is the process of anaerobic digestion (AD), purposely ongoing in biogas plants (BGPs).

2.1.4.1. Anaerobic digestion

AD is a suitable method of converting non-sterile, diverse and complex feedstocks into energy-rich biogas. It can be used for effective alternative treatment of wastes since it recovers bioenergy from the substrate with high moisture content (Pulvirenti et al 2015, Sawatdeenarunat et al 2015). The AD process is the naturally occurring biological pre-treatment of organic matter carried out by mixture of microbial communities in the oxygen free environment. The consortium of microbes works in synergy decomposing the biomass structures to the basic components. The entire lignocellulosic feedstock is fed into anaerobic bioreactor to convert complex carbohydrates and organic matter into energy-rich biogas (Weiland, 2010).

The entire AD process comprises four stages (showed in Figure 4), where each group of different bacteria decomposes complex polymers to easier compounds.

The first stage is hydrolysis, where polymer substrates are hydrolysed to monomers by hydrolytic bacteria using enzymes: amylases, lipases, proteases and cellulases.

In the second stage (acidogenesis), the acidogenic or fermentative bacteria convert the products of hydrolysis to volatile fatty acids (C3 – C6), alcohols etc., forming acetate, CO_2 and H_2 as byproducts. These compounds together with methylamines, methyl sulphide, acetone and methanol produced in this process, can be directly utilized for methanogenesis (final stage).

Final product, the biogas is produced during the last stage- methanogenesis by methanogens in two ways: by splitting the acetic acid molecules producing methane and carbon dioxide; or by reduction of the carbon dioxide with hydrogen by acetotrophic and hydrogenotrophic methanogens.

The generated biogas is composed mainly of methane (50 – 75%), CO_2 (25 – 45%) and traces of other gases like O_2, H_2S, CO, NH_3; and water vapour (Manyi-Loh et al, 2013).

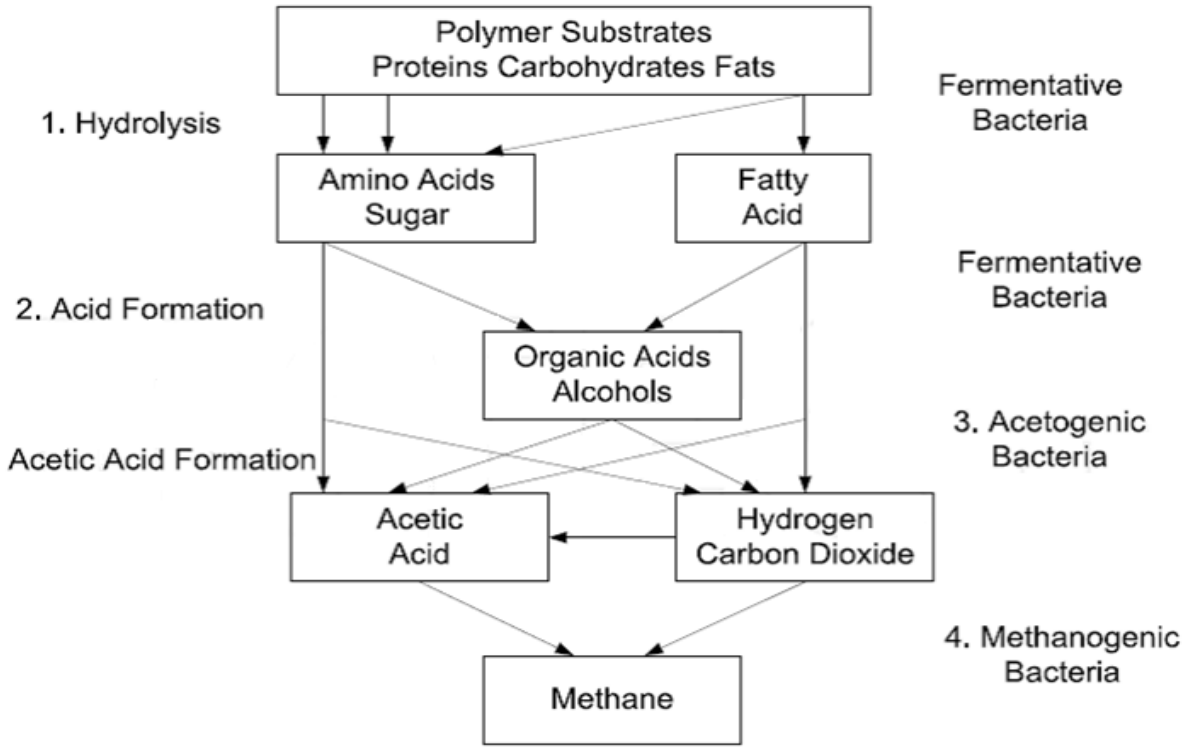

Figure 4: Stages of anaerobic digestion process (Wilkinson, 2011)

The results of different studies show that the heterogeneous polysaccharide hemicellulose was decomposed and metabolized before other structural components. Well operated AD process may have the ability to stimulate the CH_4 production from the hemicellulose leaving behind the cellulose and lignin in the fibrous solid residues. The hemicellulose removal destabilizes the hard degradable biomass structure allowing for the cellulose solubilization by enzymes (Maclellan et al, 2013). Any lignin remaining in the solid residue has little commercial value, but can be burned and used for heat and electricity generation (Sawatdeenarunat 2015).

Many of biodegradable materials and liquids such as industrial wastewater, food wastes, animal manure, agri-wastes, sewage sludge, organic fraction of municipal solid waste, among others, have been employed as input feedstock for commercial biogas production.

The lignocellulosic biomass, namely the agri-residues and energy crops, have been introduced at the beginning as a candidate of primary feedstocks for bioenergy production and bio-based products. The lignocellulosic biomass represents a highly resistant and recalcitrant biomass structure and thus, the hydrolysis stage is often slowed down during the traditional AD (Sawatdeenarunat, 2015). However, researchers have focused on enhancing the digestibility of

the lignocellulosic biomass through physical, chemical, biological and hybrid pre-treatments in the production of liquid fuels by biochemical methods (FitzPatrick et al, 2010; Takara and Khanal, 2011).

Amongst various pre-treatments, the thermochemical pre-treatment using alkali is noted as one of the most promising methods for the lignocellulose hydrolysis. It is known that the degradability of lignin by chemicals depends on its composition. The lignin polymer consists of three different phenyl-propane units; guaiacyl, syringyl and p-hydroxyphenyl lignin. Non-woody tissues (e.g., leaf and pollen) and herbaceous plants contain all types of lignin (Koyama et al, 2015).

Unfortunately, many of these pre-treatments are economically and environmentally unfavorable (Sawatdeenarunat, 2015). As already mentioned, the biomass is considerably resistant to the anaerobic biological decomposition due to the lignin barrier on cellulose and hemicellulose manifesting negative relationship between CH_4 yield and the lignin content in various biomass bodies (Koyama et al, 2015).

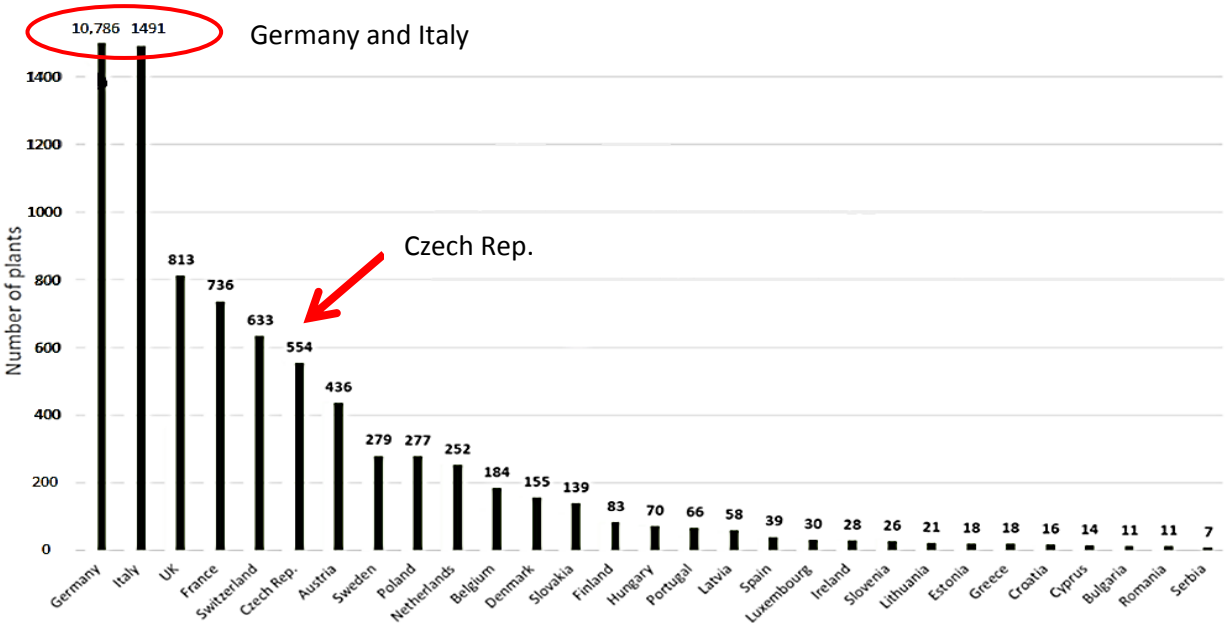

Figure 5: Biogas plants number across Europe in 2014 (EBA, 2015).

The AD process became very popular mainly among the agri-business companies and farmers and the number of BGPs is still increasing. In the Czech Republic this number represents approximately 554 of BGPs per year 2014 (Amon et al, 2007; EBTP, 2013). For example in Germany, the number of AD BGPs has increased over the 24 year period (1990 – 2014) from 100 to 10 786 facilities (Mangwandi et al, 2013). The total number for Europe was 17 240 BGPs in 2014 reaching the total installed capacity of 8 239MW_{el} and the leaders are Germany

together with Italy as shown by Figure 5 (EBA, 2015). This number of BG plants is quite high and consumes large volume of biomass matter. The BGPs became an integral part of almost every agricultural farm. For their operations, substrate of lower quality grass plants and manure is not as sufficient as intended. All BGPs are optimized in order to gain advanced biogas production yielding higher electricity production (Ward et al, 2008). That is why currently the maize grass pulp makes approximately one half of the total mass input, and this plant material is purposely grown for the BGPs' operations (Amon et al, 2007).

Unique to an AD approach, in comparison to the conventional bioenergy production, is the digestate generating (nutrient-rich residue) from the digested slurry (Sawatdeenarunat, 2015). However, high production of digestate slurry and liquor is limited by the capacity of the AD disposing facilities (Mangwandi et al, 2013).

2.1.4.2. Digestate

Digestate is the by-product of biodegradation process – the anaerobic digestion, consisting of water, cellulose residues, small quantity of bacteria and organic nutrients (nitrogen, phosphorus, potassium, calcium, etc.) (Kurchania, 2012). After processing this nutrient rich matter is more or less in a liquid form. This form is separated as required to 'liquor' and 'fibre'. 'Liquor' usually contains 10% of dry matter and in most cases is partially reused in the AD process with a new dose of input substrate or it is used as liquid fertiliser (Hills & Roberts, 1981; Li et al, 2011; ADBA, 2012). The dry matter content in the solid fraction varies according to input feedstock material (generally between 40–85 %). The feedstock material is usually animal manure, slurry, food wastes, energy crops residues and bio-wastes, so the content of the lignocellulosic components is high in digestate. Particles of the digestate matter are not size distributed, because the feedstock for the AD is chopped to same sizes (Černá, 2015).

2.1.4.3. Digestate use

The digestate is a very complex material having effect on the wide range of physical, chemical and biological properties of the soil, mainly its liquid fraction, depending on the soil types (Makádi et al, 2008). Farmers use the digestate either as a fertiliser or as a soil conditioner in modern crop management. Among the organic additives, the ratio of the liquid digestate in the agriculture is known to be around 10% (Pulvirenti et al, 2015; Schleiss and Barth, 2008).

In comparison to other organic materials, the fertilizing properties of the digestate rank as follows: compost ~ digestate > digested sludge >> ingestate (raw materials), according to OM degradability (Tambone et al, 2010). The variation of the macromolecule content in the AD process is shown in Chart 2.

Chart 2: Variation of macromolecule content in the AD process (Pognani et al, 2009)

Ingestate Type	Total solids ($g \cdot kg^{-1}ww$)		Lignin ($g \cdot kg^{-1}TS$)		Hemicelluloses ($g \cdot kg^{-1}TS$)		Celluloses ($g \cdot kg^{-1}TS$)	
	IG	DG	IG	DG	IG	DG	IG	DG
Energy crops, cow manure slurry and agro-industrial waste	127	35	49	280	35	42	50	68
Energy crops, cow manure slurry and agro-industrial waste and OFMSW	143	36	72	243	27	54	71	79

The response of plants on the digestate fertilizing could be classified as sensitive (alfalfa, sunflower, and soybean) and the non-sensitive (winter wheat, triticale, sweet corn, silage maize) groups. In case of the sensitive plants, the digestate can cause burning, thus they can be treated only in certain stages of their life, compared to non-sensitive plants, which can be fertilized by digestate at any development stage, even in rainy period, when the digestate technically could not be spread (Makádi et al, 2008). Because of its high available nutrient content, digestate application results in significantly higher aboveground biomass yields. According to nutrient analysis in research of Mangwandi et al, 2013, the phosphorus (P) content in the digestate sample was 459 mg/kg, ammonia (N) 883 mg/l and potassium (K) 1, 797 mg/kg. However the effectiveness and nutrient composition of the digestate depends on the arrangement of co-digested material, the treated plant species and the treatment methodology (Möller et al, 2008; Stinner et al, 2008).

The digestate slurry or liquor is usually applied to the soil directly; however there are some restrictions and limitations. One is established by the European Union – the European Nitrates Directive (91/676/EEC.) restricting the application of the digestate to the soil according to the location and crop demand. This directive is restricting the limit of N added to the soil, which cannot exceed 170 kg of N/ha, especially in vulnerable areas. Other limitations of liquor application can arise from possible run off, leaching and eutrophication of waterways (Ahlgren et al, 2010; WRAP, 2012). Restrictions in combination with intensive livestock imply that BGPs in nutrient rich regions should not or only sparingly return digestate in its crude, slurry form. However, the digestate in nutrient rich fertiliser, nutrient recycling and treatment

make it a costly and unsustainable alternative of energy recovery and fertilizing, whereupon innovative techniques of the digestate processing (Figure 6) are invented (Mangwandi et al, 2013). Cost of transportation and spreading make the digestate value zero or less and thus there are enhancement techniques to generate a digestate 'product'. The process of digestate enhancement is illustrated in scheme Figure 7, 8.

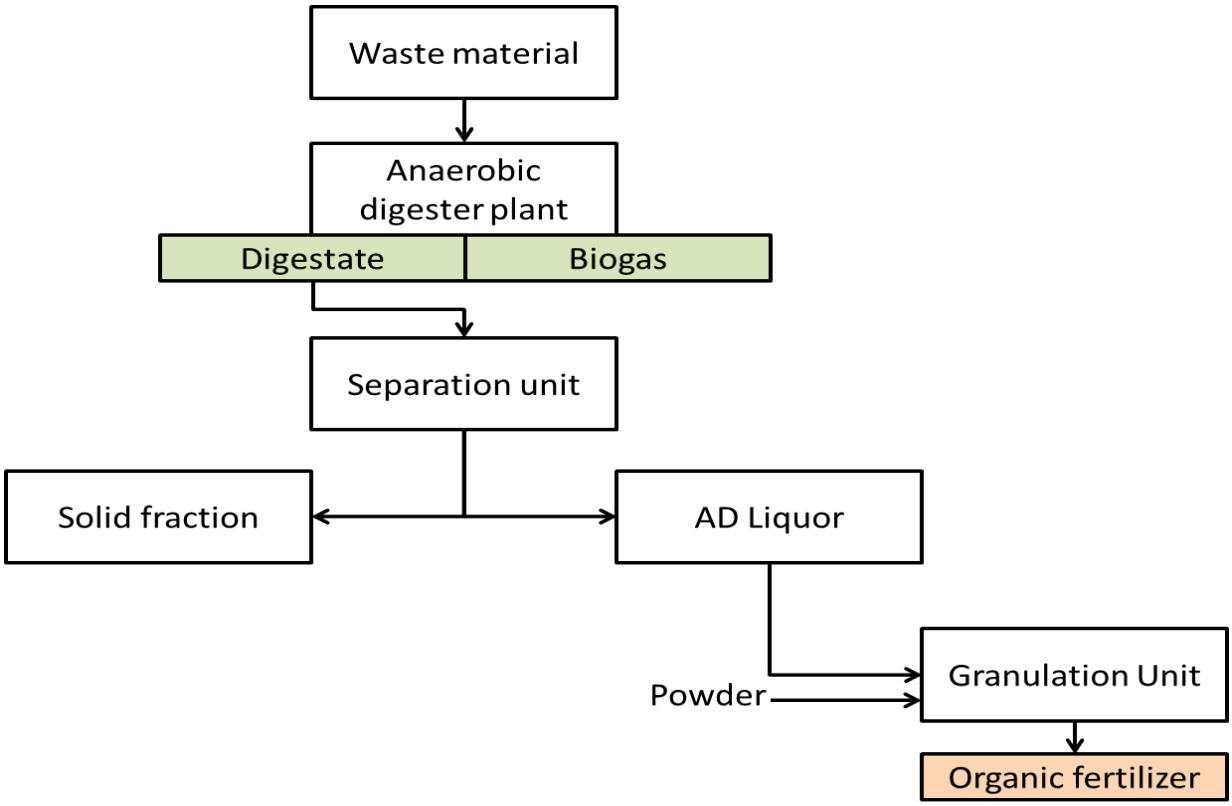

Figure 6: Scheme of digestate production and processing as fertiliser granules of reasonable strength and shape, produced by granulating limestone powder using the AD liquor (Mangwandi, 2013).

Beside the fertiliser or the conditioning properties of the digestate, there are some other ways of its utilization. These methods enable proper utilization of various quality digestates.

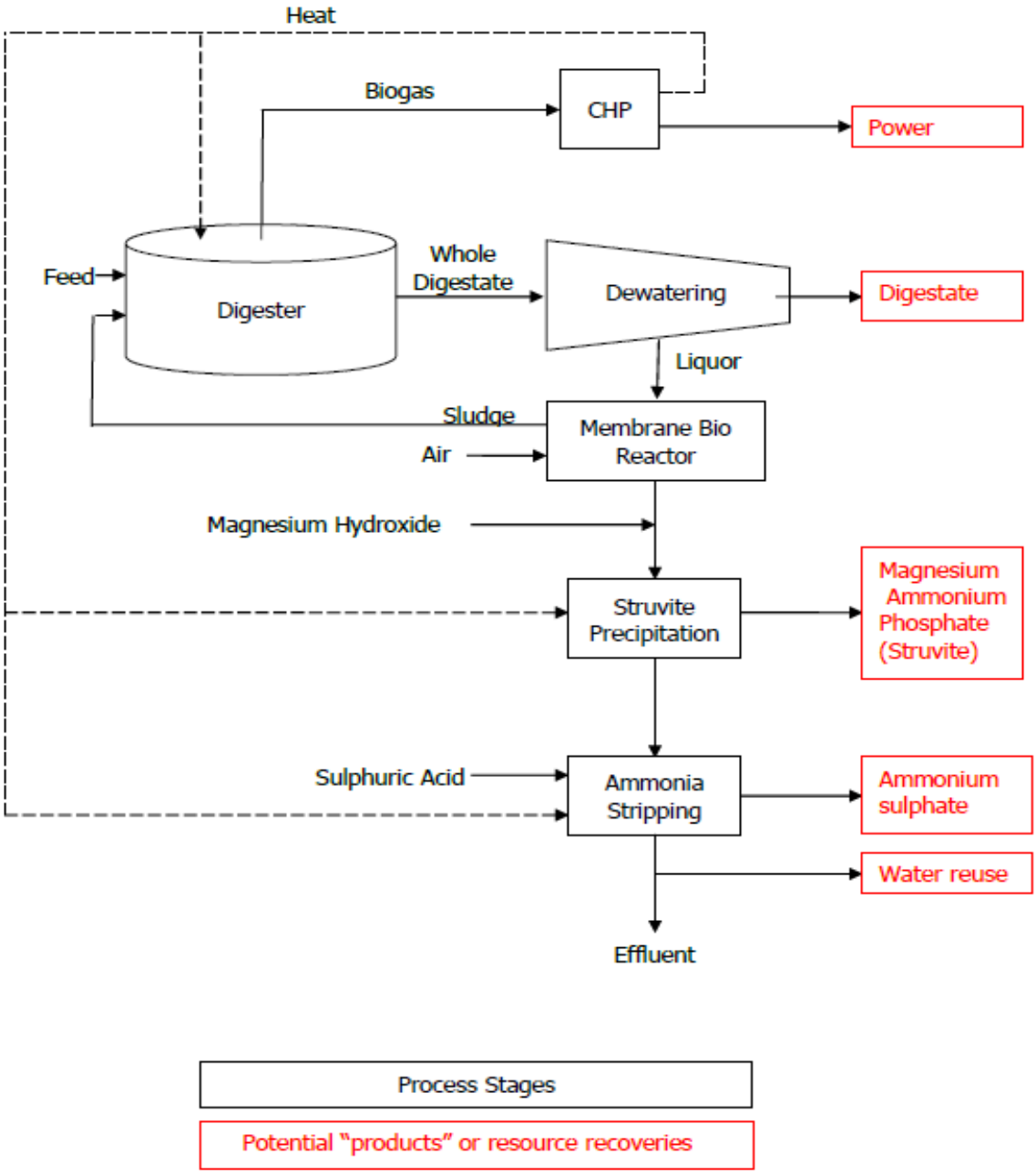

Figure 7: Diagram of potential digestate liquor enhancement (WRAP, 2013)

In one way, the digestate can be separated to liquid and solid fraction. The liquid fraction is suitable for irrigation especially due to its high N and K content. Solid fraction contains a great amount of volatile solid and P (Liedl, et al, 2006) and has also high biogas and methane content, therefore it could be used as co-ferment material for anaerobic digestion.

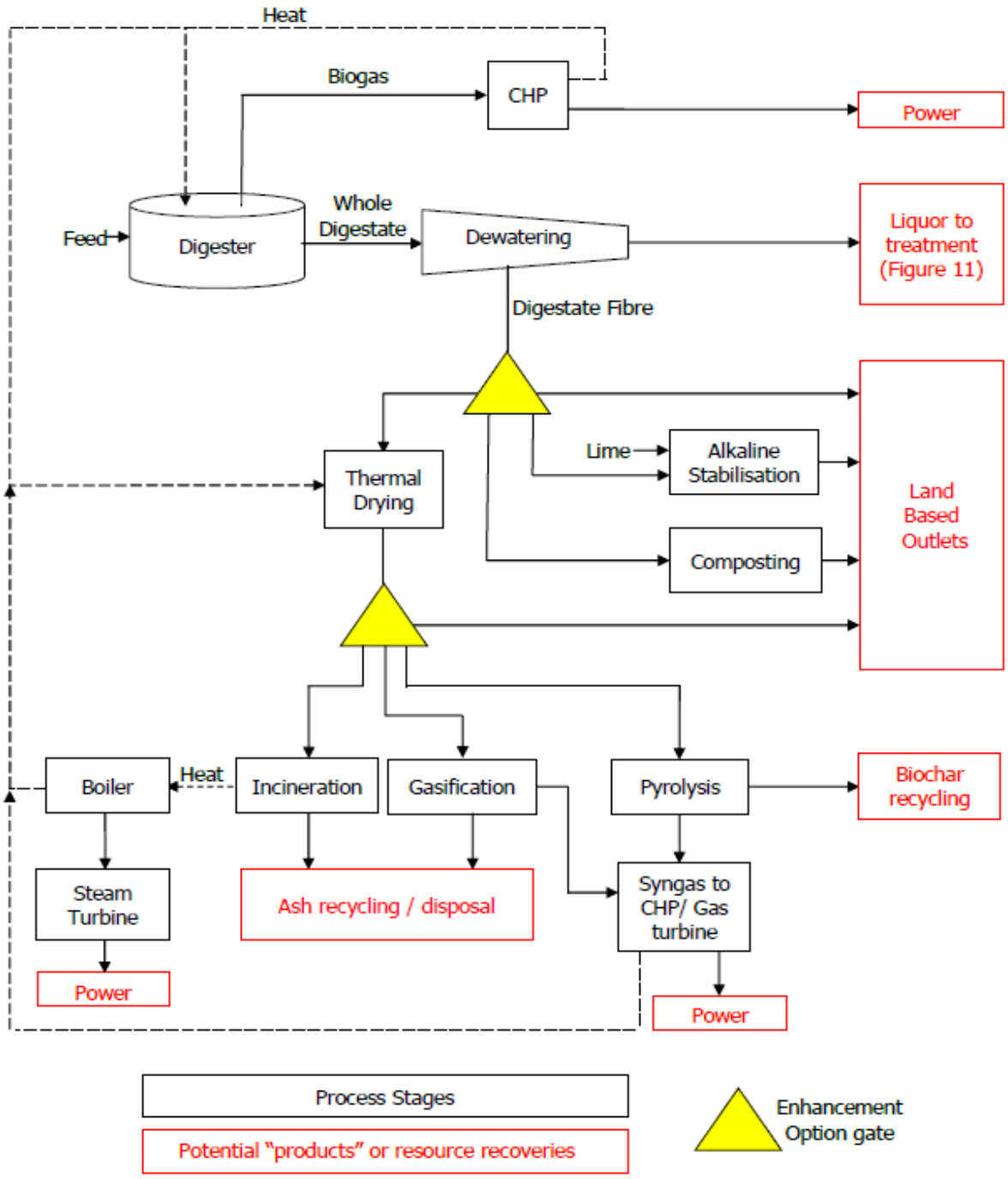

Figure 8: Diagram of potential digestate fibre enhancement (WRAP, 2013)

In second way, the digestate can be dried and pressed, after drying the water content of pellets (approx. 9.2 – 9.9%). The digestate in the pellet form has mechanical durability meeting the standards for common pellets. Moreover, the calorific value of the digestate briquettes was in several studies comparable to the calorific value of wood (Černá, 2015). Therefore, the digestate fuel pellet seems to be a good alternative for wood fuel. The solid digestate fraction is commonly used in stables as bedding for animals or it is used as fertiliser enriched by additives (Alghren et al, 2010). Another use of the separated digestate can be in the compressed form

(briquette or pellet) for direct burning, but it is not such frequent utilization, because it tends to be primarily long fibre material. The most useful application is soil conditioner (ADBA, 2012). Using the digestate for energetic purposes is not so convenient. First reason is that the digestate briquettes production process is more expensive and energy demanding than energy production itself, which is 15 – 16 MJ/kg; which is lower in comparison to other easily accessible biomass of higher calorific value. Another reason is the higher content of nutrients in the matter and ashes, which are more useful as fertilisers than an energy source (Kratzeisen et al, 2010). Very good reason to use the digestate as fertiliser in compressed form is the possibility to mix amendment additives into the briquettes without changing the compatibility of the briquettes and with good sorption properties (Černá, 2015).

Another interesting possibility of the digestate utilization is the use of digestate effluent to replace freshwater and nutrients for bioethanol production (Makádi et al, 2012). The Gao & Li research (2011) revealed that ethanol production was boosted by 18% with the use of digestate effluent in comparison to the freshwater utilization.

A common practice in agriculture is the use of biodegradable and agro-waste material of high bulk density, which is hard to store. Furthermore, inappropriate handling, storage and application of the digestate as fertiliser can cause ammonia emissions, nitrate leaching and phosphorus overloading (Wilkinson, 2011) so it is desirable to compress the biomass to much higher densities and less volume, because of transport efficiency, better biomass handling, storage and utilization of the original matter, which is due to high moisture content, irregular shape and sizes less appropriate or inappropriate for direct use (Zhang & Guo, 2014; Miao et al, 2015).

We have to go deeper in this topic, to find properties of the biomass matter. To find out how the plant matter would behave in compressed state, we firstly need to know the particle distribution and the particle properties in general. The biomass particles to be densified are the basic filling and construction material and thanks to the information obtained, we are able to predict, at least to some extent, how this material will construct the final briquette or pellet. The issue of porosity and sorption by solid materials closely relates to this topic. The diploma thesis deals with the topic of sorption and thanks to deeper knowledge of inner briquette structure; it could be further exploited and understood.

2.2.Biomass texture, inner structure and porosity

2.2.1. Biomass particles

Physical properties of solid particles are influenced by important factors such as the particle shape and size distribution. Due to high content of lignocellulosic components, the biomass particle shape is very irregular. This fact cannot be overlooked in the biomass transport, mixing and fluidization. Different particle shapes result in different surface areas of particles, which is essential for heat and mass transfer processes. It is noticed that needle shape particles of large aspect ratio are associated with particularly high internal friction. Moreover, the research showed that the particle shape influences the strength of the material making it stronger and more resistant to shear in simple shear flows. There are some shapes qualitatively described by different studies as flakes, rod-flakes, needle-flakes. In another study, shapes are described as plate, slab, prism, cylinder, rod and sphere. Particles can be spherical (shape of one dimension – diameter of sphere) and non-spherical. All biomass particles are described by two dimensions (length and width) as shown in Figure 9 (Scientific, 2012**).**

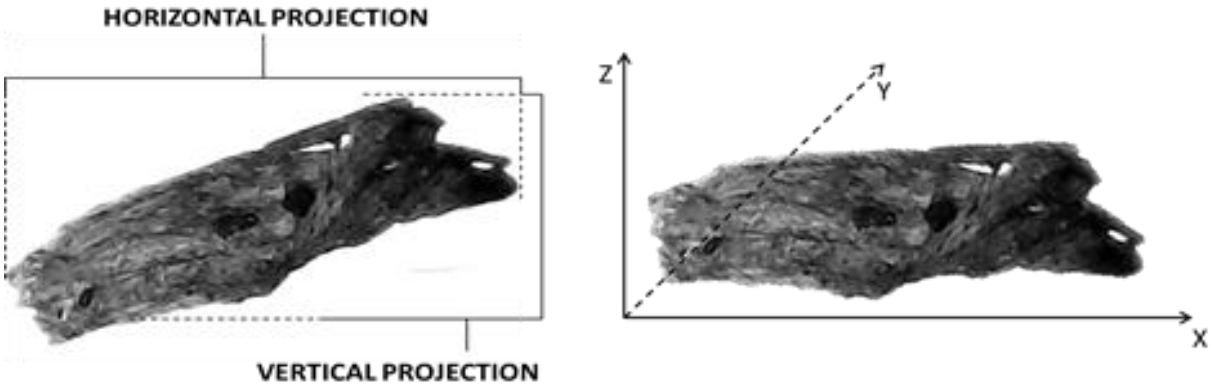

Figure 9: Non-spherical particle, described by XYZ axis in planar view (2D) (Scientific, 2012; author's picture).

Quantitative study of particle shape has not been reported yet. Particle size distribution plays its role in flow ability and other properties. Even small variation of particle size changes the resulting flow ability. Even small difference s in fine particles content results in measurable changes of cohesiveness (Guo, et al, 2012).

In the study of Hann and Stražišar (Hann, et al, 2007), they noticed that the yield strength of bulk solid would increase with the particle size. Guo and his team reached a conclusion in his study that anisotropy of biomass materials is caused by needle-shaped

particles of large aspect ratio. The particle size distribution in biomass materials brings good coincidence and cumulative mass fraction (Guo, et al, 2012).
Each particle dissimilarity and other changes, mechanical or chemical, influencing the briquette properties are reviewed in next chapters.

2.2.2. Porosity and biomass texture

Porous structure at the cell wall level of biomass refers to the pore structures among various macromolecules. Cell wall of a fibre cell is composed of primary cell wall and the secondary cell wall, the secondary mainly comprises of lignin and the primary mainly of cellulose. Corn stem – width of pores is 1 – 20 μm and the length 10 – 30 μm. (Chen, 2015)

The biomass pores represent passages between two surfaces (internal and external) of solids. The pore structure more or less influences the physical properties, e.g. density, strength and/or conductivity are (Fletcher, 2008).

Pores can be classified to four categories (see Figure 10). Firstly, the closed pores, which are influencing macroscopic properties such as bulk density, mechanical strength,

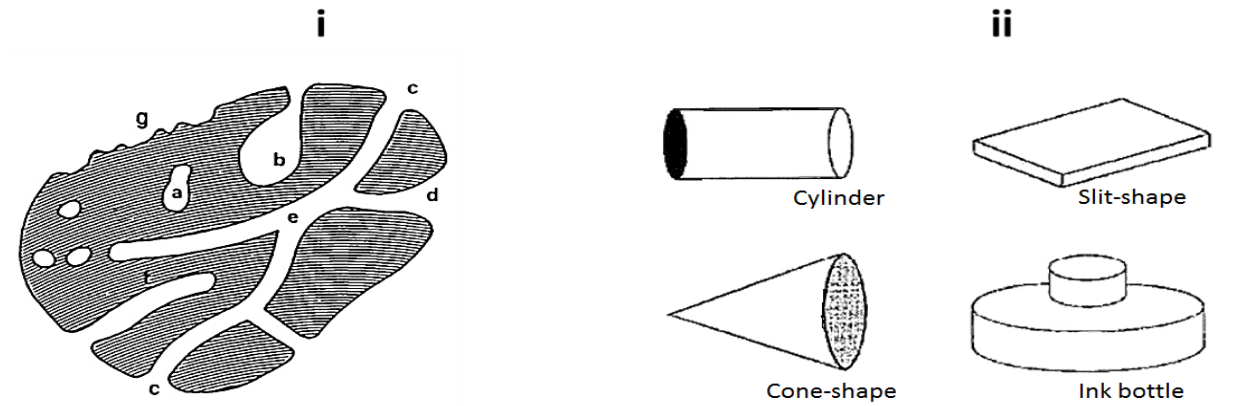

Figure 10: i) Pores categories a – closed pores, b,f – blind pores, c,d – open pores, e – transport and g – external pores (Rouquerol et al, 1994). ii) Basic shapes of pores (Kaneko, 1994)

however they are inactive in flow processes because the internal void is not connected with the exterior surface. Secondly, the open pores connected to external material surface allowing flow. Thirdly, the transport pores connecting different parts between external and internal surface. The last category are the blind pores that are connected to the transport pores and do not lead to the external surface. Pores also can be categorized according to their shape, width and routes (Rouquerol et al, 1994). The most common shapes are cylindrical, ink-bottle, funnel and/or split-shaped (see Figure 10), (Kaneko, 1994). However, real porous system is more complicated; idealized system divides shapes to cylinders, prisms, cavities, windows, spheres and slits (Rouquerol et al, 1994).

The guidelines of pore width classification are as follows:

2.2.2.1. Micropores (< 2nm)

Divided by width there are the following types of pores: ultra-micropores (< 0.5 nm), micropores (0.5 – 1.4 nm), super-micropores (1.4 – 2.0 nm). The micropores are results of imperfect packing arrangement of bulk matter of different element size and shape. These pores provide maximum water sorption, which is completely irreversible.

2.2.2.2. Mesopores (2 – 50 nm)

The mesopores are in fact defects of solid structures and form passages serving as a transport system to micropores.

2.2.2.3. Macropores (>50 nm)

The macropores provide transport access to internal surfaces; the diameter is usually of 1 – 2 mm and can be observed by optical and scanning electron microscope. Every porous structure is unique and distinctively shaped (Fletcher, 2008).

In case of biomass matter, the prevalent pore size is definitely the macropores. The porosity is changing with biomass processing, e.g. the experiment of Miao et al, 2015 shows comparison of porosity before and after the biomass compression where particles were compressed to 7.2 MPa and 750 MPa and the porousness of biomass particles has significantly decreased. However, despite the high pressure of 7 MPa, the cell walls were not disrupted. This finding could imply that mechanical compression doesn't destruct the cell walls; however more studies are needed to determine the effect of mechanical compression and its consequence on porosity decrease.

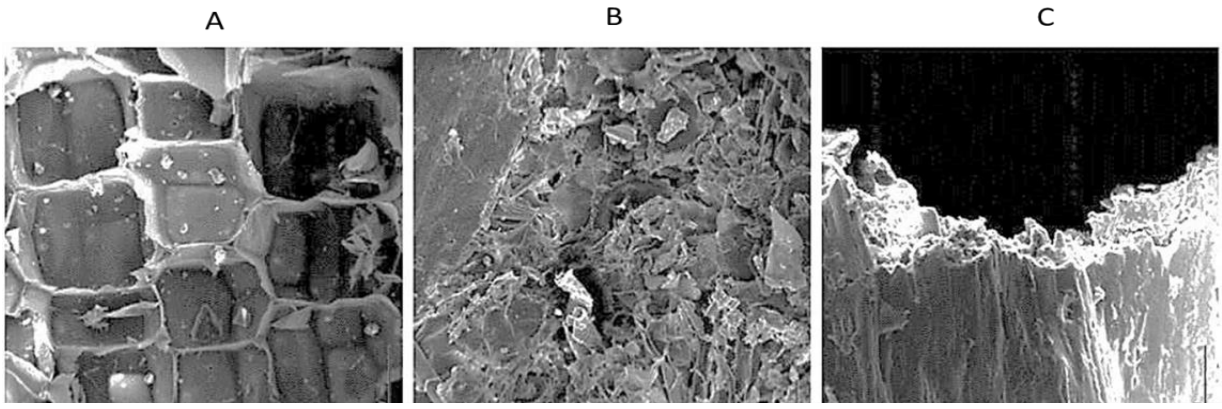

Figure 12: Microscopic images of *Miscanthus* stem porosity A) grinded by milling screen of 12.7 mm aperture without compression; B) after compression by 7.2MPa and C) after extreme compression by 750MPa (image scale 50 μm)(Miao, et al, 2015)

Figure 11 shows the comparison of microscopic images of porosity of Miscanthus material processed by milling screen with aperture size of 12.7 mm, without compression; than material after being compressed under pressure of 7.2 MPa; and material after being compressed under extreme pressure of 750 MPa. Figure 12 shows also the Miscanthus cell damage with an aperture size of milling screen of 13 mm before and after compression (Miao, et al, 2015).

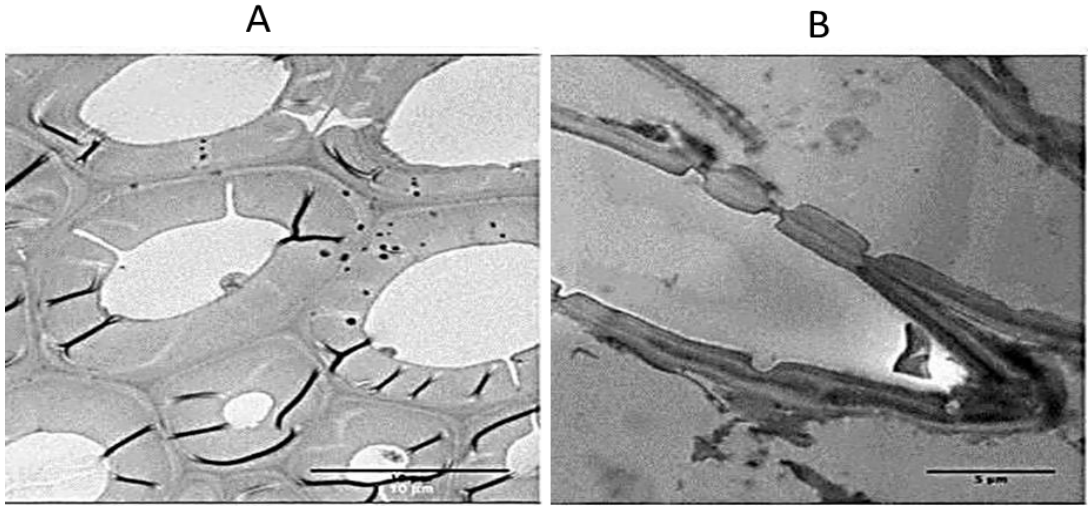

Figure 11: Microscopic images of *Miscanthus* cell walls grinded by milling screen with the aperture of 13 mm A) before compression and B) compressed by pressure of 750MPa (Miao, et al, 2015)

The moisture content and ability of solids to absorb water and fill the pores it is also related to porosity. That is why the next topic is further described in the paragraph "Sorption". The plant tissues have the ability to transport and bond water in its tissues, demonstrating the water binding capacity: water is extremely important medium allowing growth. This term refers to the water absorbed by a mass unit of dry matter. Water is held among macromolecular organs by capillary effect and surface tension. After the cellulose fibre moisture content

reaches its saturation point, water molecules keep going into the cell cavities and pores within the cellulose forming a multilayer of absorbed water or capillarity water called the unbound water (Chen, 2015). Bound water is the water held within the cell wall material. Fibre saturation point is the stage in the drying or wetting of wood when the cell walls are saturated with bound water, and the cell cavities are free of liquid water. Fibre saturation point for most wood species occurs at moisture contents of about 25 to 30% (Reeb, 1995).

2.2.3. Sorption properties

Most of biomass materials are hygroscopic and they may absorb and desorb moisture from its surrounding. The knowledge of moisture content is essential in appraising the importance of environmental and other changes observed in storage. High moisture content results in swelling and disintegration of briquettes (Singh, 2004). Sorption is described as a transport of gas or liquid into the bulk phase of the solid material; it can be divided to absorption and adsorption.

Chart 3: Characteristics Associated with Physical/Chemical Adsorption (Fletcher, 2008)

	Physical Adsorption	Chemical Adsorption
Heat of adsorption [$kJmol^{-1}$]	20 – 40 c.f. heats of liquefaction	> 80 c.f. rela bulk-phase chemical reactions
Rate of adsorption (at 273K)	Fast	Slow
Temperature relation to uptake (with Increasing T)	Decreases	Increases
Desorption	Easy- by reduced pressure or increased temperature	Difficult - high temperature required to break the bonds
Desorbed Species	Adsorbate unchanged	May be different from the original adsorptive
Specificity	Non-specific	Very specific
Monolayer Coverage	Mono or multilayer, condition dependent	Monolayer

Adsorption can be chemical and/or physical (see Chart 3). The physical sorption is a dynamic process dependent on the physical property of the adsorbent containing van der Waal's forces. The chemical adsorption is less common, enabling electron transfer between phases resulting in chemical bond formation. Chemical reactions cause adhesion of adsorbate molecules which is almost irreversible (Fletcher, 2008).

In respect of the sorption properties of material, it is difficult to predict adsorption of any material due to specific porosity (Gruszkiewicz, Simonson, Burchell & Cole, 2005). However, there are some available measurements and methods (volumetric, gravimetric, calorimetric or spectroscopic) to determine the pores sizes and distribution, and the resulting graphical form is the isotherm (Pechoušek, 2010).

2.3.Briquettes

Some materials like agriculture and forestry residues and other waste biomass matters are usually difficult to use as biofuels, because of large bulk and laborious processing. This problem can be easily solved by transforming this bulky mass into compact regular shapes (Naik, et al, 2010). Lignocellulosic feedstock, especially herbaceous biomass, has low bulk density. Depending on the densification level, the transport cost represents 13 – 28% of total costs. Bulk densities ranging from 120 – 180 kg DM m^{-3} of forage hay and biomass are traditionally achieved by using the in-field balers. Even when modern high-compression cutting balers are used, the bale density does not exceed 230 kg DM m^{-3}. It is desirable to compress the biomass to much higher densities than balers can achieve, because of transport efficiency, e.g. pellets bulk density is 850 kg m^{-3}.

Chart 4: Recommended use of briquettes (Grover and Mishra, 1996).

Boilers:	For steam generation
Food processing industries:	Distilleries, bakeries, canteens, restaurants and drying facilities etc.
Textile process houses:	Dyeing, bleaching etc.
Agro-products:	Tobacco curing, tea drying, oil milling etc.
Clay products:	Brick kilns, tile making, pot firing etc.
Domestic:	Cooking and water heating
Gasification:	Fuel for gasifies

Herbaceous crops show varying elastic and plastic qualities among various species and forms (Miao, et al, 2015). The biomass densification into pellets, briquettes or cube forms can solve the issues of the biomass handling, transport, storage and better utilization of original matter, which due to high moisture content, irregular shape and sizes and low bulk density is less appropriate or inappropriate for direct use (Zhang, et al, 2014). Chart 4 shows recommended uses of briquettes.

2.3.1. Biomass pre-treatment

Many agricultural materials before densification require pre-treatment, because they are often dusty, difficult to handle and costly to manufacture and thus poorly formed to pellets. By disrupting lignocellulosic matrix of the biomass through application of chemical, physic-chemical and/or biological treatment, the compression and compaction characteristics can be improved. Thus mechanical milling, steam explosion, hot water washing, acid and alkali pre-treatments and ammonia fiber expansion, among others, have been employed as upstream unit operations to disrupt the complex polysaccharides which are reduced to low molecular components. The polymer becomes more cohesive in presence of moisture. The biomass structure thereby increases its porosity, removing lignin and/or hemicellulose, facilitating the biological conversion of biomass into bioenergy and bio-based products (Monlau et al, 2013).

The physic-chemical methods of pre-treatment comprise the steam explosion, the torrefaction and the microwave and radiofrequency (RF) heating. The chemical methods comprise the acid hydrolysis, the alkali hydrolysis, the use of oxidizing agents and the ozonolysis. Hydrolysis is the micro biological degradation of lignocellulose by enzymes, which is the first stage of anaerobic digestion. In this process the cellulase enzyme come into contact with cellulose, bonds effectively to its active site and begins to degrade the crystalline and amorphous regions of cellulose (Chen, 2015).

Biological methods do not require expensive instruments and equipment and high energy (Tabil, et al, 2011; Chen, et al, 2015) amount as the previous two methods. The biological methods use various types of rot fungi for removing lignin from the biomass. However, this method is very slow and has to be improved for commercial application.

Pre-processing and pre-treatment methods effect on lignocellulosic matrix at the level of molecules is not well understood. Application of the pre-processing methods, such as the size reduction or increasing porosity and pre-treatment techniques, have demonstrated an improvement in pellet cohesion resulting from the lignocellulosic component changes. Traditionally, the chemical analysis of each lignocellulosic component has been performed by

acid hydrolysis and gravimetric determination of lignin, and has provided highly precise data. However these methods are very laborious, time-consuming and expensive to perform (Tabil, et al, 2011).

Structural elements of many lignocellulosic materials react to pre-treatment, e.g. high mechanical pressure collapsing the natural vascular structure (see Figure 13); ambient or elevated temperatures cause the tendency of pentosans and hexosans to decrease the water-solubility with temperature; and some pre-treatments may permit lignin to become soluble on cellulose surfaces during the cool-down stage (DoE, U.S., 2006).

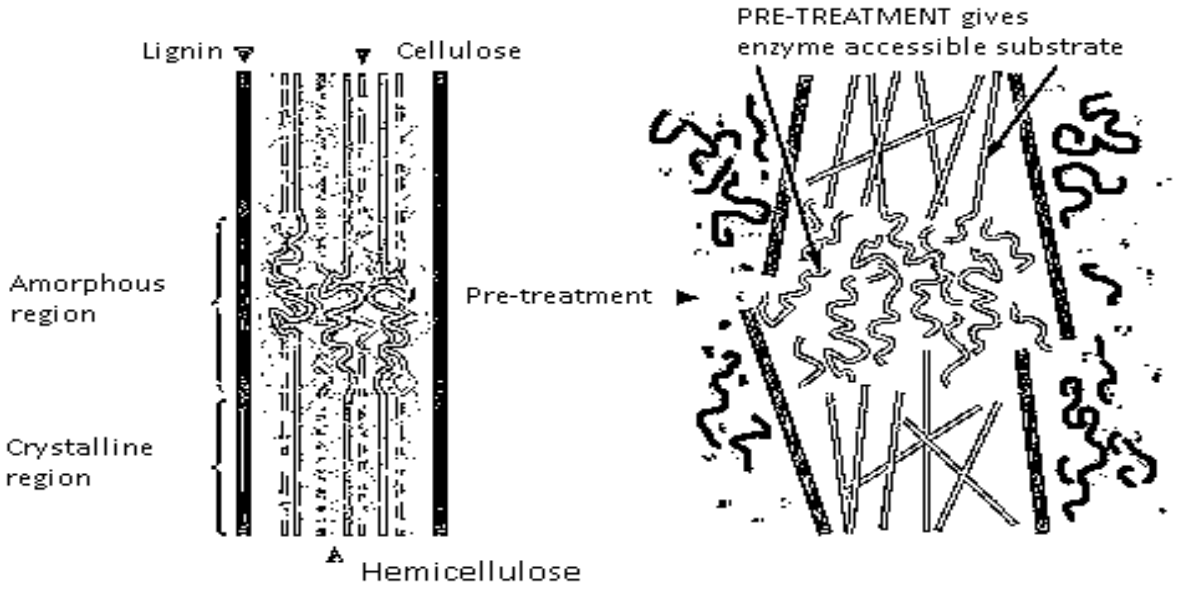

Figure 13: The biomass fibre structure, before and after pre-treatment (Antognoni, et al, 2013).

2.3.2. Pellet production technology

Manufacturing process is determined by raw material and usually comprises of these steps: the reception of raw material, the drying (optimal level 12% or less, final 6 – 8%), the grinding (milling, to size no more than pellet diameter ~ 6mm), the pellet-making (machines – extruders, flat or rotary type), the cooling (critical to pellet strength and durability, lignin solidification), the screening (passing through the vibrating screen to remove fine material), the sifting and packaging, the distribution and storage, as seen in Figure 14 (Karkania, et al, 2012). The pellet-making or densification is a process applying a mechanical force to compact biomass residues or wastes into uniformly sized solid shapes such as pellets, briquettes or logs. The aim of densification process is to increase the volumetric density from the initial 0.04 – 0.2 g cm^{-3} up to 0.6 – 1.4 g cm^{-3}, improving storage, handling and transport properties. The

final quality of pellets or briquettes depends on such factors as the fibre content, particle size, moisture content, temperature, feed rate, the size and shape of the die etc. (Chen, et al, 2015).

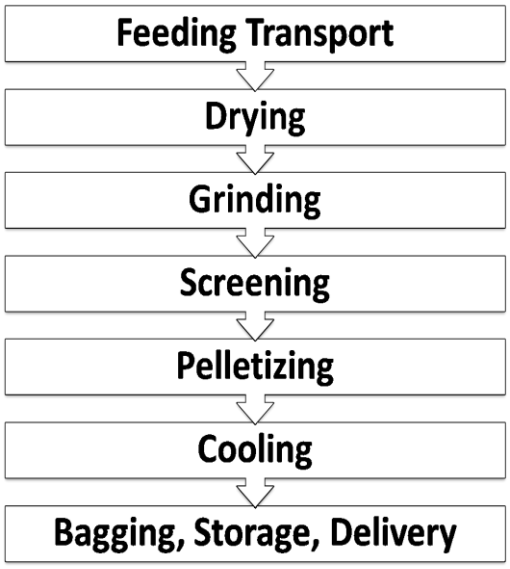

Figure 14: Manufacturing palletisation process (Chen, et al, 2015; Ciolkosz, 2015).

The method of densification (the compression in chamber presses) consists of two major stages, the pressing and the maceration. During the pressing process there is a very close correlation between the increasing density and increasing applied pressure in early stage of the compression but this correlation falls rapidly as the density of the pressed material approaches the density of water. The correlation is not so high in case of the density change and the degree of maceration (chopping, grinding and pulverizing) (Naik, et al, 2010).

The compaction technology consists of the piston press and the screw press. Most of the units are the reciprocating type, where the biomass is pressed in by a reciprocating ram in a die at a very high pressure. In screw extruder press, the biomass is extruded continuously by a screw through a heated taper die. The central hole incorporated into the briquettes produced by a screw extruder helps to achieve uniform and efficient combustion and these briquettes can be carbonized (Kurchania, 2012)

2.3.3. Particle size reduction and physical properties

The mechanical compression can influence the particle structure, including the porosity, the enzyme accessible surface area and texture, which are important parameters in the pre-treatment and the conversion processes. Although the impact of pellet-making on biomass digestibility has been studied, the influence and effects of mechanical compression on biomass particle structure have not been reported in previous literature.

The pre-processing operations, such as the particle size reduction or grinding, are important, to increase the surface area of the lignocellulosic biomass before densification. The particle size reduction increases the total surface area, the pore size of the material and the number of contact points for inter-particle bonding.

Because the agricultural biomass material from field does not have good flow characteristics and may not flow fluently to hammer mills or disc refiners, it needs to be

chopped with a chopper/knife mill/tub grinder to facilitate the bulk flow and the uniformity of feed rate. Chopping is often used for coarse size reduction (>50 mm) of the biomass.

Hammer mill grinding is used to produce wide range of particles. It is able to finely grind a greater variety of materials than any other machine. The mill performance is measured in terms of energy consumption, geometric mean diameter and particle size distribution of product (Tabil, et al, 2011).

To design efficient compression equipment, it is important to know the compressive properties such as the Poisson's ratio relative to the various particle sizes (Miao, et al, 2015).

2.3.4. Physical properties of biomass to briquette matter

2.3.4.1. Bulk density

To facilitate economic storage, transportation and handling of the material, the goal is to maximize the bulk density of agricultural matter. The bulk density is more dependent on the type of material used, than on the moisture content, grind size and pre-treatment.

2.3.4.2. Particle density

The particle size of grinds has direct effect on the final density of pellets. It can be as high as the particle density. The particle density as well depends on the biomass type, moisture content, grind size and pre-treatment. The particle density and hammer screen size are in negative correlation.

2.3.4.3. Geometric mean particle size and distribution

The size and shape of particles plays a very important role in the compression process. The biomass material of 6 – 8 mm in size with powdery component of 10 – 20% is giving the best result. When using oversized particles, the briquetting will not be smooth and clogging might take place at the entrance of the die resulting in jamming of the machine. The larger particles which are not conveyed through the screw start accumulating at the entry point and steam is produced due to high temperature (caused by screw rotation, heat conducted from the die and also if the material is preheated) inside the barrel of the machine starts condensing again. The processing conditions should be adjusted to suit the requirements of each particular biomass. Therefore, it is desirable to crush any larger particles to get a random distribution of particle size. An adequate amount of sufficiently small particles is present that will be embedded into the larger particles. The presence of different size particles improves the packing dynamics and also contributes to high static strength. Only fine and powdered particles of size <1 mm are not suitable for a screw extruder because they are less dense, more cohesive,

non-free flowing entities. (Kurchania, 2012). During the compression, smaller fine particles are reorganized and fill the void space of larger particles producing denser and durable compact forms. Ideally, grinds should be distributed normally, it means near zero skewness and lower peak than expected for normal and wider data. Decrease in biomass grind size has a positive effect on pellet mill throughput.

2.3.4.4. Frictional properties

Physical and frictional properties have a significant influence on the design of the new modification equipment. Frictional behaviour of biomass is described by two independent parameters: coefficient of internal friction and coefficient of wall friction. Classic law of friction states that frictional force, which is dependent on material nature in contact and independent of contact surface area or sliding velocity, is proportional to the total force. The friction properties are moreover influenced by the moisture content and the particle size. These coefficients are important for the design of production and handling equipment and storage structures (Tabil, et al, 2011).

2.3.4.5. Effect of moisture

The moisture aspect in relation to the feed biomass briquette-making, it is a very crucial factor. When the feed moisture is 8 – 10% the briquettes will have 6 – 8%. Having this moisture, briquettes are strong and free of cracks and the compression process is smooth. In case of higher moisture content (>10%), briquettes are poor and weak and the whole process is erratic. It is crucial to reduce the moisture content, because steam excess causes blockage of incoming feed from the hopper. On the other side, water as well plays role as film type binder by strengthening the bonds in the briquettes. Water also helps to promote bonding in the cellular matter by van der Walls' forces by increasing the true area of contact between particles. So water can be a success or failure medium of the compression process depending on its content. Appropriate amount of moisture develops self-bonding in lignocellulose substances at elevated temperatures and pressures prevalent in briquetting machines.

2.3.4.6. Temperature

Temperature is the next factor influencing the compression and the strength of briquettes. The changes of biomass temperatures can influence the briquette density, the briquette crushing strength and the moisture stability. The temperature in the extruder gradually increases. Both the internal and external friction cause local heating and the material develops self-bonding properties at elevated temperatures. Adding heat relaxes the biomass fibers and

apparently softens its structure simultaneously reducing resistance of such fibers to briquette-making thus reducing power consumed and increasing the production rate. However, the temperature should not be increased too high up to the biomass decomposition temperature (300°C) (Kurchania, 2012).

2.4.Mechanical properties influenced by quality parameters

Although production of pellets and briquettes is demanding additional energy input, pellet market has a rising tendency worldwide. The biomass pellets are cylindrical, 6 – 8 mm in diameter and 10 – 12 mm long, and wood pellets as fuel can be compared (in terms of trade volume) to biodiesel or bioethanol.

The equipment for commercial biomass densification, such as the pellet mills, the tools for other extrusion processes, the briquetting presses or roller presses are used to facilitate the feeding, handling, storing and transport problems (Hakeem, Jawaid & Alothman, 2015).

2.4.1. Quality parameters

Durability and density are the principal characteristics observed to describe physical properties and quality of densified solid biofuels such as pellets and briquettes (Zhang, et al, 2014).

2.4.1.1. Factors affecting strength and durability of briquettes

The strength and durability of the densified products depend on the physical forces that bond the particles together (Kalyian, 2009). In some experiments, the mechanical strength of the briquettes is characterized by the force necessary for its destruction, thus briquette is tested by exposition to the pressure force. This force is gradually increased until the briquette disintegration and splitting (Miao et al, 2015).

Understanding the particle binding mechanisms is important to determine which test should be used to measure the strength and durability of the densified products. The binding forces: solid bridges, attractive forces between solid particles, mechanical interlocking bonds, adhesion and cohesion forces, and interfacial forces and capillary pressure. These binding mechanisms have been observed for the densification of pharmaceutical powders, animal feeds and biomass materials (Kalyian, 2009; Tabil & Sokhansanj, 1996; Lindley & Vossoughi, 1989).

By application of high pressures and temperatures, solid bridges are developed by diffusion of molecules from one particle to another at the contact points. Solid bridges can be

formed between particles due to crystallization of some ingredients, chemical reactions, hardening of binders, and solidification of melted components. Solid bridges develop after cooling/drying of densified products.

Short-range forces such as molecular valance forces (i.e., free chemical bonds), hydrogen bridges, and van der Waals' forces, electrostatic, and magnetic forces can cause solid particles to adhere to each other if the particles are brought close enough together (Kaliyan & Morey, 2009).

2.4.1.2. Durability, density

Durability represents the measure of shear and impact forces that a pellet could withstand intact during handling, storing and transportation process (Tabil, 2011). Pellets durability remains in physical strength and resistance to being broken up. Durability is increased by moisture when water soluble compounds, such as sugar, starch, soda ash, potassium salt, sodium phosphate and calcium chloride are present in the feed. Compounds like starch, lignin and protein increase durability, while fat content results in low durability. Finally, particle size and process variables also influence durability values (Tumuluru, et al, 2011).

In research of Kaliyan[a, b] & Morey, 2009, they recognized that durability is influenced by particle size, moisture content and temperature, where the particle size and moisture content were the two dominating factors. The durability increased with decreasing particle size and moisture content. The effect of measured Poisson's ratio suggests that the matter of smaller particles (6 mm) has higher ability to withstand transverse stresses than the larger particles.

The pellet quality is usually evaluated on basis of its density and durability. Higher density presents higher energy potential per volume unit of material and the durability indicates the resistance of pellets to withstand the shear and impact forces applied during handling and transportation. Low durability results in problems like disturbances within the feeding systems, dust emissions and so on (Tabil, et al, 2011). In research of Kaliyan, et al, 2009 they as well recognized that the particle size, moisture content, and pressure significantly affected the density. The particle sizes containing moisture are the dominating factors – the briquette density increases with decreasing the particle size and the moisture content.

Next parameters are the energy content, moisture content, volatile matter, ash content and slagging characteristics, reactivity, size and its distribution and bulk density (Tabil, et al, 2011). All these parameters are measured from the aspect of the energy potential, however, that's not the topic of this thesis thus we shall not deal with this issue further.

2.4.1.3. Unit and bulk density

These parameters are important for storage and transportation. Materials with higher moisture and larger particle size have reduced the unit and bulk density, while higher process temperatures and pressures increase both the densities. It was observed that high unit dryness corresponds to high compression strength (Tumuluru, et al, 2011).

2.4.1.4. Moisture content

When initial moisture content is >15% and pressure >15 MPa, it has negative effect, cracks occur on the final product. On the contrary, moisture <5% results in a profit loss as pellets tend to break up creating more fine particles during the storage and transportation.

2.4.1.5. Percentage of fines

Fines are generated during transportation and storage by the destruction of the densified products and their presence is not desirable. Occurrence of fines increases by processing under suboptimal conditions.

2.4.1.6. Calorific value

Typical calorific value of wood- and straw-based pellets and briquettes are from the range of 17 – 18 MJ kg^{-1}. This value is dependent on the process conditions, such as the temperature, particle size and biomass pre-treatment (Tumuluru, et al, 2011).

2.4.1.7. Compressive strength

The compressive strength, more than other properties, is influenced by certain factors. Regression model shows that the particle size and the moisture content are the two dominating factors.

2.4.1.8. Impact resistance

Particle size and pressure were the key factors. Durability increased with decreasing particle size and increasing pressure.

2.4.1.9. Sorption properties

Sorption properties are influenced by the grind size; they can absorb moisture more readily than large particles and produces higher quality pellets and therefore, undergo a higher degree of conditioning. In addition, finer grinds have higher surface area of contact to form bonds/solid bridges during the compaction processes. Also, large particles are the fissure points that cause cracks and fractures in compacts. A reduction in hammer mill screen of the size from 3.2 to 0.6 mm can result in an increase of the pellet densities from 5 to 16% (Kaliyan and

Morey, 2006; Kashaninejad, Tabil, & Knox, 2014; Mani et al, 2004). However, no significant trend in the density variation was observed at the geometric mean for particles of 0.6 mm in size and smaller (Kaliyan and Morey 2006b; Mani et al, 2002). The pellet density variation depends on the biomass type (Tabil, 2011).

2.4.1.10. Quality parameters summary

The particle size and the moisture content are two dominating influencing factors where the pressure had the lowest influence, its contribution was minimal. Reducing the particle size led to increased density, durability, impact resistance and decreased compressive strength. This is supported by micrographs (the particle size significantly influences the physical properties of the briquette). The structure is than more porous (1.25 – 2.5 mm) than (<0.16 mm) which results in the increase of air volume between the particles and in the decrease of the density. Application of high pressures causes solid bond formation by short-range forces (i.e. the hydrogen bonds, van der Waals' forces and magnetic forces). Also certain inter-molecular attractive forces can cause particles to adhere to each other and form strong bonds between bordering particles if they are pressed close enough together (Zhang, et al, 2014). In case of larger particles, mutual interlocking can occur forming interlocking bonds (Kaliyan, et al, 2009).

Performed tests: moisture content, pressure, and particle size plotted (input variables) against briquette density, durability, compression, strength and impact resistance (responses). The ANOVA test showed that particle size and pressure significantly affected the compressive strength, as well as the particle size and the pressure interaction (Zhang, et al, 2014).

The compression parameters of agricultural biomass vary with different applied pressures. It is important to understand the fundamental mechanism of the biomass compression process, thus to design energy efficient compaction equipment mitigating the cost of production and enhancing the quality of the product (Mani et al, 2004). To a great extent, the strength of manufactured pellets depends on the physical forces that bond the particles together. These physical forces come in three different forms during pellet-forming operations: a) thermal; b) mechanical; and c) atomic forces as illustrated in Figure 15 (Adapa et al, 2002).

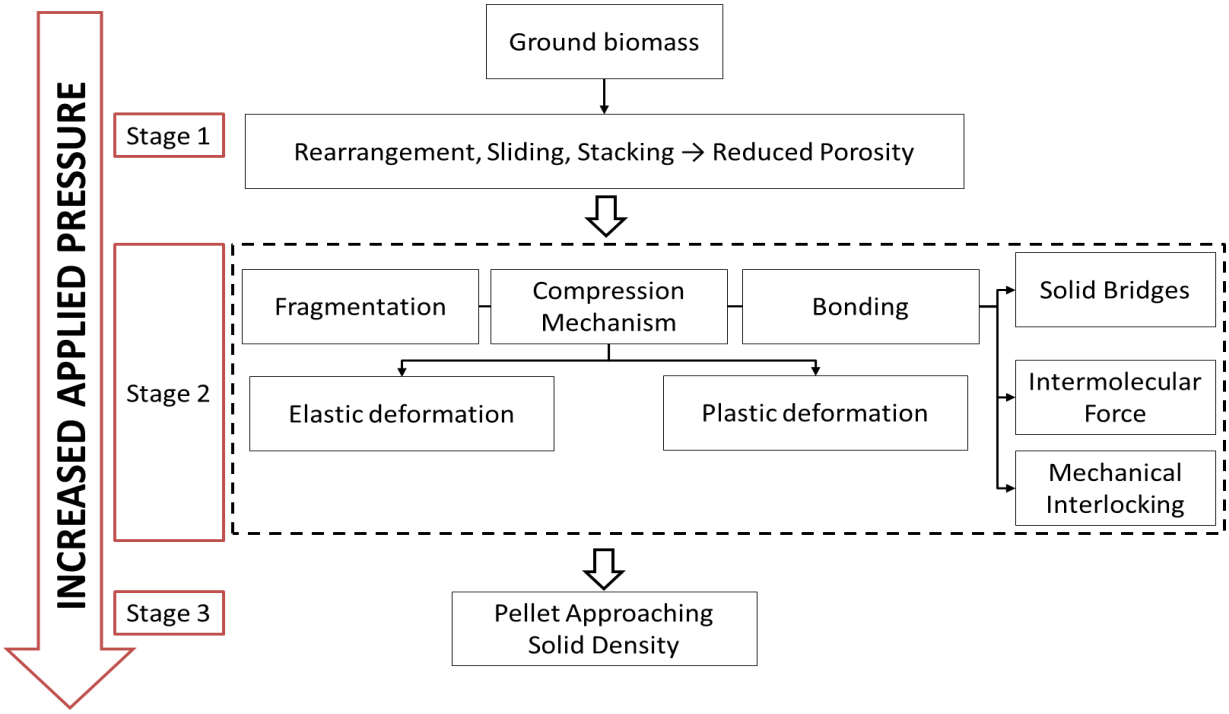

Figure 15: The deformation mechanisms of particles under compression (Comoglu, 2007; Denny, 2002).

2.5. Image analysis

In many sectors of industry is necessary to know and consider such fine and small particles such as coal and charcoal fines, nanostructures and even biomass particles. Therefore, more knowledge is needed about structures and polymer organization. Imaging and image analysis help to gain this information.

Image analysis method is a universal and accurate measuring method, which allows comparing and quantifying texture elements of different materials. The aim of the image analysis is to formulate information on material by using quantitative data, like particle size distribution in graphic or numeric form, or the mean value of monitored variables (Černá et al, 2015).

The task of setting particle size specification for material requires knowledge about what technique should be used for the analysis. In general, different particle sizing techniques will produce different results for a variety of reasons, e.g.: physical properties, algorithm used, basis of distribution (number, volume) and range of equipment. The dynamic image analysis uses techniques such as particle counting or sieving.

Static image analysis – with this system a microscope and digital camera collect images of biomass particles as the slide is scanned. Processing steps are then made using appropriate software.

The dynamic image analysis – utilizes many of the same steps as the static image analysis with few exceptions. The sample is moving during the measuring, so its preparation should improve the processing ability of the sample (Scientific, 2012). This measurement is not case of this study, thus we will not go in detail here.

Using the image analysis we can measure and define numerous parameters referring to the particle size. The definitions of these parameters and the ways how the program measures them can differ. Basically, the image analysis is based on two-dimensional images of particles.

The dimensions (Figure 16) often used in the image analysis are the minimum and maximum Ferret diameters, the maximal projected area of the particle representing the longest and intermediate dimensions of the particle; the smallest projected areas are representing the intermediate and shortest dimensions of the particle. The maximum and minimum projected areas of a particle may not always be perpendicular. Next, the particle axes as the axes of equivalent ellipse oriented at right angles are defined and the longest and the intermediate axes as the lengths of the longest and shortest sides.

The "size" of particles is a complex parameter. The IA accurately measures several parameters that can be defined as "the particle size" in contrast to the traditional sieve analysis, which does not directly measure the axial dimensions of particles. The sieve size depends upon the particle's overall shape; in particular on the shape of the particle's minimum projected area. Moreover, the IA is not dependent upon the correct estimation of the particle volume or mass. The grain-size distribution curves are normalized with respect to mass, i.e., cumulative mass

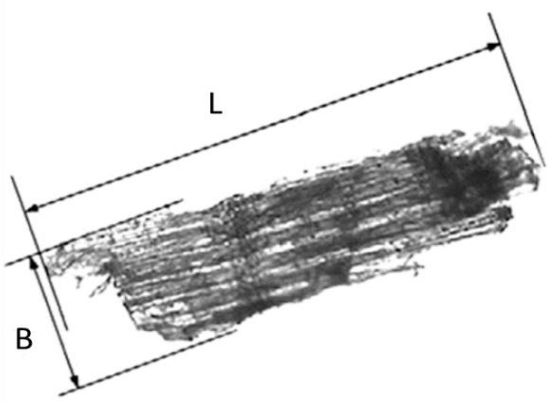

Figure 16: Biomass particle dimension measuring, where L is length and B is width (Guo, et al, 2012).

percentage, and so the mass per se has a very little influence on the results. The disadvantage of the IA against the sieve analysis is lacking the Y-axis as the height dimension resulting in the impossibility to measure volume of a particle as a three dimensional object. Much of the current research in the field of the image analysis is striving to establish better methods of volume determination, where the most important factor for accurate transposition of the IA results to the sieve method results is the IA measuring of such particle parameter which is related to sieving. Most of the existing transposition methods of the IA results to the sieve results do not take into consideration the width to thickness relationship or the shape of the particle. If the intermediate and the shortest axes are similar in length, the particle will not pass the sieve diagonally and thus the IA size would be the same as the sieve size.

The overall shape of the minimum projected area of a particle has to be considered to use the adequate method of transposing the IA size to the sieve size for each particle.

In new research approaches, the minimum bounding square was successfully tested showing good correlation between the sieve size and the image analysis size based on the minimum-bounding square. This new function, together with the axial lengths, gives a very detailed quantification of particle size distribution. This method translates the image analysis results to the sieve results, and at the same time allows numerous qualities of each particle to be evaluated. The advantage of this application is the use of comprehensive information provided by the image analysis instead of merely using the sieve size. However, it is important to determine the sieve size. With the image analysis we can link the sieve size to many other dimensional aspects of particles (Fernlund et al 2007).

2.5.1. Particle size analysis and particle size distribution

As already mentioned the particle size influences many properties of particulate materials and is an important indicator of quality and performance. The size and the shape influence the flow and the compaction properties. For these and other reasons, it is essential to measure and assess the particle size distribution of many materials. Lab measurements take part during the size reduction operations like crushing and homogenization, etc. Also the separation steps, such as the screening and the filtering should be monitored before and after the process.

When measuring the size we can recognize spherical particles, which can be described by one number – the diameter, but this is not the case of this study. Non-spherical particles can be described by the length and the width. These techniques provide more accurate and complex results. Problems can arise at particles with large aspect ratio, such as fibres or needles. Each

measurement technique detects size by using a particular physical principle. But the only techniques that can describe particle size using multiple values are the microscopy or the automated image analysis. This system can describe the non-spherical particle using the longest and shortest diameters, perimeter, projected area, etc. In particle size distribution, for any elongated and fibrous particles the x axis is typically displayed as length rather than the equivalent spherical diameter (Scientific, 2012).

Most often, the first measurement is the projected two-dimensional area - *S*. The area of a particle is calculated as a sum of areas of each individual pixel within the borders of the particle. Note that the units of *S* are given in pixels, but assuming the system has been calibrated in millimeters, the area may then be converted to units of mm^2.

Length (L) and Width (B)

The length is the maximum distance between any two points at perimeter of a particle parallel to the major axis. Likewise, the width is the maximum distance between any two points at perimeter of a particle parallel to the minor axis. The units for length and width are most often expressed in μm. The length and the width are illustrated in Figures 16 and 17.

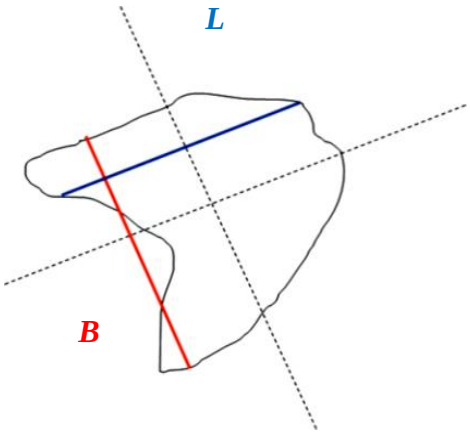

Figure 17: The length and the width projection in image analysis (Olson, 2011).

Beside the image analysis, the sieving test is used to determine the size distribution. For graphical plotting of the sieving test results it is advised to assess their full significance. Many methods of have been developed over the time, the most plotting of the relation of the cumulative undersize (or oversize) over the particle size. For this purpose, various combinations of axis scales can be used (linear, logarithmic and double-logarithmic). Most documents used the Rosin–Rammler (RR) and the Gates–Gaudin–Schuhmann (GGS) function to describe the size distribution. We have chosen the Rosin-Rammler plot as the most

convenient; and as a tool for the RR plot creation, we used the MATLAB® software, which is a powerful, high-level programming language and interactive environment exploited in many fields of scientific and engineering activities.

The tool of RR distribution can assist to evaluate the size distribution analysis results. It is used to determine and calculate the size distribution of particular material parameters and to calculate the percentage of material retained by the mesh size and vice versa (Brezani & Zelenak, 2010).

These analyses have been calculated using the distribution function F (ϕ) (mass fraction) and density function f (ϕ) (number of particles retained between two given mesh sizes) (Macías-García, Cuerda-Correa Díaz-Díez 2004).

The particle size distribution parameters based on the image analysis include the mean, arithmetic and geometric mean values. According to Bitra et al, 2009 the Rosin–Rammler equation stands as follows:

$$M_{cu} = 100 \left[1 - e^{-\left(\frac{D_p}{a}\right)^b}\right] \quad 1.$$

where $\mathbf{M_{cu}}$ is the cumulative undersize mass [%]; $\mathbf{D_p}$ is the particle size assumed equivalent to nominal sieve aperture size [mm]; **a** is the size parameter or the Rosin–Rammler geometric mean diameter [mm]; and **b** is the distribution parameter or the Rosin–Rammler skewness parameter (dimensionless). In basic conditions, the equation is:

$$R(d) = 100 \cdot e^{\left(\frac{d}{d'}\right)^n} \quad 2.$$

where: **R(d)** is the cumulative percentage of material retained on the screen; **d** is **the** mesh size, **d'** is the specific dimension of the mesh size on which % wt. of material is retained. This parameter can also be used to determine, whether the material is fine or coarse. Function **n** is the uniformity parameter characterizing the material based on the proportional content of individual size classes in the overall size distribution. The plot diagram of this function (Figure 19) is linear in case of special curves used - logarithmic vs. double logarithmic scale. Functions determining the individual parameters are part of the tool as well (Brezani & Zelenak, 2010). Figure 18 shows how the data is entered to the MATLAB® graphic application. To create the RR diagram the following data are needed: the mesh size with corresponding unit percentage of passing particles and percentage of particles retained on the sieve. From this information the MATLAB® is able to calculate and create the plot diagram.

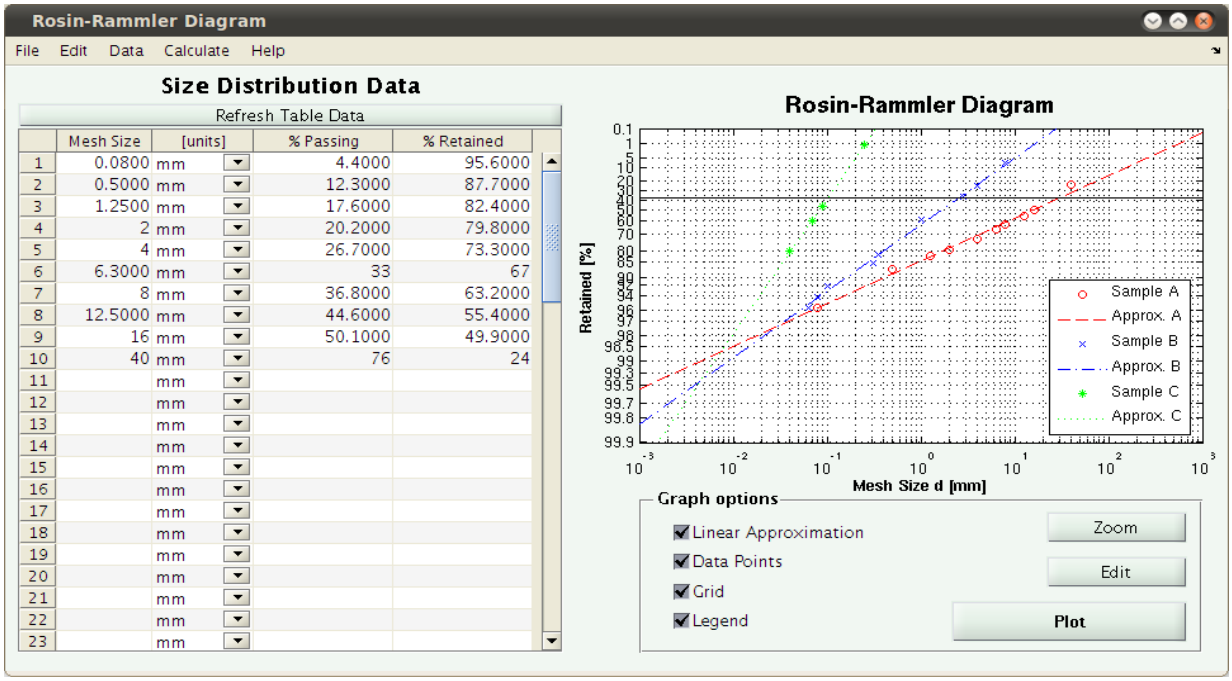

Figure 18: The MATLAB® plot diagram creation (Brezani & Zelenak, 2010).

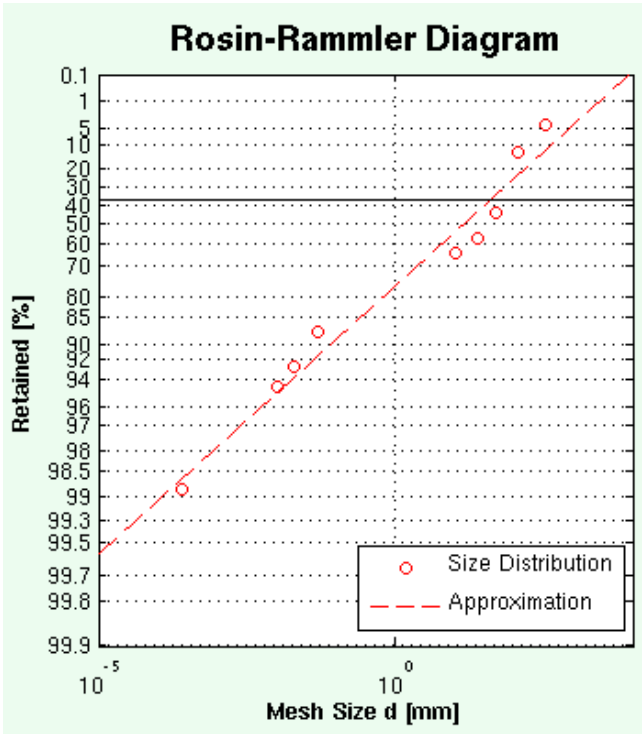

Figure 19: Example of the Rosin-Rammler distribution plot (Brezani & Zelenak, 2010).

Needle-like mineral particles can be compared geometrically to approximately ideal cylindrical rods. The aspect ratio A of a particle is defined as the ratio between its largest dimension and smallest dimension, which - in case of the rod of **length L** and **width B** - can be expressed as:

$$A = L/B \qquad 3.$$

The surface area SA of one such rod-like particle is given by:

$$SA = \left(\frac{\pi \cdot B^2}{4}\right) + \pi \cdot B \cdot L \quad 4.$$

The specific surface area (SSA) ε for a single particle is defined as:

$$\varepsilon = SA/M \quad 5.$$

where M is the mass of the particle having the surface area SA (Gantenbein et al 2011; Guo et al, 2012).

Particles were analyzed as the biomass changed. The reduction process changes the particle size and shape, increases the bulk density, improves the flow properties, increases the porosity, and generates new surface area. Larger surface area increases the incidence of contact points for chemical reactions and the capacity to adsorb water in higher volume, which may require grinding to a nominal particle size of about 1 mm. Efficient size reduction enables proper particle size distribution, though there is insufficient information to predict the particle size distributions for most of the newly considered biomass sources.

Rosin and Rammler with their equation started finding suitable mathematical functions to describe particle size distribution. This equation proved as a universal law of size distribution valid for all powders. The Rosin–Rammler function has proven as the best function based on the analysis of variance among at least three common size distribution functions, which are the log-normal, the Rosin–Rammler and the Gaudin–Schuhmann functions tested on different fertilisers (Bitra, Womac, Chevanan, Miu, Igathinathane, Sokhansanj Smith 2009).

For irregularly-shaped, non-spherical particles the size characterization must include information on the type of particle shape beside the diameter measured. The image analysis is used for the interpretation of such non-spherical or irregularly shaped particle information. Time constraints and the elaborateness may limit the use of the image analysis so the technique will probably never be faster than the laser diffraction or the sieving analyses. There may be situations where a single particle size value is insufficient to properly characterize a material (Olson, 2011).

Particle size analysis gives a variety of approaches to the result reporting. Result than can be expressed by one number – the average size, but a single number cannot describe the distribution of the sample. So there is better way to express the result: it is to report both the central point of the distribution and one more value to describe the width of the distribution. With regards to the particle size measurement, the most common quoted statistic information is the linear dimension of symmetrical peak tendency, most often of an equivalent circle or sphere (i.e., the mean, median, or mode equivalent spherical diameter of a particle size distribution)

(Olson, 2011). There are central values, which is important to define their terms for correct use in both statistics and the particle size analysis. The distribution can be symmetrical and non-symmetrical, bimodal, normal and Gaussian distribution shown in Figures 20 and 21.

2.5.1.1. Mean

The mean is the arithmetic average of data, the geometric mean. This value is associated with the distribution calculation (number, surface and volume). The best way to illustrate this value is a histogram chart, which shows upper and lower limits of n size channels beside the percentage.

2.5.1.2. Median

The median is a value of particle size, which divides the sample group exactly to two parts, for example, there is 50% above some value and 50% below. The median describes the volume distribution, the count distribution and the surface distribution and belongs to one of the easier statistics to understand and the most useful for particle size distribution.

2.5.1.3. Mode

The mode is the most common value of frequency distribution, the peak in the distribution. It represents the particle size (range) most commonly found in the distribution. The mode is not as commonly used, but it is descriptive, if there is more than one peak to the distribution, it determines the mid-point of different peaks (Scientific, 2012; Rawle, 2003).

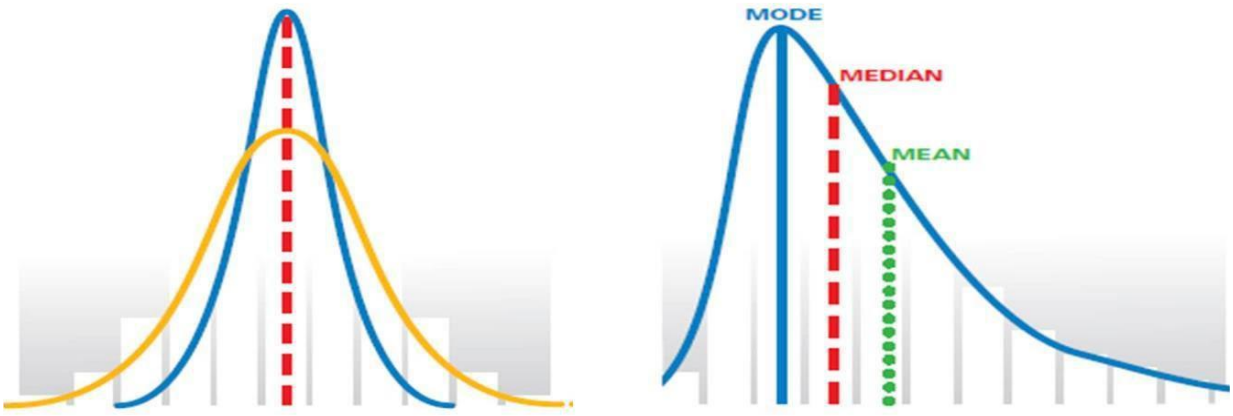

Figure 20: Left-symmetric distribution, where mean=median=mode; Right-non-symmetric distribution, where mean, median and mode will be three different values (Scientific, 2012).

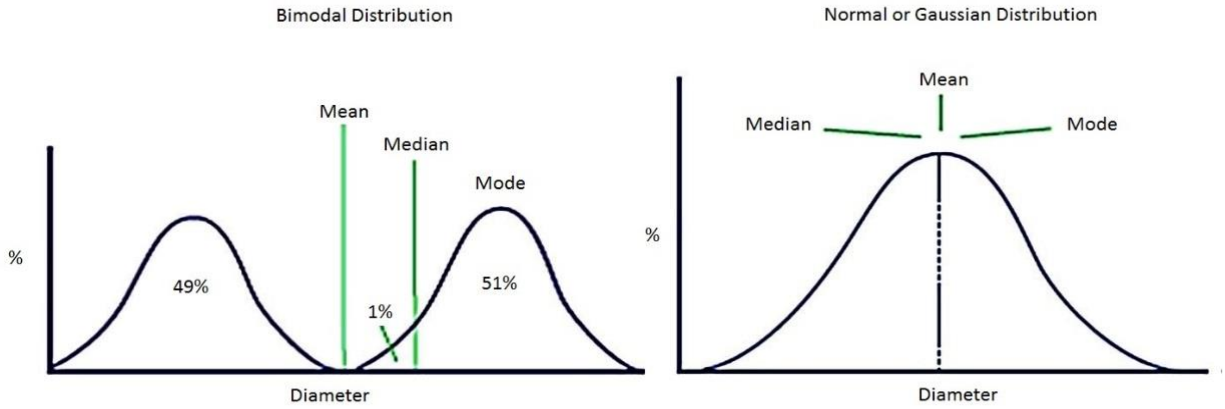

Figure 21: Bimodal, Normal and Gaussian distribution / mean, median, mode (Rawle, 2003).

2.5.2. Particle shape measurements

Shape measurements can be made after obtaining all digitally defined edges of the imaged particle. Among many parameters, the aspect ratio is calculated. It is defined as the ratio of the Feret's minimum length to the Feret's maximum length as given below.

$$A = \frac{x_{Fmin}}{x_{Fmax}} \qquad 6.$$

Thus, the width and length of the shape are nearing the same value. It does not mean the shape is circular; a perfect circle has an aspect ratio of 1.0 (Figure 22, shape 1). Very symmetrical shapes also have a very high aspect ratio. For example, shapes 7, 12, 14, 15, 21, and 20 all have aspect ratios >0.95 as measured. As the measurements of the width and length of certain shape diverge, the aspect ratio approaches zero. Examples of this are given by shapes 2, 3, 4, 5, 6, 8, and 9, which all have aspect ratios ≤ 0.25.

Shape 17 from a geometric point of view is interesting, the width should be one diameter and the length should be two diameters, the aspect ratio (Chart 5) is 0.5. Shape 10 is a common shape particle often seen in crystals that are aggregated. The result of so called twinning for most types of aggregation is the measured aspect ratio, which is larger than the A of individual particle. Shape 10 (twinning) can be compared to shape 8 (long rectangle), in which the aspect ratios were 0.49 and 0.10, respectively (Olson 2011).

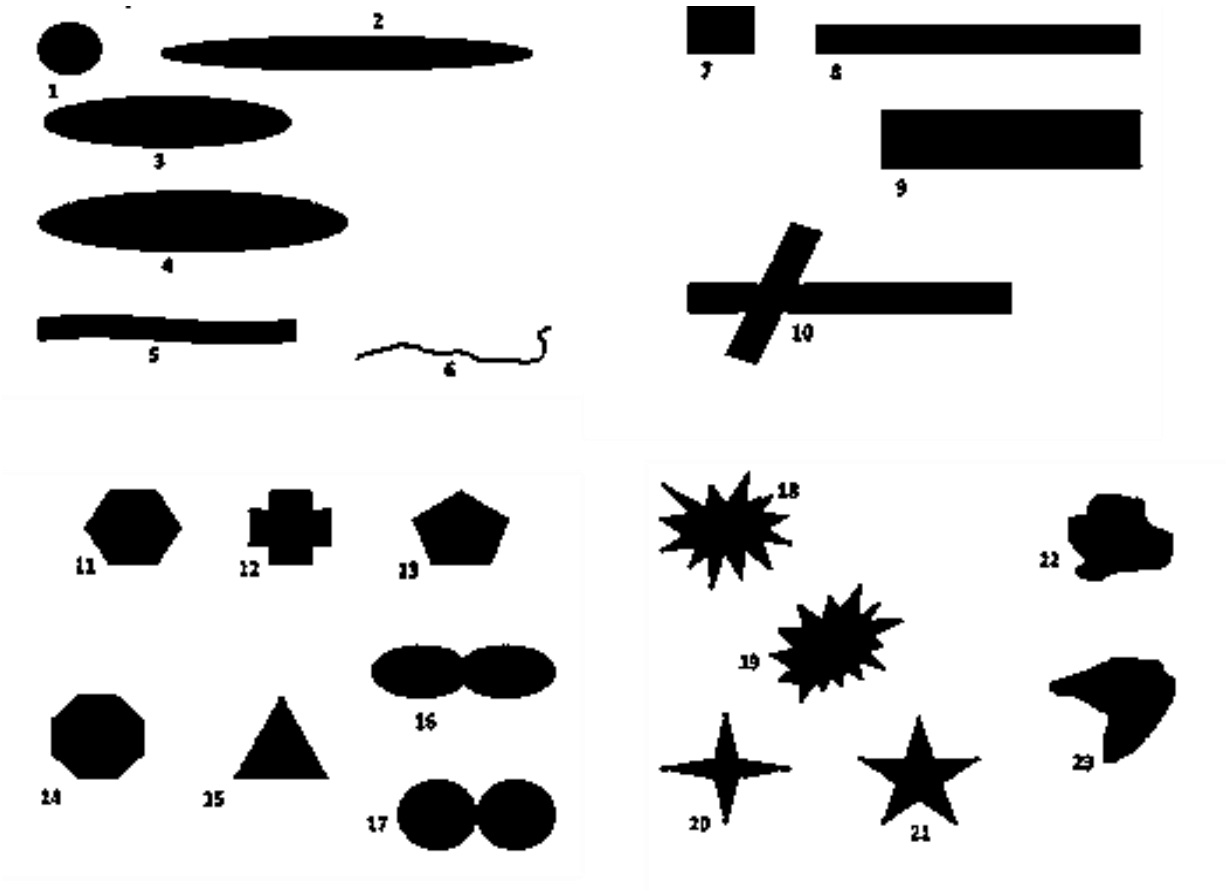

Figure 22: Various particles shapes (Olson, 2011)

Particle Shape can be also defined as:

Acicular - needle-shaped
Angular - sharp-edged or having roughly polyhedral shape
Crystalline - freely developed in a fluid medium of geometric shape
Dendritic - having a branch- shaped crystals
Fibrous - regularly or irregularly thread-like
Flaky - plate-like
Granular - having approximately an equidimensional irregular shape
Irregular - lacking any symmetry
Modular - having rounded, irregular shape
Spherical - global shape

Table 5: Aspect ratio of different particle shapes (Olsen, 2011)

ID	Shape Description	Aspect ratio	Circularity
1	Circle	1	1
2	Torpedo	0.10	0.49
3	Long ellipse	0.22	0.69
4	Medium ellipse	0.23	0.71
5	Ribbon	0.11	0.49
6	Fiber	0.20	0.14
7	Square	1	0.89
8	Long rectangle	0.10	0.51
9	Medium rectangle	0.25	0.71
10	Twinning	0.49	0.45
11	Regular hexagon	0.90	0.95
12	Symmetric cross	1	0.79
13	Regular pentagon	0.86	0.93
14	Regular octagon	1	0.97
15	Equilateral triangle	1	0.78
16	Peanut	0.33	0.77
17	Touching circles	0.50	0.75
18	Star	1	0.42
19	Star	0.81	0.49
20	4-points star	0.96	0.45
21	5-points star	0.98	0.52
22	Random shape	0.94	0.86
23	Random shape	0.92	0.79

At the research of Guo et al, 2012, a particle shape has been described, which was needle-like shape with large aspect ratio. The aspect ratio in study of Guo et al, 2012 was in range of 2 – 9, which refers about the shape. The aspect ratio was calculated according to equation 3. The bigger the Aspect ratio the bigger the particle length dimensions.

2.5.3. Image J

In this study, two types of software were used for particle dimension measurement. Firstly, it was the ImageJ software. However, some functions were missing and secondly, the lab equipment used the NIS elements software, which I find more user friendly.

After capturing the particle by a camera or the charge coupled device (CCD), the image is transferred to pixels. The pixel is than defined as the smallest unit of light. The pixel is of

rectangular or square shape, the construction unit of the image, which can be recreated by certain devices. Pixels contain two parameters - the location and the intensity. Depending on the camera features, image can be in colour or black and white. The intensity of white light than determines the greyscale. The value of zero indicates no presence of white light, hence it is black; and the value of 255 indicates the highest intensity of white light. Values between 0 – 255 represent the shades of grey. The edge of a particle is defined by thresholding. The threshold defines the surpassed edge of a particle by which it is indicated. The thresholding is a process that may lead to biased data. An image in the threshold can be too low (known as erosion). As the threshold is decreased, more of the particle edge is eroded. Because erosion eliminates pixels from the actual particle edge, the general effect is a bias of the data towards the smaller size (Olson, 2011).

A program for basic image analysis known as Image J is a very efficient tool for measuring particles dimensions is–. This freeware is a program developed by the National Institutes of Health and it is designed specifically for processing and image analysis based on the Java. This program is able to calculate the areas and the pixel statistics in user-defined selection. The Image J allows to measure distances, angles, can create histogram line profiles and other features. The biomass properties of individual particles play an important role, because it influences the properties of the final product (Černá et al, 2015).

2.5.4. NIS elements

The NIS-Elements is an integrated software imaging platform developed by the NIKON Company used in laboratories, research centres, and at universities, where image analysis is needed. It features the microscope control, the image capturing, the documentation, and the image analysis and data management.

There are three levels of NIS-Elements according to how demanding tasks shall be done:

- Advanced Research (Ar)
- Basic Research (Br)
- Documentation (D)

The functionality of each of them can be further extended by additional modules. For the purposes of this thesis, the Advanced Research level software was used for measuring which is optimal for advanced research applications, featuring fully automated acquisition and device control and a wide range of image analysis functions (Nikon Instruments, 2016).

3. Objectives and Hypotheses

The aim of this research was:

Finding and/or quantification of the relation between the **texture of biomass briquettes and their durability and hardness** of shape during manipulation, storage and use.

Specified: to investigate an influence of biomass particle size in relation to biomass particles durability and hardness of the briquette.

This is a part of wider specialization on identifying and quantifying the texture of the material of most the microscopic particles of biomass except the smaller ones.

The secondary, related objectives were:

- to compare the size distributions of different digestate samples (and of different materials, if possible);
- to observe the shapes of particle and establish the prevalent dimensions;
- to identify the relation between the briquette density and its texture,
- To quantify, when applicable, the relation between the material type and its water sorption under different conditions.

The basic hypothesis of this work is based on the presumption that a briquette **texture is dependent on many parameters** of quantified values (type of material, moisture content, eventually chemical composition, size of particles, porosity of material, way and conditions of briquette processing, the storage environment and time, etc.). While for the same type of material of briquettes we can obtain significantly high variability of briquette properties. For example, just the mere **change in the size or conditions** during the production process can cause quality fluctuation.

From this side of view, the texture of briquettes is a complex variable, of which we were trying to determine the **importance of each component** in relation to chosen properties of the briquette.

Our goal was to find and establish the relation between the texture, the durability and the shape stability during storage. To reach these objectives, the method of image analysis was used in comparison to the size analysis and additionally the mechanical measurement.

4. Materials and Methods

4.1. Place

The digestate samples used in this thesis were supplied by the Research Institute of Agricultural Engineering, p.r.i., (VÚZT v Praze) - from their biogas plant. The briquettes pressed from the digestate were produced at the faculty of engineering of the Czech University of Life Sciences Prague (CULS Prague). The image analyses of particles was possible thanks to the image analysis laboratories at the Faculty of Forestry and Wood Sciences, CULS Prague. All the remaining laboratory tests and experiments were conducted in the C63 lab of the Faculty of Tropical AgriSciences, CULS Prague.

4.2. Materials used

The primary material used for this research was the digestate in a solid form. The choice of this material arises from the digestate availability and from the consistency with the diploma thesis research, which showed good results. Moreover, the digestate came up as a useful material in agriculture and thus it deserves more attention.

4.2.1. Digestate samples

The digestate was obtained from one experimental biogas plant. The feedstock material for anaerobic digestion was 40% maize (green plant stems), 20% grasses and the maize silage, clover and alfalfa fodders. The sample was dehydrated and separated to solid and liquid part after the AD. After mechanical dehydration, the sample was additionally dried in laboratory conditions to lower its moisture content (max. 14.5%) required for pressing purposes. Most of the dried digestate, (moisture content 13% and 18%) was compressed to briquette form and the uncompressed rest of the digestate (of moisture content 9.5%) was used for the sieve and the image analysis to assess the size distribution of particles.

The nutrient composition of the solid matter was also analysed and the results are presented in Chart 7 (Results). The digestate matter was not size-treated after the digestion, because the biomass matter is disintegrated before the AD process. All measurements were conducted under the laboratory conditions, with the ambient temperature of 20 – 22°C and the humidity of 45 – 60%.

4.2.2. Designation of samples

The main sample designation was D3. This matter was sieved and divided to sub-samples according to diagram in Figure 23. Thus D3 is the initial dried matter of the digestate, which has been sieved through a square sieve mesh (size of 8.7 mm). Particles that did not pass the sieve holes were designed as D3-I; those particle which passed through were designed as D3-II-0. The same system was applied to particles that did not pass the mesh of 3.8 mm holes (D3-II-A) and particles smaller than that mesh holes were marked D3-II-B. Particles bigger than

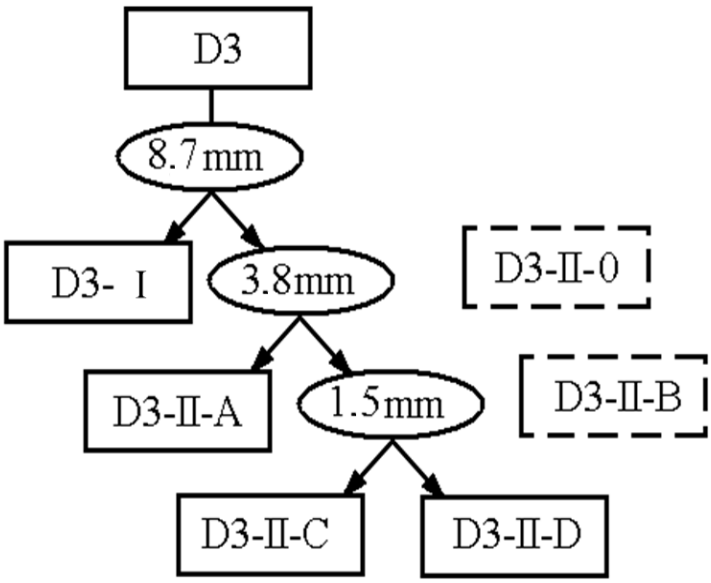

Figure 23: Division and designation of D3 digestate matter.

1.5 mm were retained and marked as D3-II-C and smaller particles D3-II-D. Thus particles were divided by the sieve analysis to categories >8.7 mm, 3.8 – 8.7 mm, 1.5 – 3.8 mm, <1.5 mm (Chart 6). The next digestate sample D4 was separated the same way.

Comparative samples for the previous tests were also made and designated as D1 (sieve mesh size – 1 mm) and D2 (not sieved). These samples are of the same composition as D3, the difference is in the size of the solid matter particles.

Table 6: Particles sizes scaling for D3 sample.

SAMPLE	MESH SIZE [mm²]
D3-I	>8.7
D3-II-A	8.7-3.8
D3-II-C	3.8-1.5
D3-II-D	<1.5

The sample of crushed plant *Miscanthus Giganteus* L. (MG) was processed the same way. The crushing process took place in the 9FQ40C hummer biomass crusher, equipped with circular-hole sieve mesh of 8 mm in diameter. Woodchip briquettes (WCH) made of spruce (*Picea abies* L.) compressed under the same conditions as the digestate D1 and D2 have been used as a comparison material for sorption properties measurements.

4.3. Material processing

Following the basic division of the material the digestate, the matter marked D3 and D4 were separated by the AS 200 sieving machine to various size fractions using square sieve meshes of 0.1, 0.25, 0.5, 1.0 and 2.5 mm (see Figure 24). Particles smaller than 0.1 mm were collected in a bowl. The weight ratio of each size fraction was expressed as a percentage relative to the weight of the initial sample.

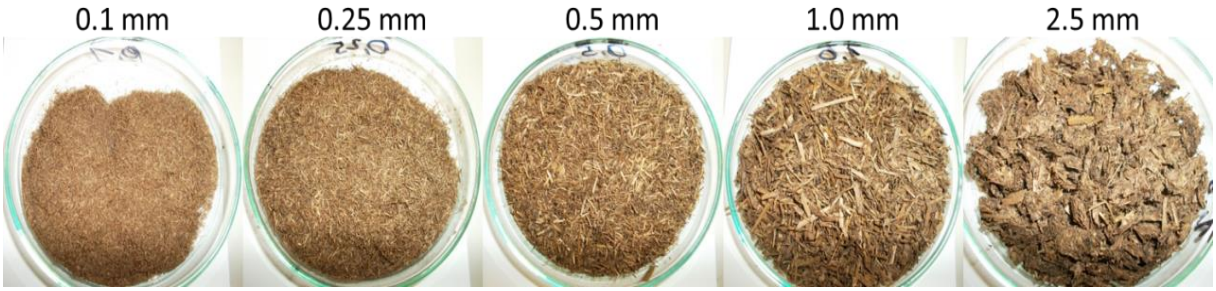

Figure 24: Digestate particle size fractions.

Before pressing the digestate material to the briquette form, the sieve analysis was conducted. This test was implemented to assess the particle weight distribution for each size fraction corresponding to the sizes of the sieving mesh. After this stage, the mean values from five repeating sieving procedures were recorded; one procedure lasts 10 min without interruption.

The briquettes were produced (Figure 25) in compliance with the International Standard EN ISO 17225–1:2015 by hydraulic piston press BrickStar model CS25; made by the Bricklis Ltd. Company, using the pressure of 12 MPa. The briquette diameter was measured ranging between 65 and 67mm.

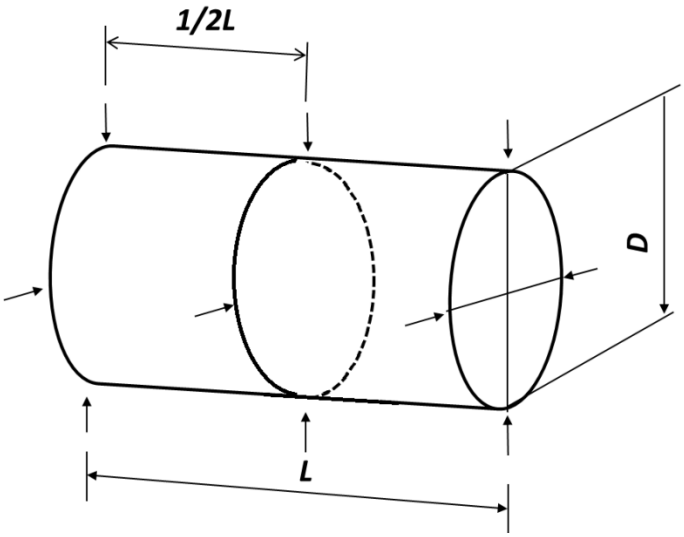

Figure 25: Produced briquettes of D~6.60cm and L~4.30cm.

4.4.Measuring

4.4.1. Durability and abrasion rate

Mechanical durability of the briquettes was measured according to the European Standard EN 15210-2:2011. The durability (DU) test was performed in dustproof rotating drum powered by electricity and equipped with a partition wall. The drum construction is shown below in Figure 26.

The minimum mass of tested group of samples is stated to 2 ± 0.1 kg, unfortunately due to lack of material, some samples are under the limit. Test duration time has been set to 5 minutes, which corresponds to 105 ± 0.5 rotations (21 rotations per minute) of drum; a special bowl was used to collect the abrasion residue from the briquettes after the testing, which was weighted as well.

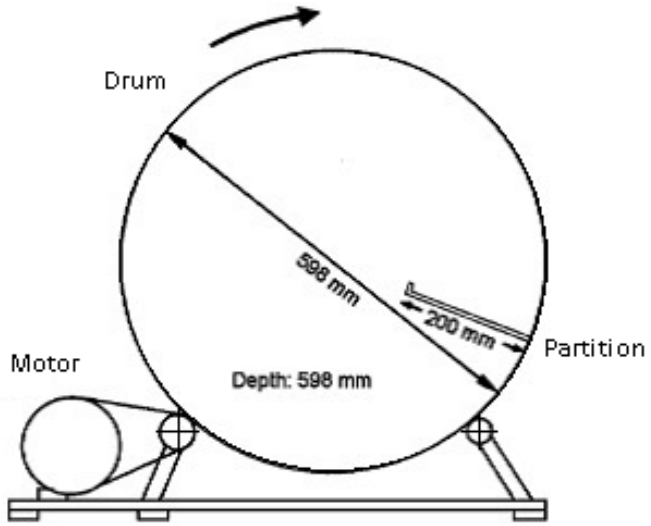

Figure 26: Durability test drum (Kaválek, Havrland & Pecen, 2012).

Durability test of the D3 and the D4 digestate briquettes was performed for briquettes with moisture content of 5.1–5.5%. The abrasion rate expresses the cohesion of the briquettes in relation to the number of manipulations with them (number of drum rates in a given cycle, corresponds with the number of manipulations). The briquettes were tested six times consecutively.

The briquette initial values: D3-I, n=13 samples having total weight of 2,013.06g, D3-II-A, n=12 samples of total weight 1,780.99g, D3-II-C, n=5 samples of total weight 639.04g, D3-II-D, n=5 samples of total weight 945.41g, D4-0, n=15 samples of total weight 2,036.77g. The differences between the initial mass are caused by lack of material to make so many briquettes and related number of samples. As a comparative factor the Shattering index (S_{Index}) or the Durability index (%) was calculated. The S_{Index} represents the handling durability. It indicates the ability of densified materials to resist when handled during storage and transportation (Tumuluru et al, 2011). The definition of equation is following: the weight of briquette after testing is divided by the weight before testing. This expresses the mechanical durability.

4.4.2. Hardness

The hardness tester is one of the most commonly used measurement devices to assess and compare the mechanical behaviour of materials (Qi, Joyce & Boyce, 2003). The operation of a hardness tester is based on the penetration of an indentor into the material being tested under specific conditions. The movement of the indentor is related to the hardness tester used for various types of material, e.g. the more the indentor moves the higher the indicated hardness test value of the material. The penetration of the indentor (Figure 27) into the test specimen is inversely proportional to the hardness test value of the tested specimen, e.g., the deeper the indentor penetrates into the test specimen the lower the hardness value (CCSi, 2006).

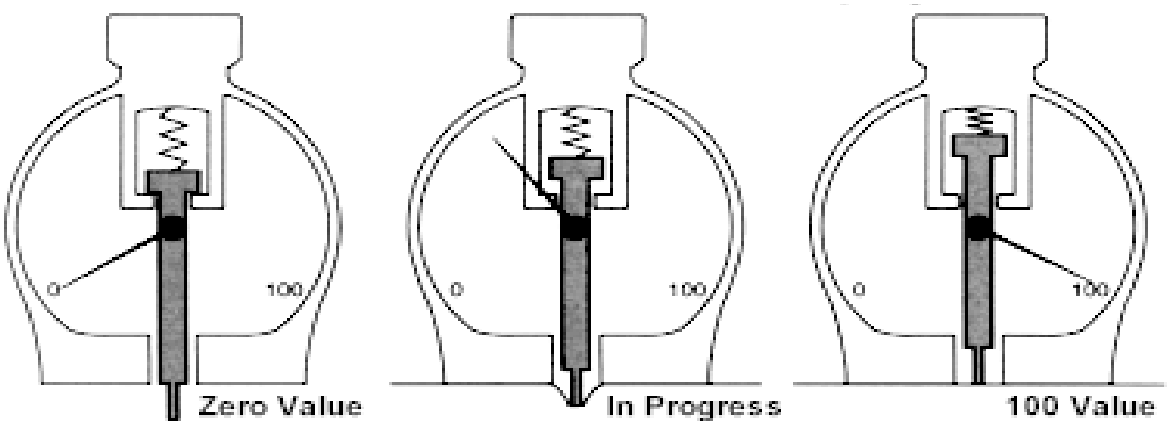

Figure 27: Hardness tester function – relative indentor position and displayed value (CCSi, 2006).

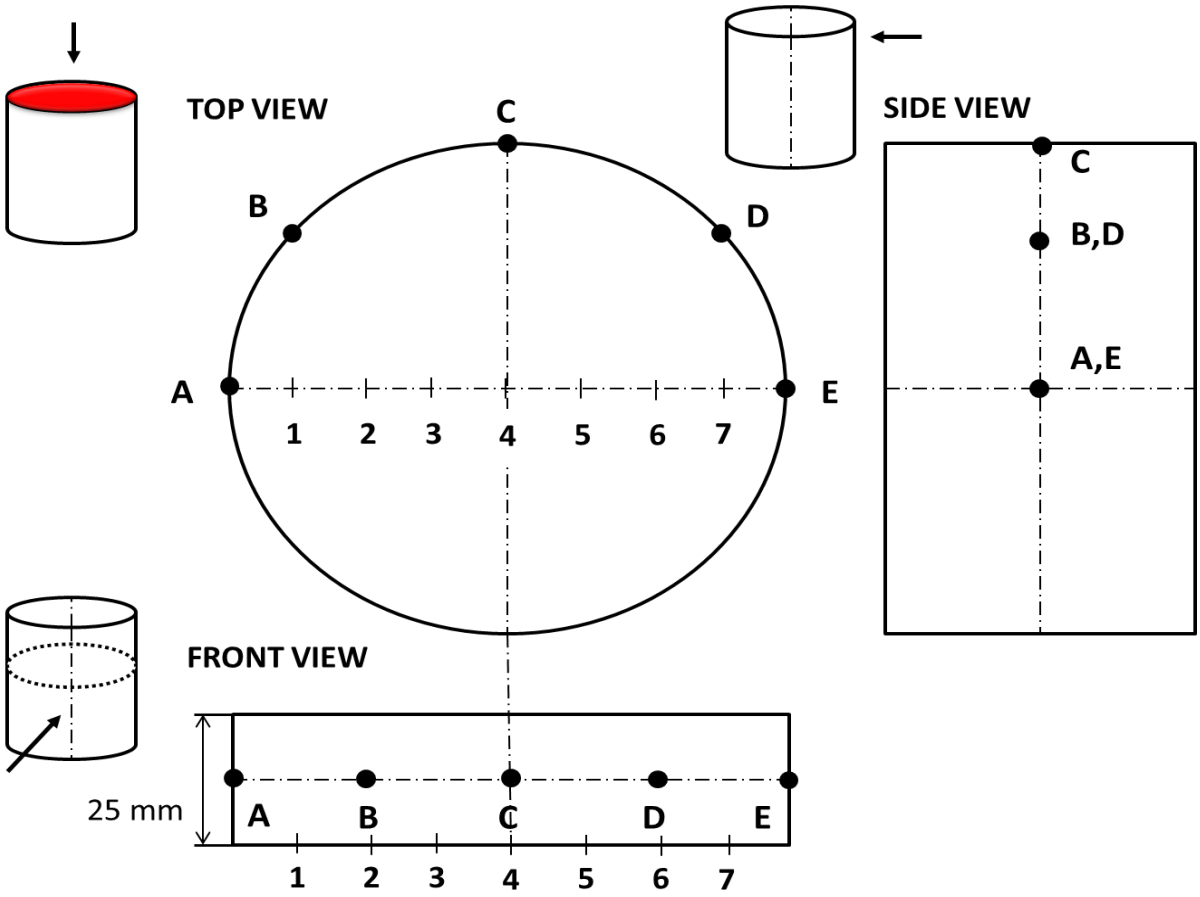

Figure 28: Measuring points of digestate briquette (of Ø 60mm) by hardness tester. View from above, front and side of the briquette.

The briquette hardness was measured by the hardness tester using 'Shore' hardness scale (0 – 100) where the basic unit is $N \cdot mm^{-2}$ (or in this case without the unit). The briquettes were tested in groups of 3 samples for each digestate specimen D4, D3-II-A to D. The values were measured at five points at perimeter (marked A, B, C, D, and E) and in seven points across the briquette diameter. The briquette was measured at points shown by Figure 28. The measured values were averaged and used for graphic illustration.

4.4.3. Particle size – sieve analysis

The sieve analysis was done on the digestate samples D3-II-A, D3-II-B, D3-II-C, D3-II-D and D4-0, D4-II-A, D4-II-C and D4-II-D. A mechanical AS 200 sieve of mesh sizes 10.00, 5.60, 2.50, 1.00, 0.50, 0.25, 0.10 and 0.00 mm has been used for the analysis. The duration of each sample processing was 10 minutes and sieving was repeated five times. The result of the sieve analysis is represented as the weight fractions. The arithmetic mean was calculated from the measured values and the standard deviation (STD) was determined. All the results from the sieve analysis were graphically rendered. The sieve mesh size influenced the width of particles,

which were very flat and the length was determined mainly by to mechanical treatment before the next AD processing.

4.4.4. Particle size – image analysis

All the values of the particle image analysis were measured automatically by the NIS elements AR program and the final value was stated as the average of those components. The measured set volume was dosed to 60 particles as a statistically sufficient sample. The particle sample had been selected by gradual mechanical reduction of the particle size, to satisfy the condition of random particle selection. The evaluation of each particle set consisting of 60 pieces was repeated several times and statistically processed. The result was expressed by the average values. The particle dimension measurement technique was modified several times during the research to ensure the most realistic data. Before the NIS software was available, all measurements were performed by the ImageJ measuring program, which is less sophisticated and harder to use. Samples D3-II-A, C, D have been used for the image analysis by NIS elements (Figure 29).

Figure 29: Digestate samples used for the image analysis.

Samples D1 and D2 have been analysed by ImageJ software. Both D1 and D2 matter is very similar, measurements of particle dimensions were conducted only for D1 sample, for particles of 1mm sieve. Particles of 1mm were chosen because of direct measuring possibilities; each particle could be measured by the image analysis and in parallel by calliper thanks to its easily visible size. Surely, powder particles making up about 1% of the sample, are well measureable in image analysis, but manually they cannot be comparably measured.

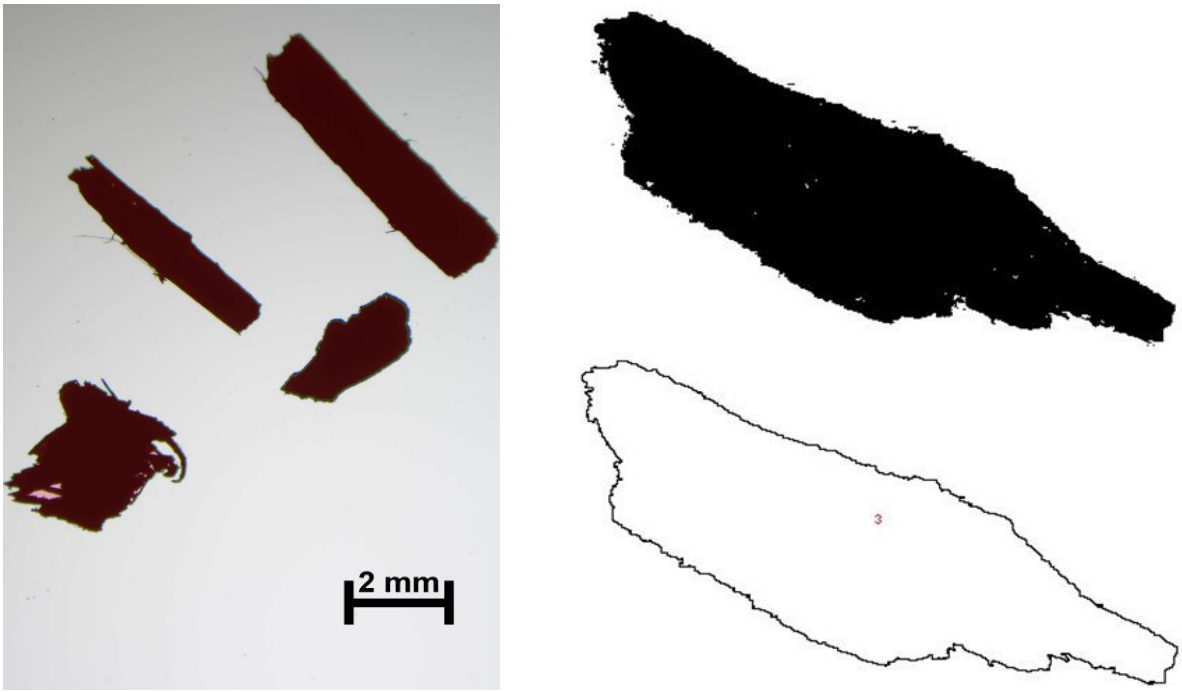

Figure 30: Image analysis of particles. Left – NIS elements Threshold/Binary function.

Right – Binary image, boundaries of particle.

The process of analysis (Figure 30, 31, 32) consisted of the following steps: first, selecting a particle and scanning it by camera to computer via magnifying glass or a microscope. Then, calibrating the image and programming the scale of the screen and the particle. Units used for our purposes were millimetres (or μm). After calibration we could use the "Threshold" function and/or switch the image to the binary view as per Figure 30. When the image is in 'Binary view' we can see if the mask corresponds to the particles boundaries, if not we can adjust the "Threshold" scale to fit. Finally, we can press the "measure" button and the program measures all required variables automatically. The data can be converted to an Excel spreadsheet and/or to graphs. Measured variables in this research were: length (L), width (B), area (S).

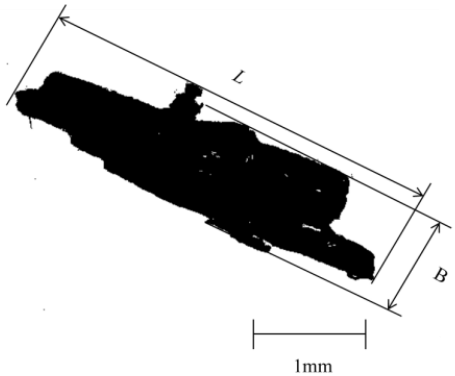

Figure 31: Measured variables of a particle.

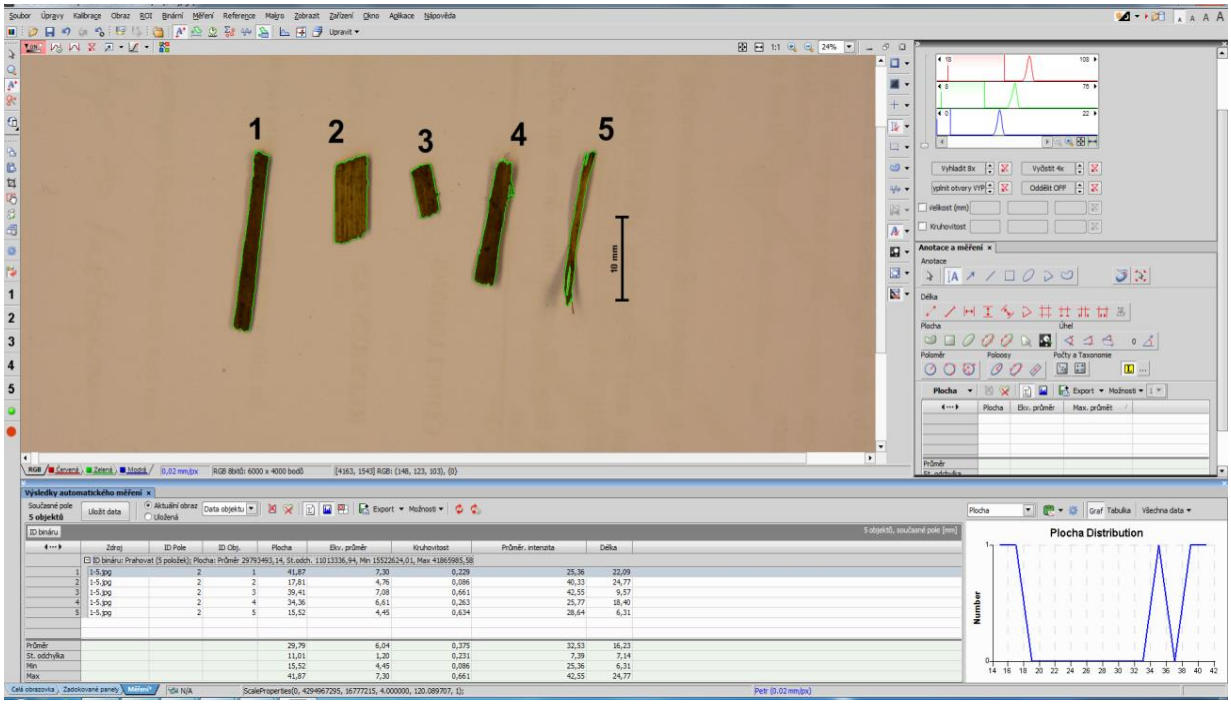

Figure 32: NIS-elements particle size measurements.

4.4.5. Measuring by calliper

Particles were measured physically by calliper as well. Method of measuring by calliper is not comparable to image analysis (because of different the measurement point count) but it is an easy method of manual verification of the program settings and measurement correctness. This approach was established to compare the accuracy of both measurement methods and the influence on particle dimensions assessment; eventually to establish the relation of the briquette strength to the size of particles.

Because the digital images are in a planar view (2D), just length, width and area were measured (see Figure 31). Thickness (Y) dimension is invisible in this kind of images. Thus this variable was additionally investigated by using a digital calliper. This method is not standard and in most cases it is inaccurate, but it was used as comparative and supplementary method. The size of the digestate sample set for the calliper measuring was 64 particles; the set for image testing of the same particles was smaller (54 particles) due to difficult handling and fragility of particles.

All measurements and verifications described above were exercised on the above described digestate materials, for comparison to different kind of biomass The Miscanthus sample was measured as well its particles retained on a sieve mesh of 1.00 mm size holes.

This direct method of calliper measurement is labour intensive. The image analysis is more reliable but it could be used as comparative method. Critical factor of this method could be the precision of measuring.

4.4.6. Water sorption

As a follow-up to my diploma thesis this research implies experiments with sorption properties of the digestate briquettes in comparison to a highly sorbent material, such as the spruce woodchip briquettes (WCH). The produced briquettes were left in the laboratory environment for two weeks to even out the difference of moisture content. The initial values are noted in Chart 8 "Results". The water sorption was measured simultaneously and repeatedly for

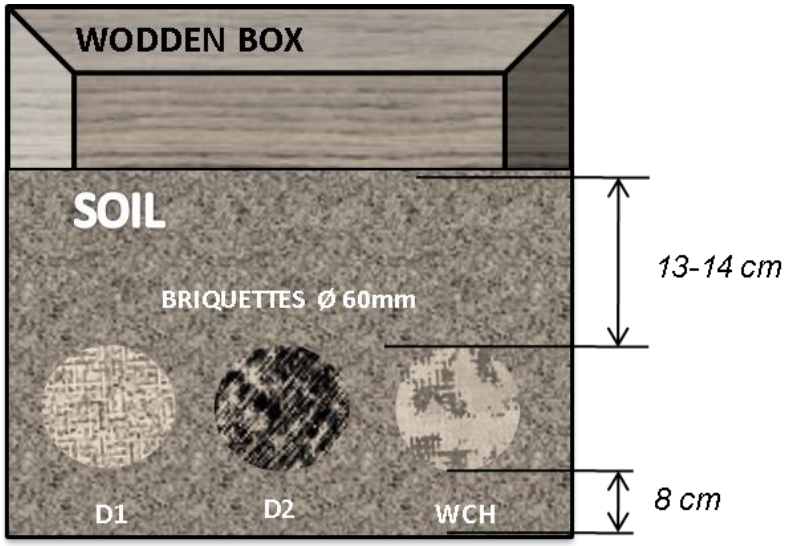

Figure 33: Experiment box for sorption observation

D1, D2 and WCH briquettes in special wooden boxes (flow boxes, see Figure 33). The briquettes were put into the same type of soil to simulate soil conditions, with the same initial moisture content without adding water in the course of the experiment. Water adsorbed by the briquettes was observed and measured by evaluating the change of the briquette dimensions and their moisture content fluctuation in relation to the period of time when the briquettes were in the soil. The system simulates closed environment soil conditions. The briquettes were placed in a flow box in three parallel lines (see Figure 33). To prevent evaporation through the box walls they were lined with PVC foil.

4.5. Used equipment and technology

- The sieving procedure was realized by standard AS 200 sieving machine using sieve meshes of 0.10, 0.25, 0.50, 1.00 and 2.50 mm.
- The Miscanthus comparative sample was pulverized by the 9FQ40C hummer biomass crusher equipped with circular-hole sieve mesh of 8 mm diameter.
- The briquettes were produced by hydraulic piston press Brick Star model CS25; company Bricklis Ltd. with working pressure of 12 MPa.
- All dimensions were measured by standard laboratory equipment, e.g. meter, calliper, scale KERN ABJ, model 124 – 4M.
- The abrasion of biomass briquettes was tested using standard test drum equipped with a partition piece.
- The hardness of briquettes was measured by the hardness tester.
- For the particle size analysis we used a specially equipped laboratory. Particles were handled with tweezers, than stored in special boxes for subsequent processing and measuring. The NIS elements AR 4.50.00 64 bit program was used for the image analysis. The NIKON D7 100 camera, by NIKON Corporation, with shutter curtain f/36, ISO speed ISO-250 and focal distance 105mm was used to capture the particles to the image form. The digital image dimensions were 6,000×4,000 with distinction 300 dpi. For smaller particles was necessary to use the Nikon SMZ1270 magnifier with focal distance of 35mm and 1×magnification. Software used was the ImageJ, free download. For the image scanning the Bresser electronic microscope was used.
- The sorption potential of biomass briquettes was observed in special wooden boxes with dimensions of 26×56.4×26 cm with openable front side. Plastic foil was placed under the soil layer as a protection against moisture.
- The data analysis was processed in Excel application and the Statistica 13, the Rosin-Rammler particle size distribution - MATLAB® software.

4.6. Calculations, statistical data evaluation

Exponential regression: $y = a + e^{bx}$

Rosin-Rammler Distribution: $R(d) = 100 \cdot e^{\left(\frac{d}{d'}\right)^n}$

Density: $\rho = \frac{M}{V}$ (kg·m^{-3})

Shattering index = $\frac{Weight\ of\ briquettes\ retained\ on\ the\ screen\ after\ a\ test\ round}{Weight\ of\ briquettes\ before\ testing} \cdot 100$ (%)

Particle size distribution: $D = {}^{d}/_{d_a}$

5. Results and discussion

All results were gained according to methods designed and described above in the 'Materials and methods' chapter and the data was processed, rendered in graphic form (as charts or graphs) and presented below in the chapter "Results and discussion", to meet the set objectives.

5.1.Nutrient composition

The nutrient contents identified in samples D1 and D2, D3 = D4 of 100% dry matter are listed in Chart 7. The content of tested ingredients such as ashes, nitrogen, nitrogen-free extracts fats, fibres and organic matter; expressed as percentage volume.

Chart 7: Nutrient composition of digestate matter, 100% DM.

[%]	Ash	N · 6.25	NFE	Fats	Fibre	OM
D1	11.9	12.3	40.8	0.3	34.8	88.1
D2	12.4	20.3	40.4	1.0	25.9	87.6
D3	11.2	17.2	35.2	0.2	31.2	91.2
D4	12.7	22.3	43.1	0.7	26.7	88.3

* DM – Dry Matter, N – Nitrogen, NFE – Nitrogen Free Extracts, OM – Organic Matter

As description of different digestate samples (D1-D4), all samples are organic matter rich materials, having the share of ashes ~12%, nitrogen content of 12 – 22%; fibres represent 26 – 35%. All samples were made of very similar feedstock and values of each observed category are not significantly different, particle size was not influencing the result.

For discussion we can see that all samples contain relatively high amount of organic matter (from 88% up to 91%) and fibres (30 – 35%) in comparison to earlier experiments where digestate sample (100% DM) consisting of 60% of corn silage, 10% of pig slurry and 30% of manure, had 75% of OM and 23% of fibre; and sample (100% DM) consisting of 20% of corn silage, 20% of grass silage and 60% of cow manure contained 83% of OM and 31% of fibres (Černá, 2015).

The digestate nutrient composition is, according to analysis, influenced by used feedstock to AD. The more crop character the feedstock is, the more fibre and OM contains. It can be said that the digestate material is more or less fibrous material containing particles of

non-spherical shape as documented in scientific articles (Hann & Stražišar, 2007; Guo et al, 2012). This shape was observed also in this study.

The ash content varied in range of 12–13%, which is - in comparison with the samples from the Černá, 2015 study - less than the digestate sample composed prevalently from animal manure (25%). If we compare digestate briquettes to wood pellets (1.5%), the value is ten times higher (EN 14961-1, 2010). According to another paper, the ash content of wood briquettes measured according to ÖNORM M 7135 is in average 0.88% and varies in range 0.21% – 1.88% and bark briquettes 3.31% and 6.39% (Obernberger & Thek, 2004). However these values are not the target for this research, just informative data useful for fuel utilization focused topics. The digestate is not suitable as fuel, due to high value of ashes; however, the calorific value is comparable, for example, to hemp (18 MJ/kg) (Mankowski & Kolodziej, 2008). Thanks to the rich content of nutrients, the digestate is a valuable soil fertiliser, in which the nitrogen content is comparable for example with the di-ammonia phosphate (DAP) fertiliser having the weight contents of NH_4 – N as high as 18 % (Ashiya et al, 2015). On the other hand, the NPK fertiliser contains 30% of nitrogen (Abubaker et al, 2012).

Conclusion: The digestate nutritional composition is based on the feedstock input to the AD process. Based on the investigations and the consultation with other sources, the digestate matter is highly organic and fibrous; consequently, there are non-spherical particles the size of which depends on the chopping and pre-treatment processes. Due to high value of ashes, the digestate matter is not suitable as fuel, but due to high content of nitrogen it is a very valuable fertiliser.

Recommendation: For future experiments, it is advisable to compare more samples of the digestate from different feedstock materials of different ratios of animal and plant material content in terms of particle size distribution and nutritional characteristics influenced by pre-treatment processes affecting the properties of briquetting and the final product.

5.2. Briquette characteristics

Before any testing, briquette samples dimensions and basic physical properties were measured. Results were recorded in Chart 8, namely the diameter, height, volume; moisture content and density were listed. The units were expressed in ‘cm’ for measured variables because of easier orientation and description of the unit.

Chart 8: Initial characteristics of made briquettes.

Briquettes	Diameter [cm]	Length [cm]	Volume [cm^3]	Moisture [%]	Density [$g \cdot cm^{-3}$]
D1	6.70	4.83	169	4.90	0.787
D2	6.70	4.08	142	5.20	0.769
D3	6.80	5.02	183	5.20	0.850
D4	6.80	4.76	170	9.50	0.892
WCH	6.50	4.11	137	5.60	0.792

The result indicates that all briquette samples had the diameter in range of 6.50 – 6.80 cm, length in range of 4.08 – 5.02 cm. The measured moisture content of the briquettes ranged 5 – 10%; the density was 0.769 – 0.892 g cm^{-3}, where in samples of smaller particle size, the density is higher in comparison with the bigger particles and volume of 140 – 180 cm^3.

The measured diameter values vary around the 6.6 cm with length of 4.3 cm. In comparison to study (Obernberger & Thek, 2004) using different norm namely ÖNORM M 7135, the average value of diameter was 7.9 cm and length 2.5 cm for briquettes from wood biomass; diameter 9.6 cm and length 2.8 cm for bark briquettes. The moisture content should not exceed 14% to ensure good coherence of the briquettes. The average moisture content of our briquettes was 5.23%; in earlier observation the average moisture of the digestate samples was 8 – 10% (Černá, 2015) and in comparison to the moisture content of wood briquettes in the Obernberger & Thek, 2004 study reaching 8.0 – 10.4% we can say the standard was met. The moisture of samples was observed because of potential storage conditions influencing its cohesiveness as briquettes may be stored in interior conditions or outside protected against precipitations.

The density of the tested digestate briquettes is rather high for the digestate, even if we compare it with different kinds of biomass briquettes like rice husk 0.129 g cm^{-3} – 0.371 g cm^{-3} (Yank, Ngadi & Kok, 2016). However, the digestate briquette measured density was a high value; the wood briquette density in different study was 1.060 g cm^{-3}. Ordinary wood briquette density was ~0.490 g cm^{-3} (Onuegbu, Ogbu & Ejikeme, 2012); the water density is 1 g cm^{-3} (VŠCHT, 2008). Most technologies produce briquettes of densities above 1 g cm^{-3}, thus in water test the briquette is sinking. The physical upper density limit for ligno–cellulosic materials is about 1.500 g cm^{-3}. High pressure processes produce briquettes with density range of 1.20 – 1.40 g cm^{-3} (Antwi-Boasiako & Acheampong, 2016). From earlier observations, it is possible to compare different material briquette densities, listed in Chart 9.

Chart 9: Observed densities of different material briquette samples (Černá, 2015).

Material Briquettes	**Mean Density value [g·cm^{-3}]**
Pure digestate	0.814
Digestate + Dolomite lime	1.045
Digestate + Zeolite	1.083
Miscanthus sinensis	0.783
Sorghum (pure)	0.709
Sorghum + pine chips	0.885
Hemp	0.947
Spruce bark	1.034

According to the studies (Moreno, Font & Conesa, 2016), the higher the briquette density (when moisture content is 6 – 8%) the higher the cohesiveness (compaction) of briquettes.

Conclusion: The digestate is good material for compression, as proven in previous research and confirmed in this study. In the compressed form, the digestate material shows high density value but less than water. When using additives, e.g. zeolite or lime, the digestate briquette density value exceeds the water density and will be comparable to wooden briquettes. Worked into the soil, this could be successfully used in agriculture to prevent acidification of soil. Average density value calculated from the briquette mass and volume depends mainly on the applied pressure, and the briquette density increases with increasing working pressure.

Recommendation: The briquette characteristics are closely related to feedstock composition, the compression techniques and settings and the possibility to add some mixtures and additives approved by current standards. Because the digestate itself has been proven as a proper material for compression, with high density value, it could be recommended to exploit the options of incorporating other different enhancing additives, beside the zeolites and lime. The best particle composition (powders, granules) of additive can be assessed to support the final structure of the briquette improving its physical properties, e.g. density, durability, hardness and water sorption.

5.3.Durability

In this research, the briquette durability (or abrasive-resistance) has been tested in mechanical drum, and the ratio of the abraded biomass from the briquette was weighted. The abrasion rate represents the resistance of densified fuels against abrasion during handling. Each

round of durability testing represents a number of manipulations, which is theoretically equal to the total number of drum rotations of the test device.

The result is illustrated as scatter chart with exponential logarithmic tendency line. The results are also expressed as the Shattering index (S_{Index}) equation to be comparable with other publication results. The higher the S_{Index} is the more durable the briquette. Actually, the kinetic energy of a briquette sample when hitting the internal drum surface is converted into mechanical work, which causes abrasion of the briquette sample. Then the rate can be comfortably measured through mass losses. It should be taken into account that the abrasion values are average, because it is impossible to monitor with good accuracy the abrasion of the individual briquettes in the sample.

The result of durability testing was rendered in a chart. Graphs for D3 briquettes samples were drawn based on the average values of differences, (see Figure 34).

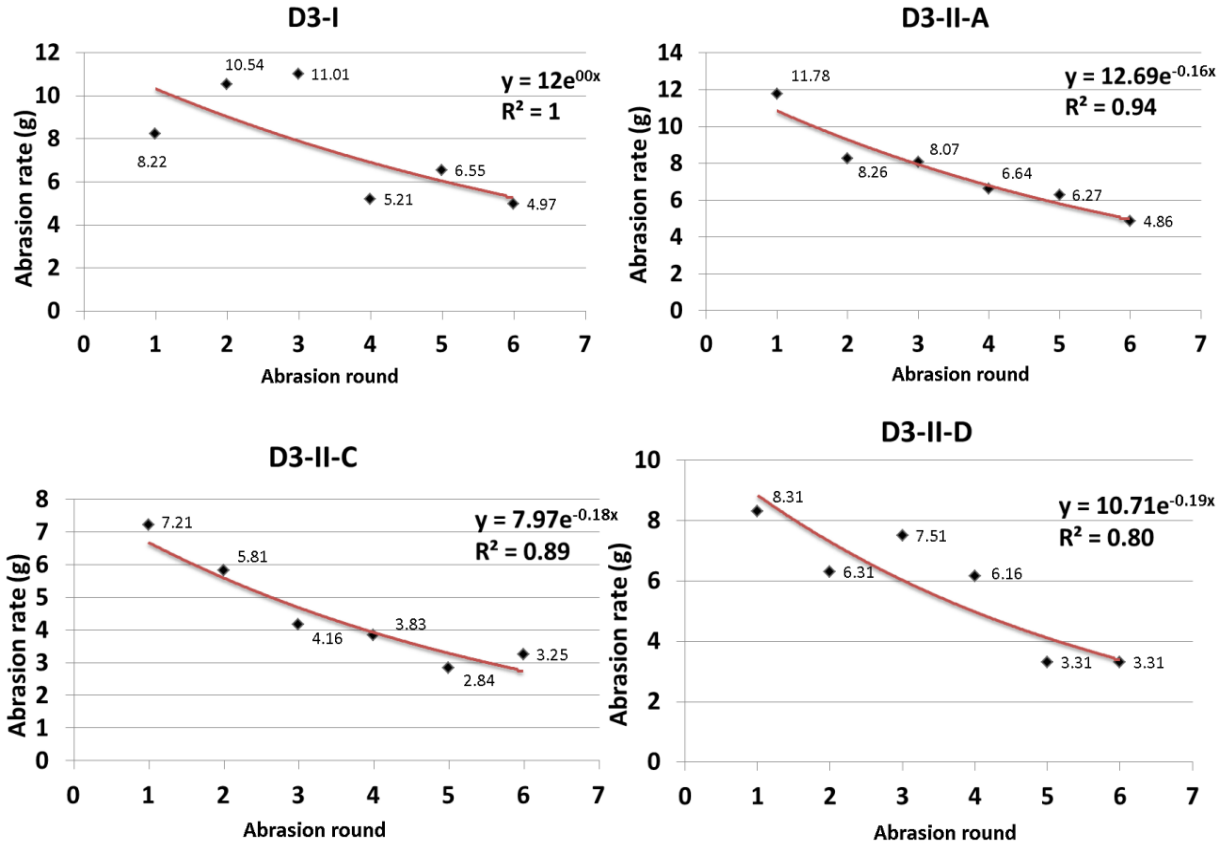

Figure 34: Abrasion rates of D3 samples, completed with regression (ER) expressed by exponential logarithmic line and coefficient of determination R^2.

It is evident from Figure 34 that the first and the second round of the durability test exhibits the highest rate of abrasion from the entire cycle. This trend is obvious in all tested samples except D3-I. The regression is the same for all measured values, it is decreasing. In the

first round of testing the AR is in range of 7 – 12 g while for sample D3-II-C is the lowest. The highest rate is in the D3-II-A sample. The lowest rate is in the sixth round of test (3 – 5 g).

The overall value of the S_{Index} was **99%** (for D3 samples); see Chart 24 – 27 (Appendices). The coefficient of determination R^2 is at all cases approximately close to 1 and we can observe the same tendency in other tests. The difference between the first round and the last round is as follows: D3-I = 3.30 g, D3-II-A = 6.90 g, D3-II-C = 3.96 g and D3-II-D = 5 g.

In comparison to previous samples D1 and D2, the rate here was 2 g and 4 g. As shown in Figure 35, the difference between round 1 and round 6 is not so as high as for the previous D3 samples. In fact, it is the lowest difference of 1.20 and 2.80 g.

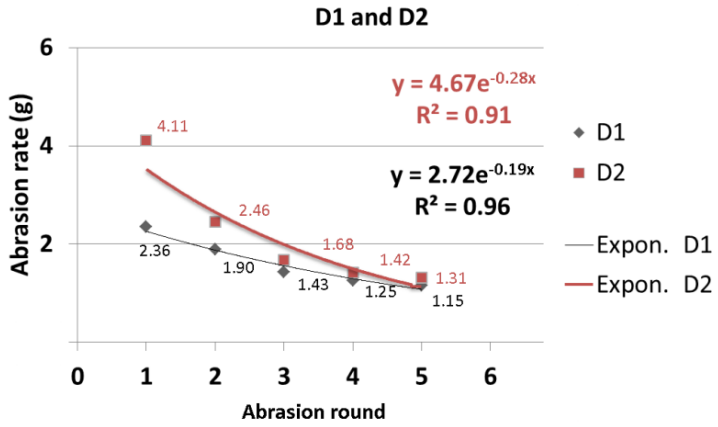

Figure 35: Abrasion rate of D1 and D2 briquettes from previous testing.

Figure 34 and 35 above shows the graphic expression of abrasion progress during the DU test - not in percentage, but in the unit of measured values (g). Thanks to the graph and the regression line, the decreasing tendency of the abraded matter is clearly evident. It can be noted that the difference of abrasion between samples D1 and D2 is probably caused by a greater volume of longer particles in D2 which are considerably flat and straight. Such particles do not form solid mechanical connection after compression, therefore, they are easier to crumble. Whereas, particles of D1 sample, are shorter in average, but they are not straight and their mutual mechanical interlocking within the briquette, is therefore stronger (Rawle, 2003; Kakitis et al, 2011; Guo et al, 2012).

When comparing the result with other publications, important for us will be the S_{Index}. From different research: Brunerová et al, 2016, with the same material (digestate) but different composition (40% of cattle manure, 30% of grass silage and 30% of maize forage) the durability value was in average equal to 99.44% (minimum 96.25% and maximum 99.99%). This value corresponds to the highest grade of quality indicator DU ≥ 95%, consistent with the international standard for solid biofuels EN ISO 17225–1:2015. The same research reports that

the rate of abrasion in the first and the second round of testing is the highest because of sharp edges of made briquettes and low cohesion of marginal particles. The same result was approved by this paper. The trend of decreasing abrasion rate refers about increasing cohesion of briquettes samples thus less briquette surface to be abraded. As many authors have reported, it is clear how important parameter is the type of material to be used in briquetting and the briquette moisture content (Zhang & Guo, 2014; Brunerová et al, 2016). Other materials which have the same durability category ≥95.0% were listed in paper by Brunerová et al, 2016: digestate (Authors data), cotton (Eissa et al, 2013), hemp (Ivanova, 2014), soybean (stalk) (Rajkumar & Venkatachalam, 2013) and paper + board (Brožek, 2013), barley (42 – 92%), canola (72 – 95%), oat (43 – 91%) and wheat (45 – 95%) (Tumuluru et al, 2011).

From other parameters influencing the durability, it has been established that the durability is increasing with the compacting pressure (12 – 35MPa). Also, the moisture increases the durability when there are soluble compounds in the matter, e.g. sugars, starches, soda ashes, potassium salts, calcium chloride etc. Lignin (to 35% of content) demonstrates the same result in elevated temperatures (140˚C). To the contrary, fats and their high content result in low durability. Finally, the particle size, the die dimensions, the L/D ratios and he rotation speed are also influencing durability (Tumuluru et al, 2011). It seems that particle size in fact influences the durability values in this research as well. Particles with bigger dimensions (≥3.8mm) D3-0 and D3-II-A both have slightly higher values that D3-II-C and D3-II-D (smaller particles, ≤3.8mm).

Conclusion:

Significant quantifiable parameters thus are the pressing temperature and the material moisture content. The pressing temperature significantly influences certain material properties, changing and influencing the material structure and the chemical composition during the process (Menind et al, 2012). The influence of the particle size and shape (Miao et al, 2015) on the durability of briquettes is demonstrated under the assumption that the abrasion of different samples of briquettes happens in the same way and at the same device. Thus the undertaken durability test represents "coherence" of briquettes. It was proven that sizes of particles are important variable in case of abrasion rate (D1, D2 and D3-II-C, D sample showed less abrasion than those with bigger particles D3-I and D3-II-A) and the same trend was found in terms of the hardness.

Recommendations: This testing should be performed on more samples for longer time using digestate briquettes differentiated by various particle sizes considering the possibility of mixture and additive use. Observation should focus on the significance of the particle size influence on the durability and other variables, such as moisture, time, compression procedure, temperatures etc.

5.4. Hardness

During the hardness testing, mainly the D3 sample briquettes were used, always repeating for three samples. Tests were measured as for fibre materials according to the Shore scale (0 – 100).

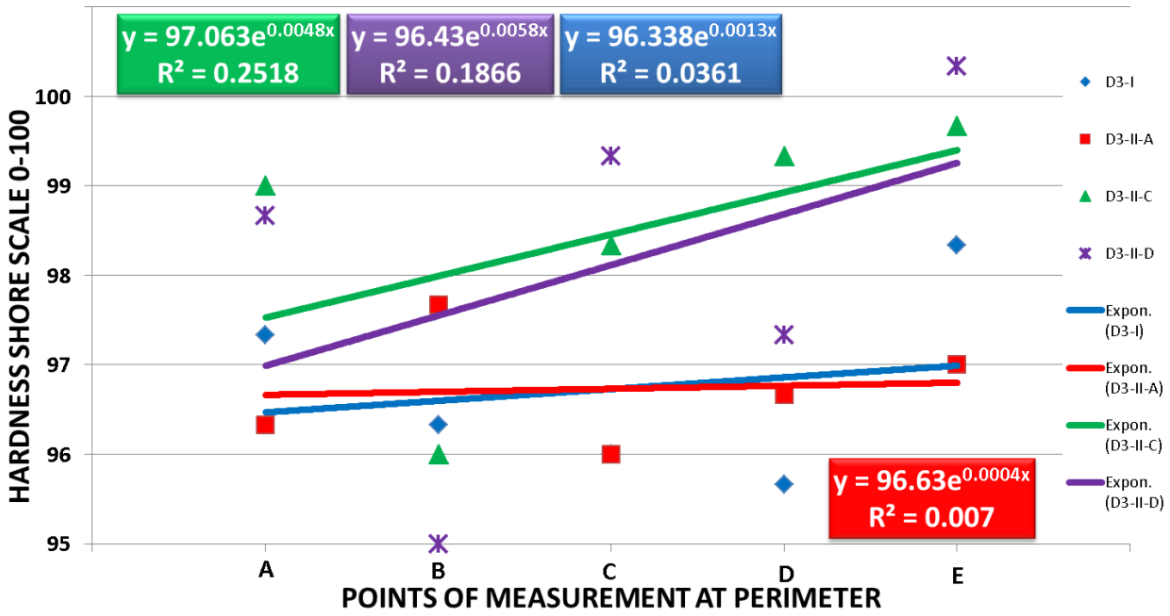

Figure 36: Hardness testing of D3 samples on the briquette perimeter.

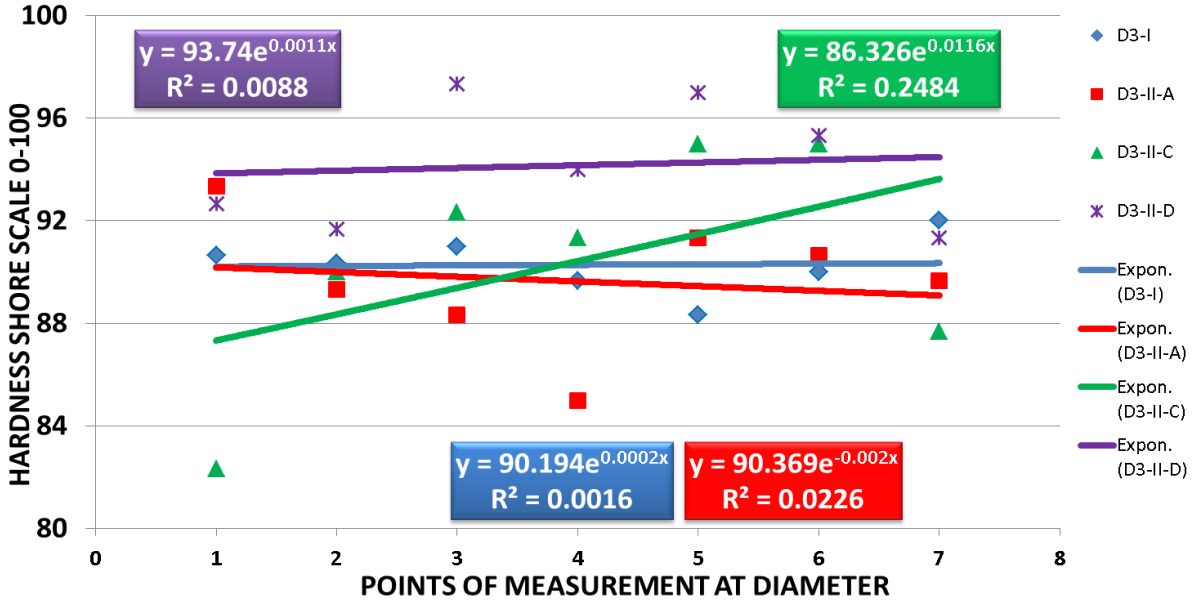

Figure 37: Hardness testing of D3 samples on the briquette perimeter

Points (A, B, C and D) at the perimeter and diameter (1 – 7), where hardness was measured are illustrated (Figure 28) in the "Materials and methods" chapter, first along the perimeter and secondly across the diameter. Results were presented in a scatter plot showing the exponential logarithmic regression and the coefficient of determination.

From Figure 36 the difference between two size groups of samples is evident, measured on perimeter. The first group is D3-I and D3-II-A (≥3.8 mm) samples situated in the lower part of the graph and the second group consists of the D3-II-C and D (≤3.8 mm) samples. The difference between these groups is not so big, but obvious. Because the R^2 indicates a very low number, the tendency of the graph regression is not well determined and accurate. There is

Chart 10: Average values of hardness measured at the perimeter. Shore scale.

Perimeter	A	B	C	D	E	AVERAGE
D3-I	97.3	96.3	96.0	95 7	98 3	96.7
D3-II-A	96.3	97.7	96.0	96.7	97.0	96.7
D3-II-C	99.0	96.0	98.3	99.3	99.7	98.5
D3-II-D	98.7	95.0	99.3	97.3	100.3	98.1

possibility that values of the measured hardness for samples D3-I and D3-II-A (≥3.8 mm) have the hardness lower than 98 compared to samples D3-II-C and D (≤3.8 mm) with hardness value of 99. Values of each sample in corresponding measured point are described in Chart 10.

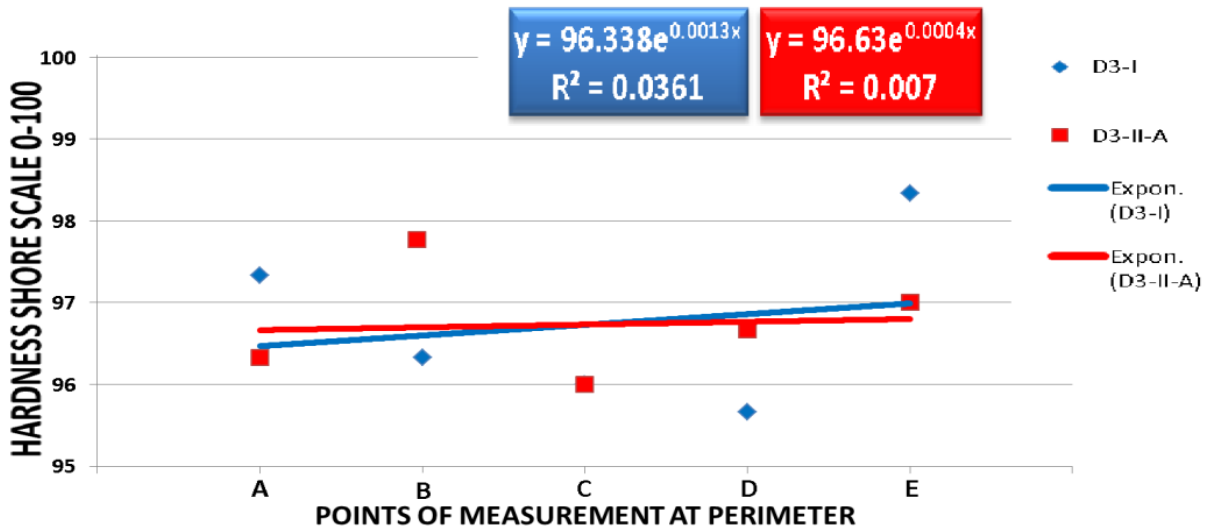

Figure 38: Comparison of hardness values for samples D3-I (particles >8.7 mm) and D3-II-A (particles 3.8-8.7 mm) measured at perimeter.

At Figure 38, samples D3-I (particles >8.7 mm) and D3-II-A (particles 3.8-8.7 mm) were compared, showing that the tendency of average values is at the same level (range 96 – 97). Values are very similar; however the coefficient of determination is very low.

Figure 39 comparing samples D3-II-C (particles 1.5 – 3.8 mm) and D3-II-D (particles <1.5mm), shows the tendency of average values rather maintains the same level (range 97 – 99). The tendency of the graph is rather incising and the coefficient of determination is higher than in Figure 38.

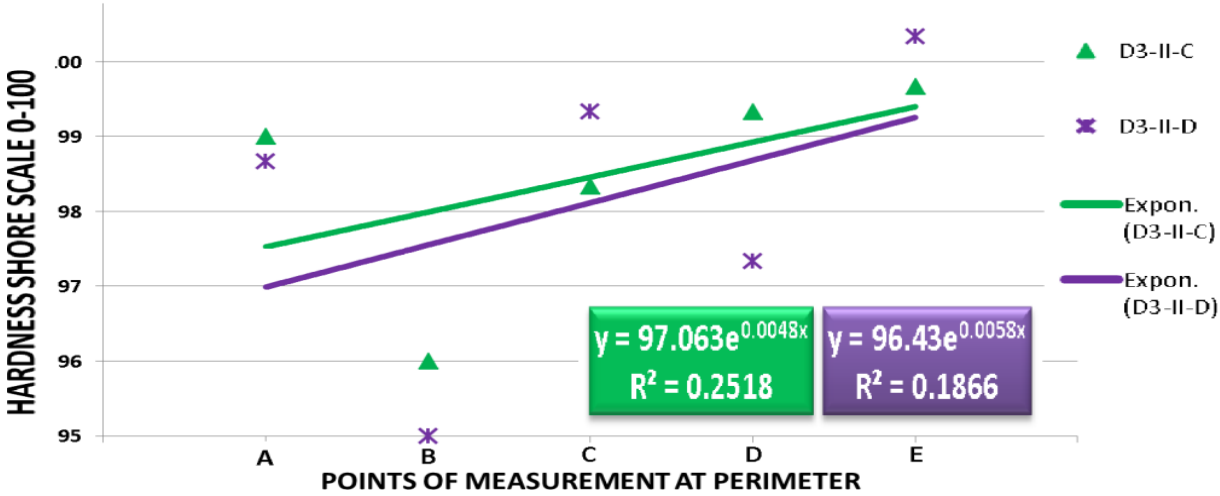

Figure 39: Comparison of hardness values for samples D3-II-C (particles 1.5 – 3.8 mm) and D3-II-D (particles <1.5 mm) measured at perimeter.

Chart 11: Average values of hardness measured at the diameter. Shore scale.

Diameter	1	2	3	4	5	6	7	AVERAGE
D3-I	90.7	90.3	91.0	89.7	88.3	90.0	92.0	90.3
D3-II-A	93.3	89.3	88.3	85.0	91.3	90.7	89.7	89.7
D3-II-C	82.3	90.0	92.3	91.3	95.0	95.0	87.7	90.5
D3-II-D	92.7	91.7	97.3	94.0	97.0	95.3	91.3	94.2

Values of each sample in corresponding measured point at diameter are described in Chart 11. The values of hardness for samples D3-I and D3-II-A (≥3.8 mm) have the same hardness of 90 as the sample D3-II-C (particles size 1.5 – 3.8 mm) with hardness of 90; there is a difference in sample D3-II-C, where the hardness is 94.

In Figure 40 comparing samples D3-I (particles >8.7 mm) and D3-II-A (particles 3.8 – 8.7 mm), the tendency of average values is at the same level (range 89 – 90). Values are very similar; however the coefficient of determination is very low.

Figure 41 comparing samples D3-II-C (particles 1.5 – 3.8 mm) and D3-II-D (particles <1.5 mm) shows that the tendency of the average values was quite constant (range 97 – 99). The tendency of the graph is rather incising and the coefficient of determination is similar as in Figure 40.

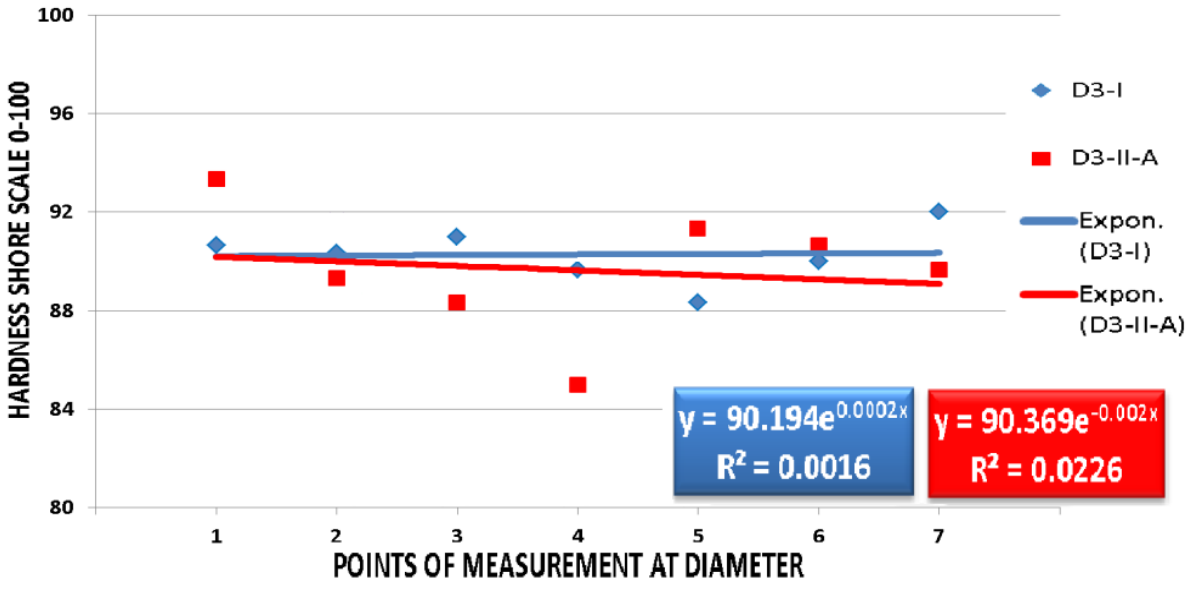

Figure 40: Comparison of hardness values for samples D3-I (particles >8.7 mm) and D3-II-A (particles 3.8 – 8.7 mm) measured at diameter.

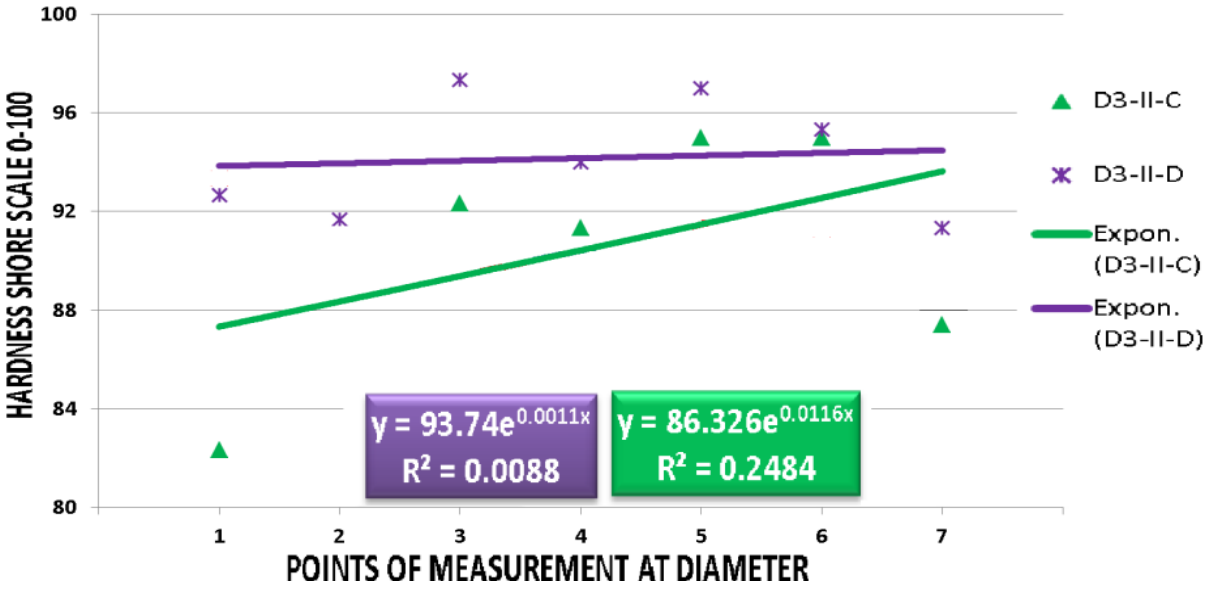

Figure 41: Comparison of hardness values for samples D3-II-C (particles 1.5 – 3.8 mm) and D3-II-D (particles <1.5 mm) measured at diameter.

The result of this test indicates that the group of briquettes made of smaller particles (C and D) has higher hardness values varying around 94 in diameter and 98 in perimeter of Shore scale. We can also consider the difference between the perimeter and diameter points, where points at perimeter have higher values than those in diameter. This is caused by the process of briquette forming, where the compression force is causing the friction among the perimeter particles (along the wall of the compression chamber), thus increasing the temperature of briquette as well as the temperature of the wall. If the compressed material contains lignin polymers than lignin serves as the bonding agent among the particles. That is why the perimeter areas are smooth and harder than the diameter areas. This is illustrated by the hardness test.

In comparison to study of Rynkiewicz et al, 2013, the values of hardness were conducted for briquettes of different materials and temperatures: hay 58.20 – 99.09, 50% hay 50% wheat straw 9.46 – 21.48, 100% rapeseed straw 16.50 – 34.00 and 100% rye straw 4.75 – 5.05.

In most studies, the Shore hardness test is not used. In the most scientific papers, the scientists use different tests (as The Meyer hardness or compressive strength, etc.) (Peng et al, 2015) The study of Mitchual et al, 2013 investigated the effect of the biomass type, the particle size and the compacting pressure on the compressive strength and the relaxed density (Mitchual et al, 2013).

Conclusion: Measuring the hardness by the hardness tester with the Shore scale is not typical for briquettes. Anyway, values of hardness are high ranging between 89.7 and 98.9. The

observed relation of particle size and hardness tested was rather obvious; samples of smaller particles reached higher values of hardness than those with bigger particles. It could be said that the smaller particles the higher the hardness. This test was just tentative, because of low number of repetitions.

Recommendation: I recommend repeating this hardness test with more representative samples using various approaches in measuring and observing the relation between the briquette ingredients e.g. digestate with different feedstock or digestate with additives. Finally, the relation between particles size and hardness should be established.

5.5. Size analysis

The size of particles is of key importance. It was observed that the presence of particles of different size improves the dynamic complementation and strength of briquettes. Finer particles give briquettes a higher density and better mechanical properties (Miroljub & Savic, 2013).

The size analysis in this work comprises three stages of the experiment: first is the sieve analysis that establishes the mass fraction of matter retained at different sizes sieves, expressed in percentage share; second is the image analysis of sample D3 using the NIS elements AR software, through which particle sizes are expressed by length, width and area in mm. Result of these analyses are graphs using average values.

5.5.1. Sieve analysis

To investigate the fraction size distribution of the digestate briquettes, the Rosin-Rammler test was conducted using the MATLAB® software.

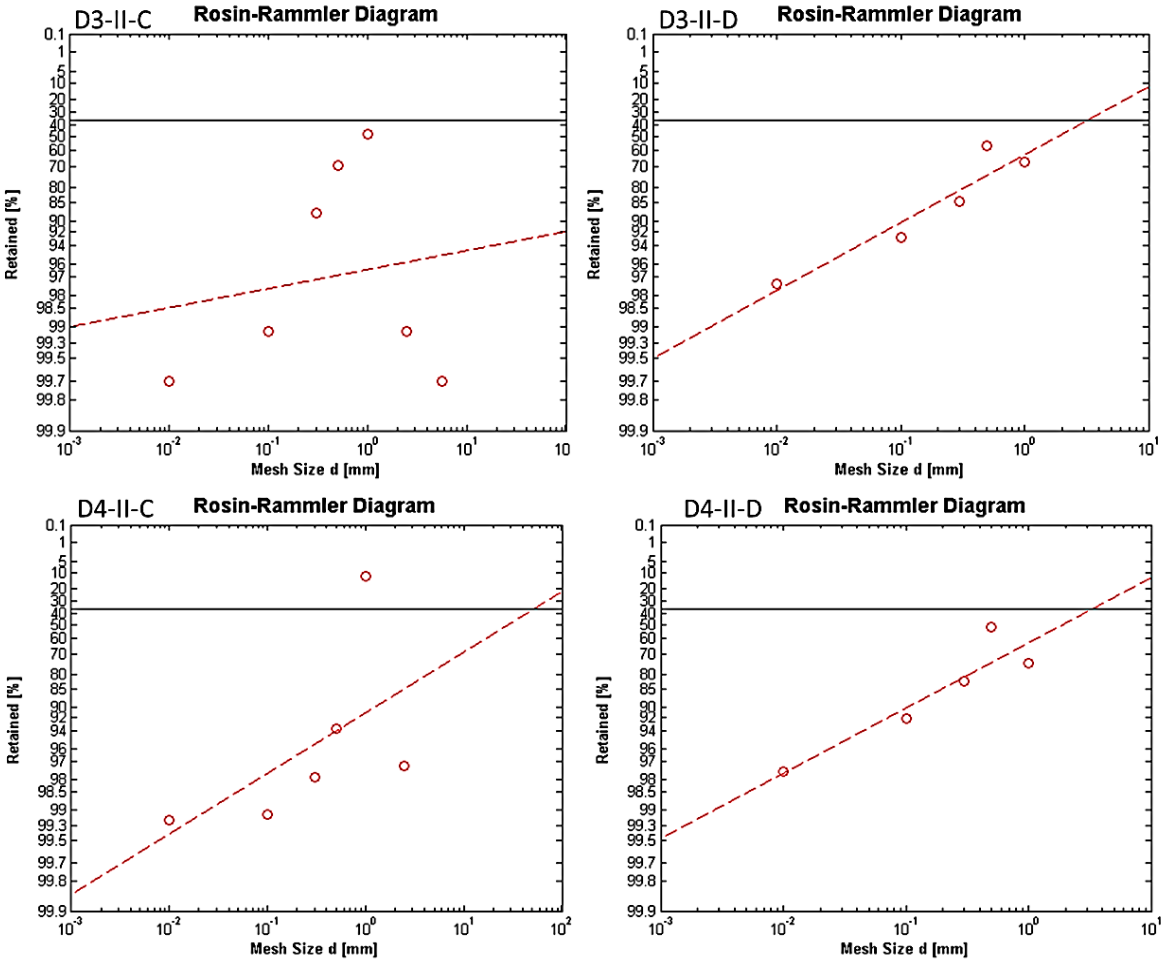

Figure 42: Rosin-Rammler plot diagrams for digestate briquette samples D3 and D4.

The Rosin-Rammler graphs (Figure 43) illustrate the percent share of the sieving matter, which remains retained at the sieve of a given size. Represented were mainly data of D3 samples. For comparison, even D4-II-C and D were tested. From the graphs for D3-II-A and B it is evident that the lowest percent (30 – 40%) of particles was retained at sieve of the size 0 – 0.5 mm. The highest share (99.5%) of particles was those of 0.01 mm size. In D3-II-C sample there were bigger particles (10 mm) from 99.7%.

The following histograms (Figure 44 – 50) contain the same data as the Rosin-Rammler diagrams, but their concept is a little bit different. Firstly, they contain information about the weight share of each size group of particles (in grams), secondly the percentage shares of each size group. The differences are obvious on the first sight. This type of graph is more suitable for these purposes and the number of observed samples.

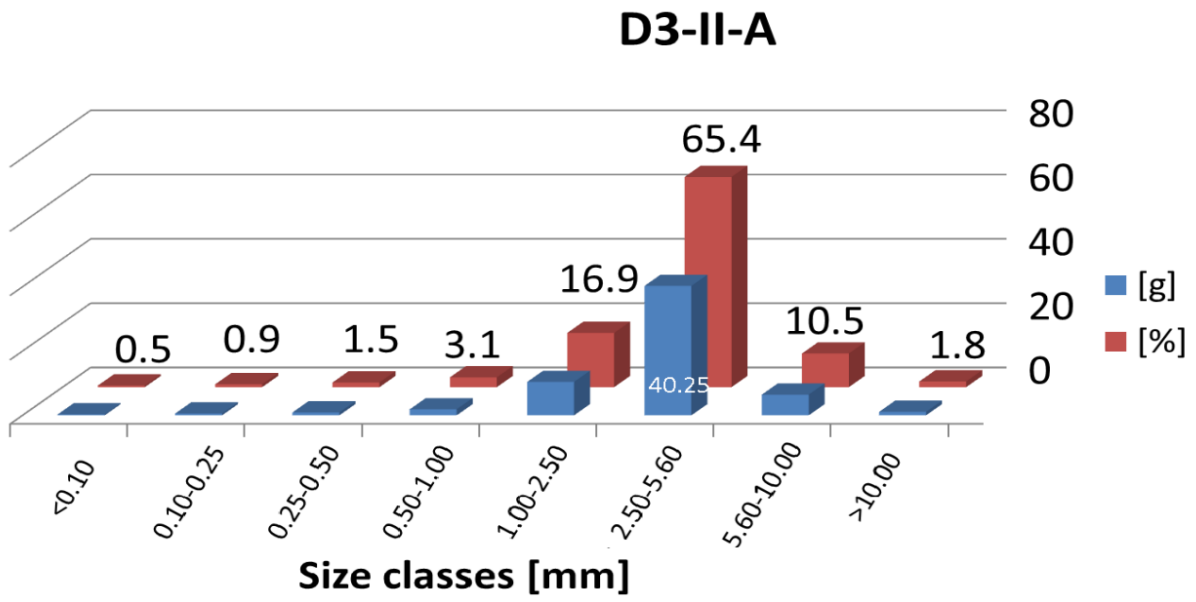

Figure 43: Size distribution of sieving analysis for D3-II-A sample.

From Figure 44 we can see that in the D3-II-A sample (sieved at 3.8 mm mesh size) the highest percentage of particles (65.4%) is in the range of 2.50 – 5.60 mm.

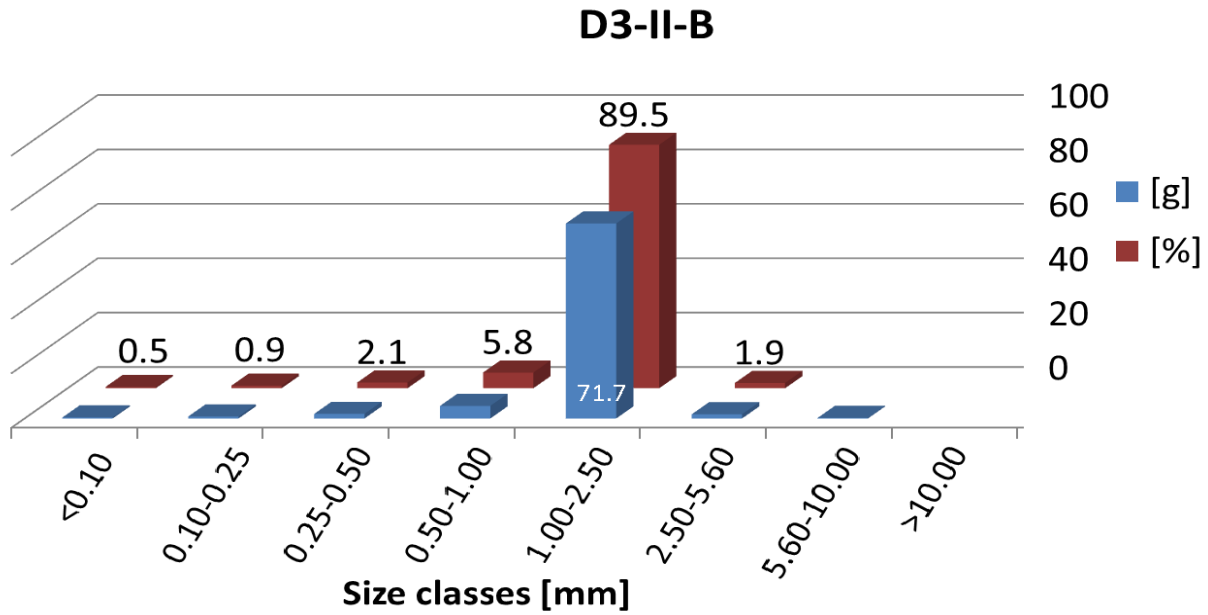

Figure 44: Size distribution of sieving analysis for D3-II-B sample.

In Figure 45 the D3-II-B sample (1.5 mm mesh size) has the highest percentage of particles (89.5%) in the range of 1.00 – 2.50 mm.

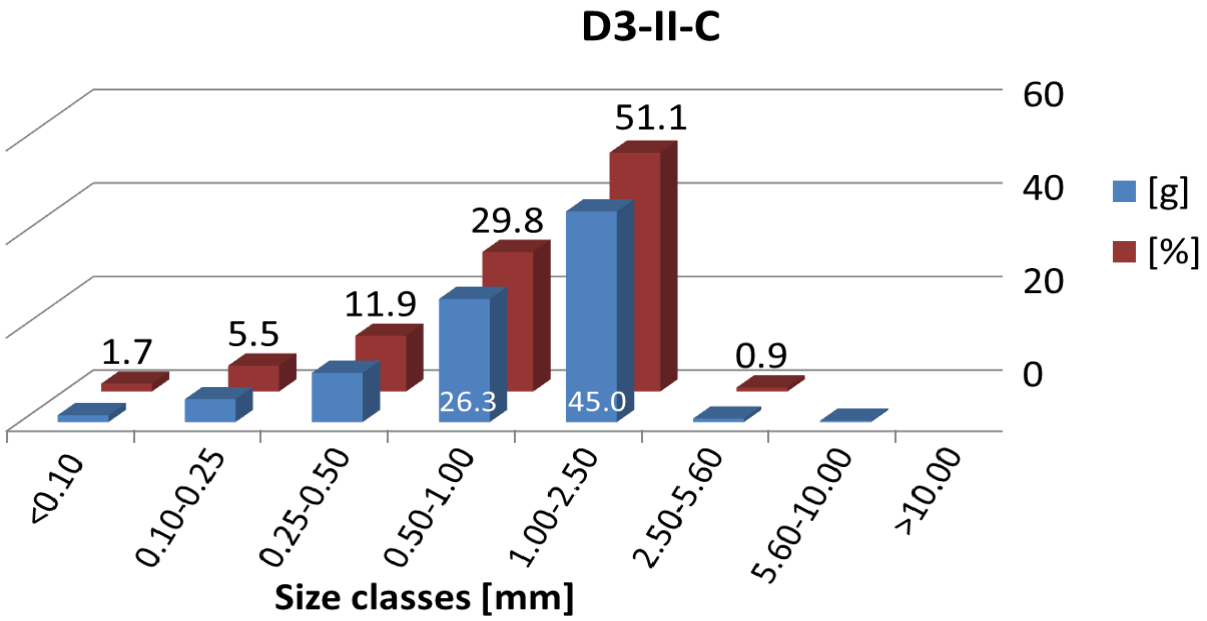

Figure 45: Size distribution of sieving analysis for D3-II-C sample.

In Figure 46 the D3-II-C sample (1.5 – 3.8 mm mesh size) has the highest percentage of particles (51.1%) in the same range as D3-II-B 1.00 – 2.50 mm, but distributed by the size of 0.5 – 1.00 mm.

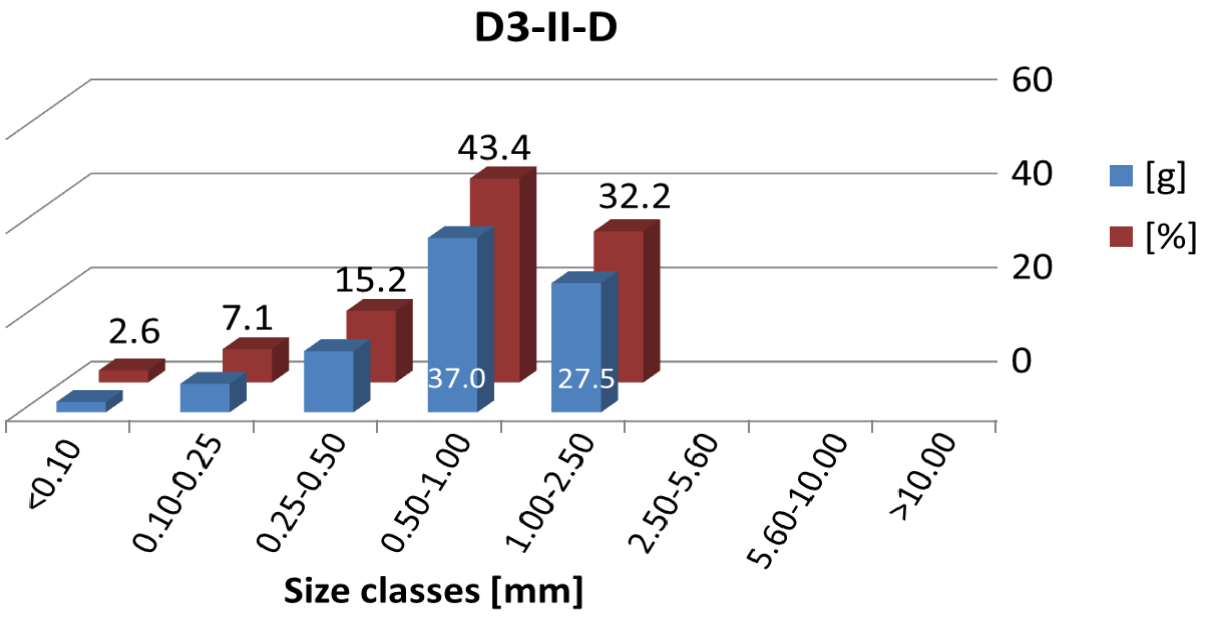

Figure 46: Size distribution of sieving analysis for D3-II-D sample.

The last sample (Figure 47) of the D3 series consists of 43.4% particles of size 0.50 – 1.00 mm, 32.2% particles of size 1.00 – 2.50 mm and 15.2% particles of size 0.25 – 0.50 mm.

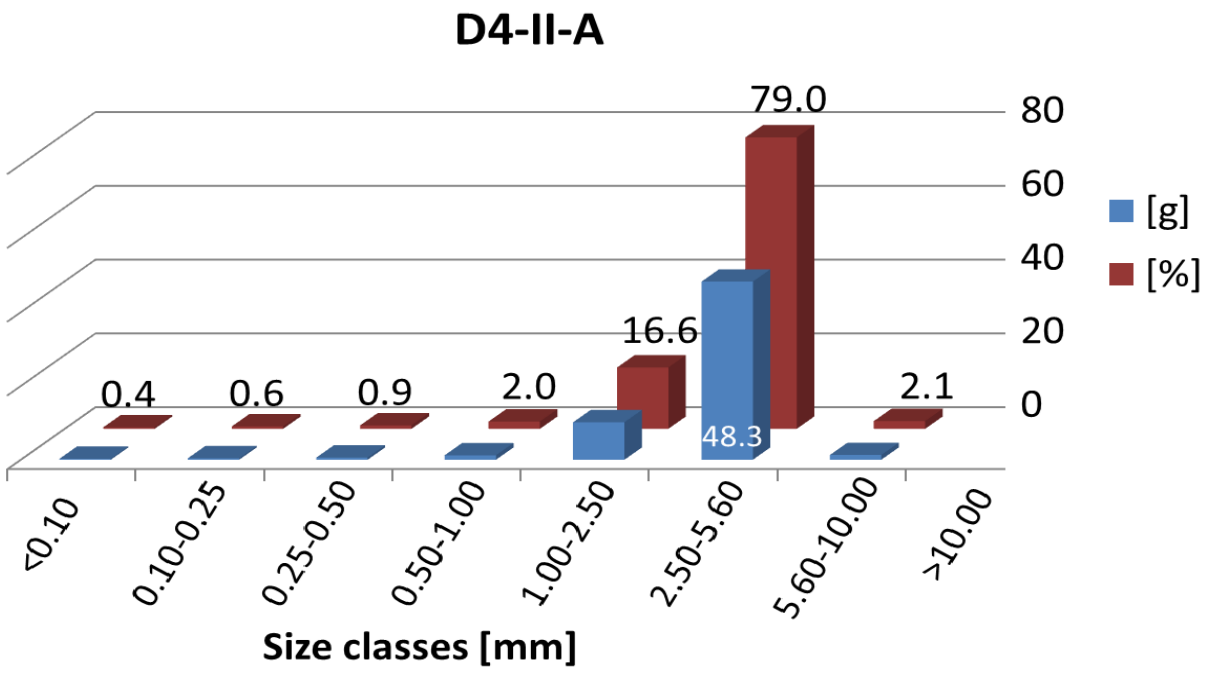

Figure 47: Size distribution of sieving analysis for D4-II-A sample.

For comparison and verification, the D4 sample was tested with result corresponding to the D3 sample. In Figure 48, the D4-II-A sample has the highest share of particles (79%) of the 2.50 – 5.60 mm size range.

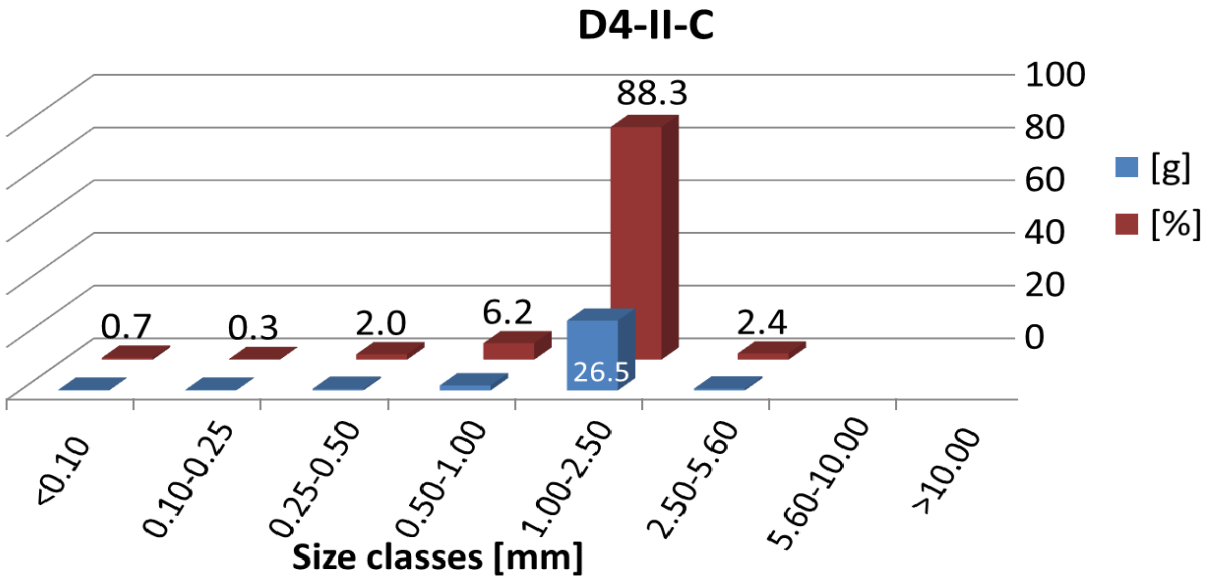

Figure 48: Size distribution of sieving analysis for D4-II-C sample.

In Figure 49, the D4-II-C sample (1.5 – 3.8 mm mesh size) the highest percentage of particles (88.3%) is 1.00 – 2.50 mm in size.

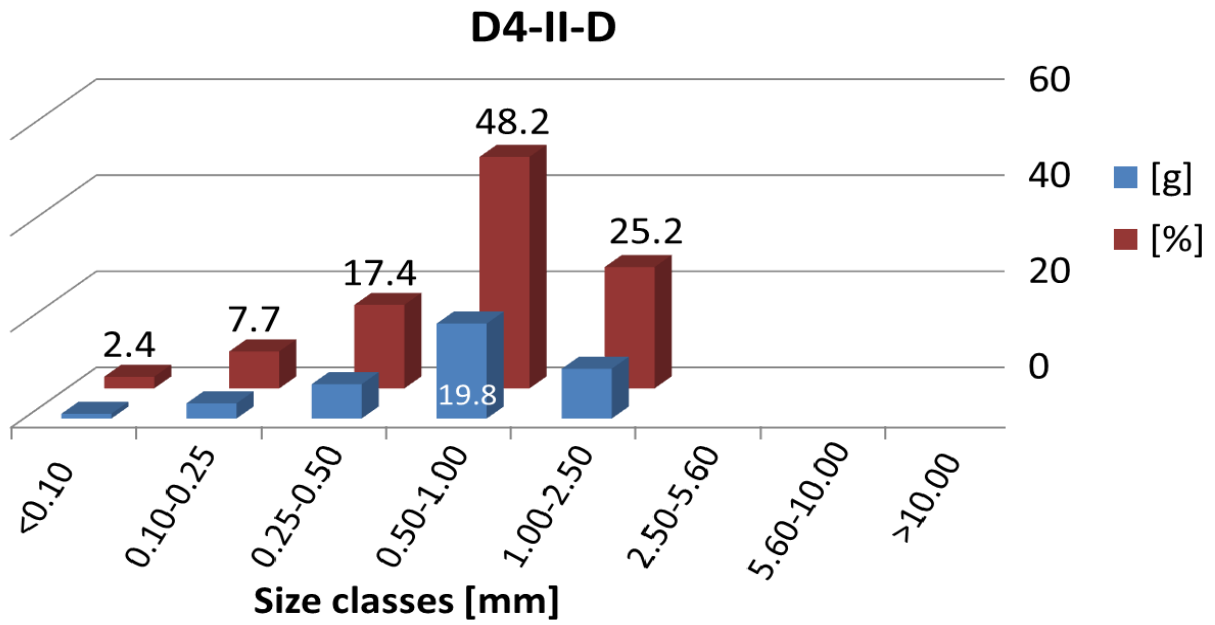

Figure 49: Size distribution of sieving analysis for D4-II-D sample.

The last sample (Figure 50) of D4 series contains 48.2% of particles from the 0.50 – 1.00 mm size range, 25.2% of particles from the 1.00 – 2.50 mm size range and 17.4% of particles from the 0.25 – 0.50 mm size range.

To summarize see Chart 12:

Chart 12: Summary of the resulted particle size distribution from the sieve analysis.

D3	D4	Particles size sieve mesh [mm]	Particles size sieve analysis [mm]	Share	
				D3	D4
D3-II-A	D4-II-A	3.8 – 8.7	2.50 – 5.60	65%	79%
D3-II-B	-	<3.8	1.00 – 2.50	89%	-
D3-II-C	D4-II-C	1.5 – 3.8	1.00 – 2.50	51%	88%
D3-II-D	D4-II-D	<1.5	0.50 – 1.00	43%	48%

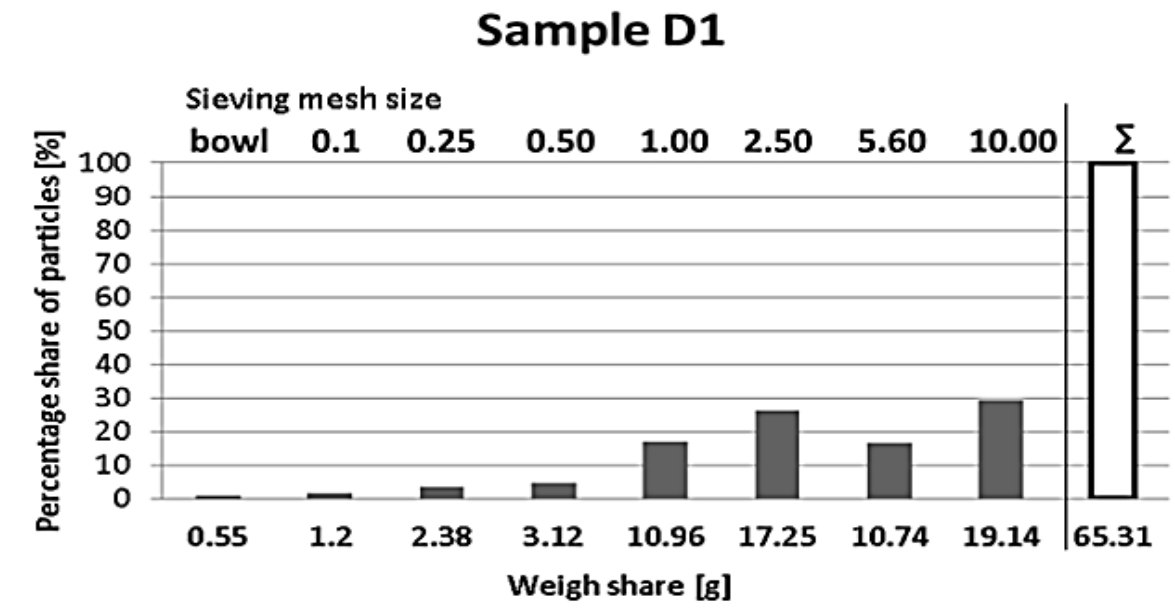

Figure 50: Illustration of mass distribution in whole sample D1 according to the sieve mesh size [%].

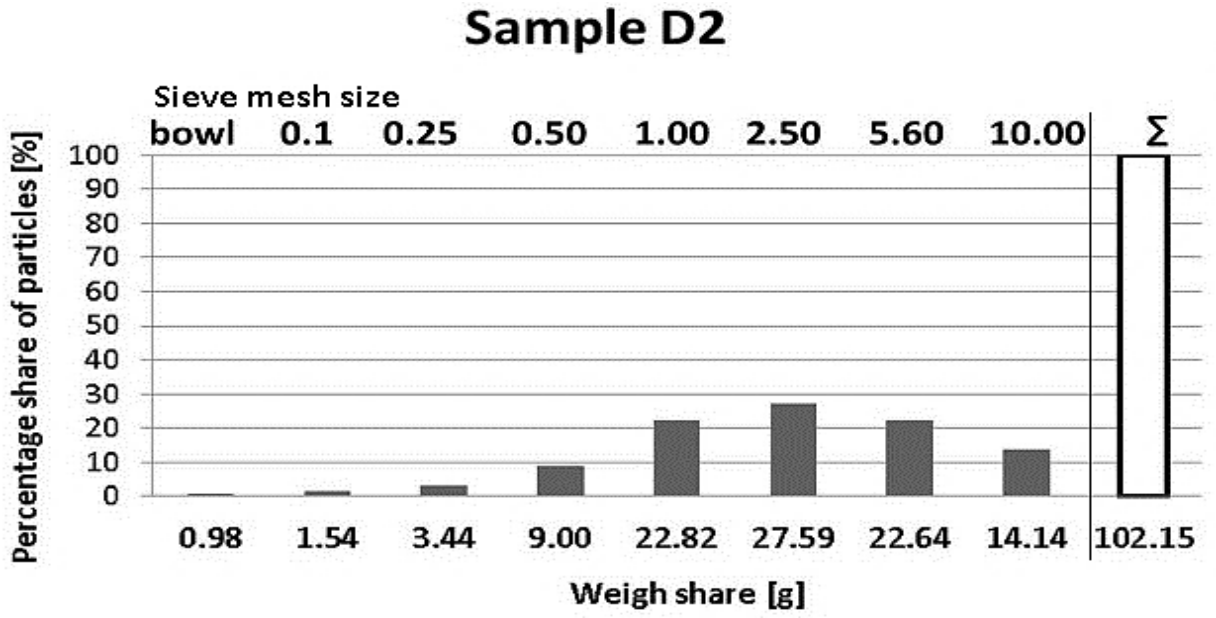

Figure 51: Illustration of mass distribution in whole sample D2 according to the sieve mesh size [%].

The sieve analysis was established also for the D1 and D2 samples. For these samples, the Rosin-Rammler analysis was not performed with the intension to compare the understandability of these two result renderings. Figures 51 and 52 show more clearly the distribution of each fraction in mass. In the D1 and D2 samples, particles were mainly 2.50 mm in size and bigger (Figure 52).

In the D1 sample, the biggest size fraction was represented by particles between 2.50 – 5.60 mm in size; and in sample D2 it was >10.00 mm.

In comparison to particle size analysis of palm shells in a different study, the biggest size fraction of particles was of the sizes 5.00 – 10.00 mm (Kaválek, Havrlan & Pecen, 2012). In another study of collective of authors Guo et al, 2012 measured the most frequent fraction size for pine, and rice straw and reed biomass briquettes in scale 0.30 – 0.43 mm, in case of beanstalk it was 0.30 – 0.18 mm. Antognoni, et al, 2013 investigated the size distribution of digested triticale and wheat biomass matter used for biogas production. Particle size of digestate both treated and untreated by digestion was less than 0.50 mm. The briquettes used in this research contain less particles than in this study. Conclusion of the Guo et al, 2012 authors was the description of a particle shape, which was a needle-like shape with large aspect ratio. The shape will be discussed in next subpart of size analysis. What should be mentioned is that particles passing through the sieve have a smaller width than the sieve mesh, but particles can be different in lengthwise. It was observed that particles have bigger length to width ratio, expressed as the aspect ratio.

Conclusion: The sieve analysis is used in many branches of science and industry. It serves to analyse particles size distribution in the sample of a given matter. In this study we investigated the particle size distribution in the digestate dry matter intended to be formed into briquettes. The sample consisted of different size groups separated by the sieving process. The most frequent size group was 0.50 – 5.60 mm. Sizes were separated correspondingly through the sieving process, thus the sample with the smallest particles (D) according to the sieve mesh, had the most frequent particle sizes of 0.5 – 1.00 mm. Sample with the biggest particles (A) according to the sieving process, had particles of 2.50 – 5.60 mm in size. Due to the fresh feedstock pre-treatment to AD and due to the digestion process itself, the particles are sized in such dimensions as mentioned above, with negligible amount of fine particles (up to 2.6%). In terms of graphic form, the histogram size distribution is easier to understand and clearly organized. On the other hand, the RR diagram is used more frequently in different scientific researches and is less laborious.

Recommendation: This research shows good approach to analysing the particle size distribution in biomass matter samples such as the digestate. It could be used for analysing the size optimization of additives in the digestate matter intended for compression.

5.5.2. Image analysis

Considerable attention was paid to the analysis of the digestate particle size. It was examined in two ways, first electronic, using the image analysis by the NIS elements program and second using digital callipers (with a resolution of 0.01 mm), just for physical reference.
The length, width and area of each particle were measured electronically. The obtained data were statistically projected into plots and normal distribution using the STATISTICA 12 program. In this method, the surface area was measured directly as well. The figures show that both methods of measurement are suitable under the assumption of normal distribution of the sample (measured values of particles length). A similar result can be obtained also for the width and height of the individual particles (Rawle, 2003).

Length

First, the D3-II-A sample is described by graphs of normal distribution histogram, normal p-graphs and the box plot (Chart 13), where we can see that particles in range of 5 – 10 mm have the highest occurrence. Some of particles are out of distribution curve and thus there are some exceptions with lengths of 40 – 50 mm. In average particles of 11.59 mm in length represent this group. But the scale of sizes is very large varies from the smallest particles (4.90 mm) to the biggest ones (40.25 mm). The standard deviation is 6.58 mm.

Width

For the width dimension the most frequent are particles in range of 1 – 2 mm. The distribution in this case is more normal and the standard deviation is lower (0.78 mm). The average width of the particles is 1.72 mm and the size range varies from the minimum value of 0.56 mm to the maximum of 4.80 mm. The values of width obtained by the image analysis and the calculated average value can show the accuracy of measuring. The data of this sample, according to the statistics, are almost clinically significant. The standard error of measurement of the individual particle dimensions and their mass was, when using a higher precision procedure, within the range of several percent.

Chart 13: Statistical data of the length and width dimensions from the image analysis. Sample D3-II-A (particle size 3.8 – 8.7 mm).

D3-II-A	
WIDTH (mm)	**LENGTH (mm)**
N = 60	N = 60
AVERAGE= 1.72	AVERAGE= 11.59

MINIMUM= 0.56

MAXIMUM= 4.80

STD= 0.78

MINIMUM= 4.90

MAXIMUM= 40.25

STD= 6.58

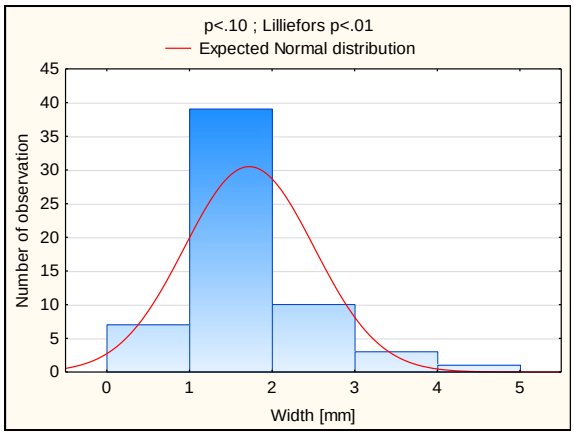

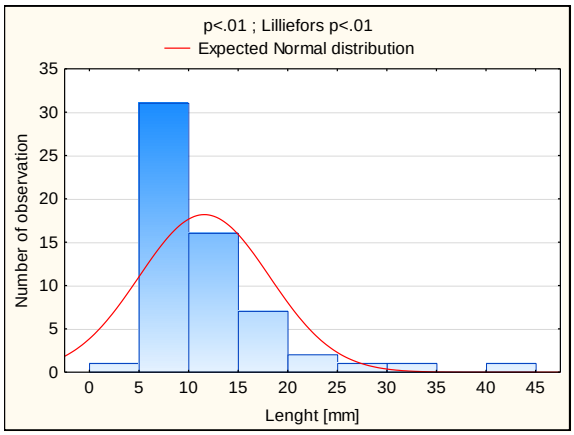

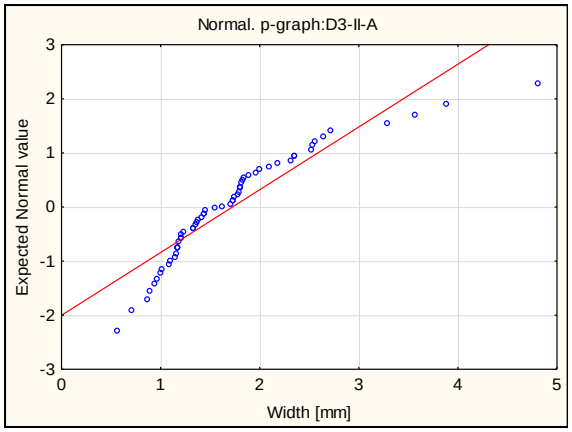

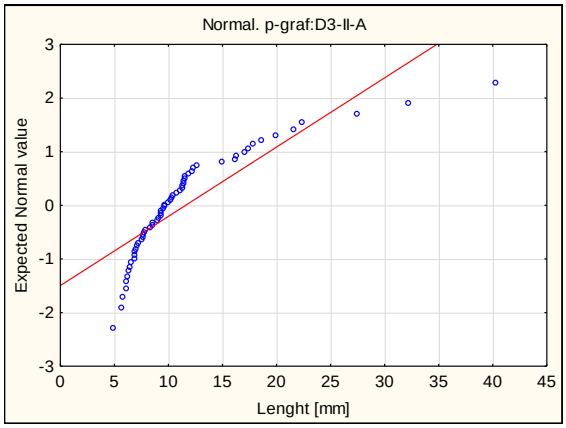

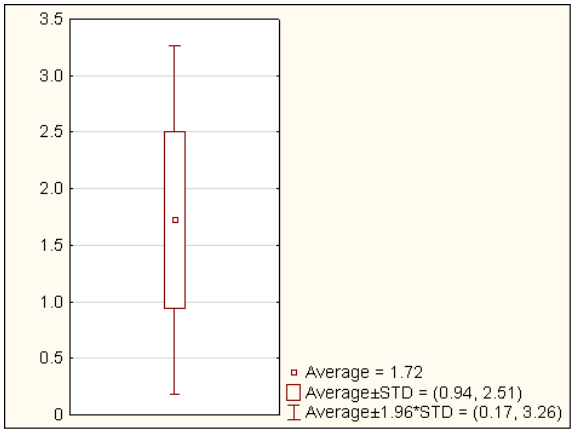

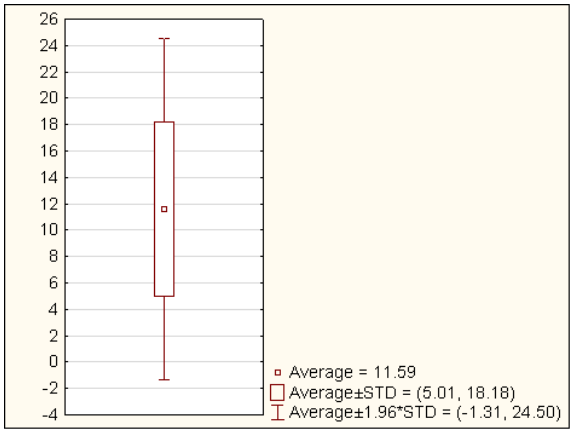

Data of D3-II-C (Chart 14) according to the statistics are not moderately significant. In case of D3-II-C, the sample values are lower than those from the D3-II-A sample. The average length was 6.50 mm and the width 0.86 mm. The length varies in the range of 2.60 – 13.25 mm with standard deviation of 2.10. The width was in the range of 0.12 – 2.01 mm with standard deviation of 0.40. In this sample, the distribution is more or less normal as well.

Chart 14: Statistical data of the length and width from the image analysis. Sample D3-II-C (particle size 1.5 – 3.8 mm).

D3-II-C	
WIDTH (mm)	**LENGTH (mm)**
N = 60	N = 60
AVERAGE = 0.86	AVERAGE = 6.50
MINIMUM= 0.12	MINIMUM= 2.60
MAXIMUM= 2.01	MAXIMUM= 13.25
STD = 0.40	STD = 2.10

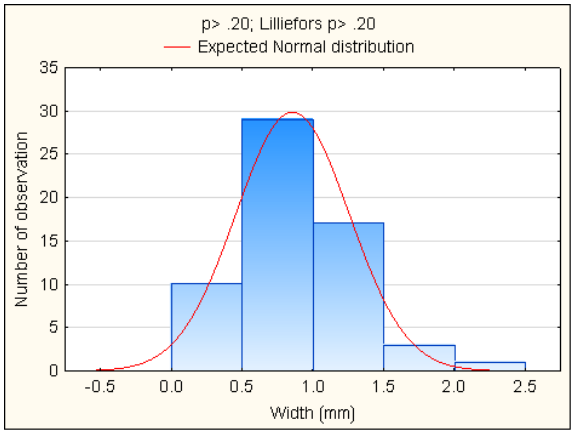

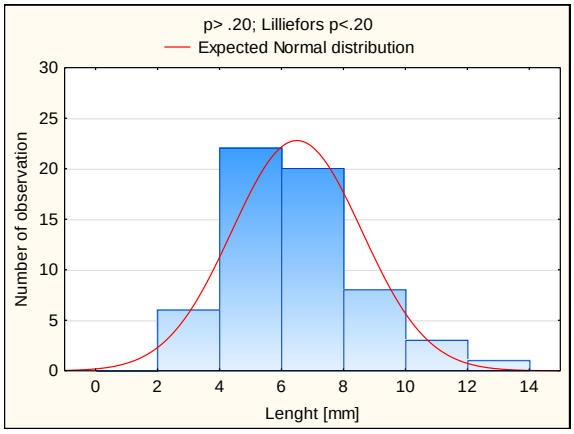

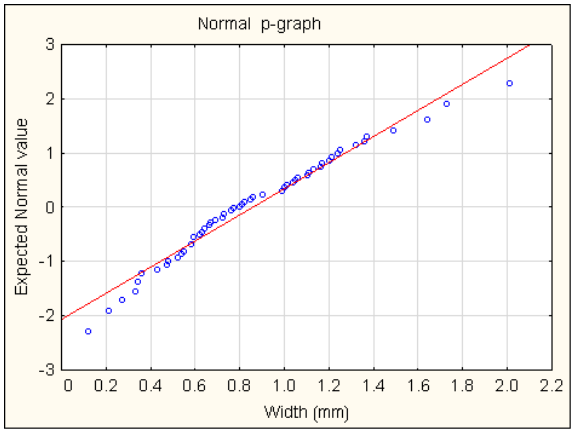

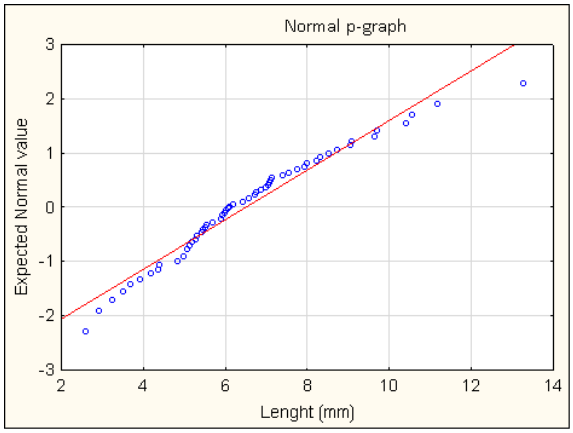

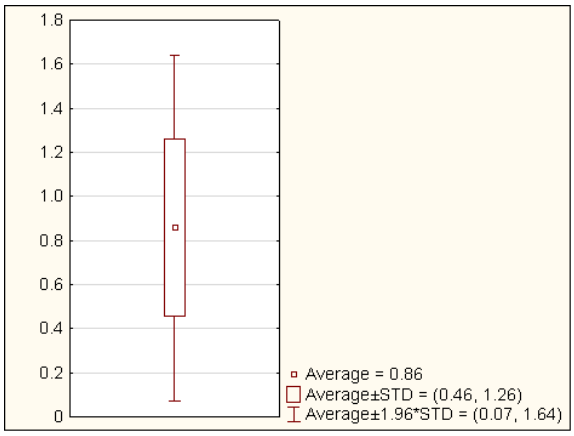

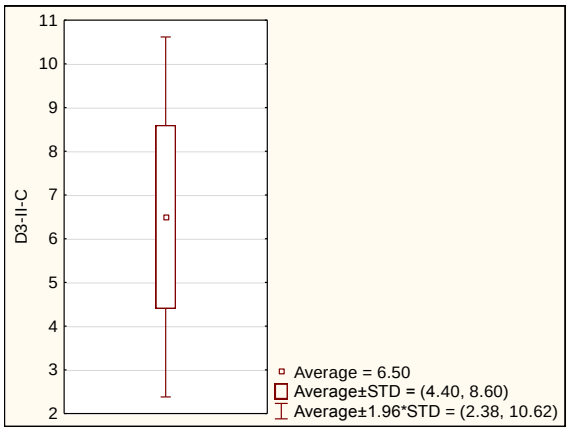

Chart 15: Statistical data of the length and width obtained by the image analysis. Sample D3-II-D (particle size <1.5 mm).

D3-II-D	
WIDHT (mm)	**LENGTH (mm)**
N = 60	N = 60
AVERAGE= 0.42	AVERAGE = 4.01
MINIMUM= 0.08	MINIMUM= 1.86
MAXIMUM= 0.99	MAXIMUM= 8.33
STD = 0.20	STD = 1.51

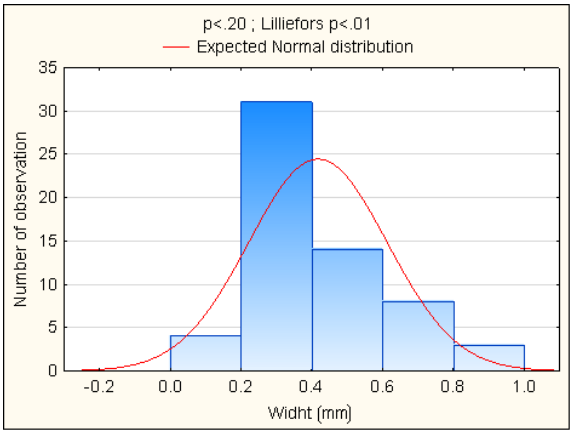

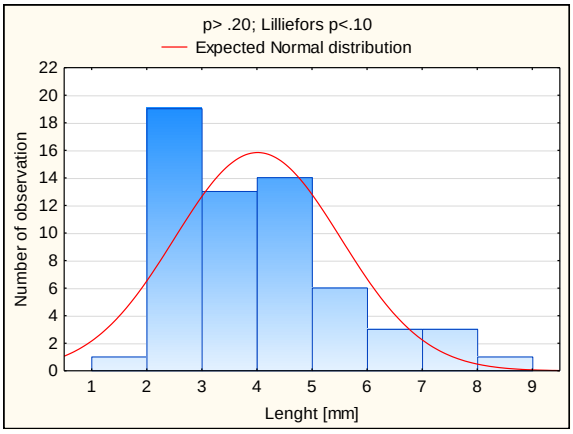

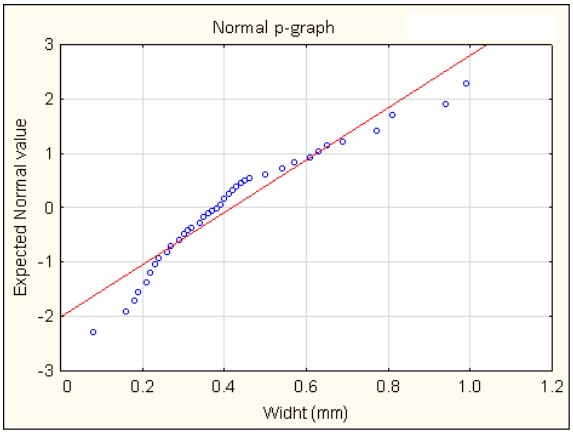

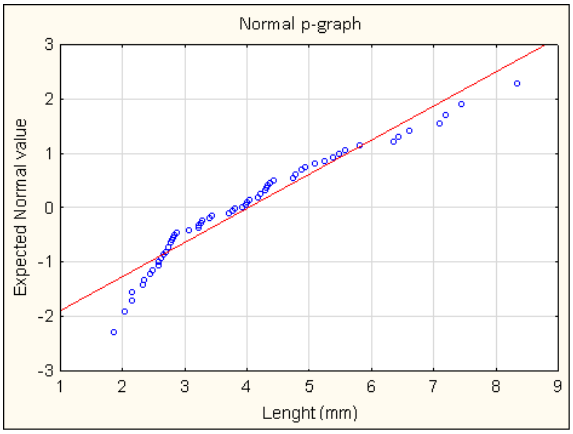

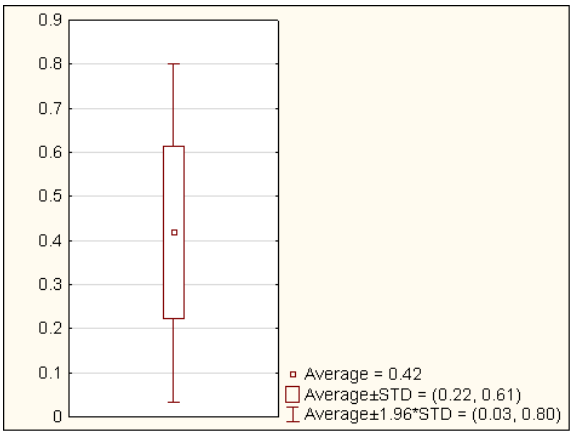

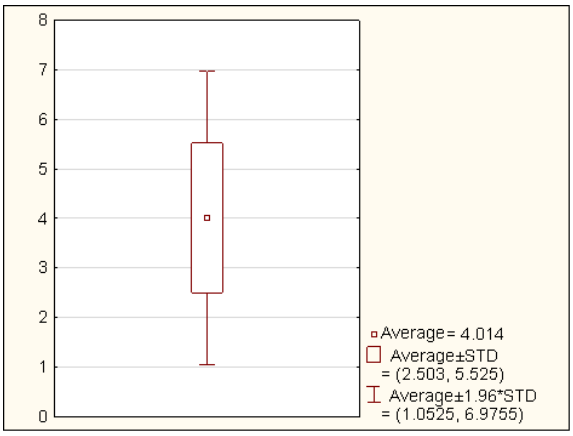

The data of the D3-II-D sample (Chart 15) according to statistics are not moderately significant for length and a slightly incline towards significance for width. The values of the D3-II-D sample are the lowest. The average length was 4.01 mm and the width 0.42 mm. The length varied within the range of 1.86 – 8.33 mm with the standard deviation of 1.51 mm. The width was within the range of 0.08 – 0.99 mm with the standard deviation of 0.20 mm. For this sample, the distribution is also more or less normal.

The following box graphs (Figures 53 and 54) describe the average values of length of all measured samples, namely the D3-II-A, C, and D. The longest particles are in sample A, but with the higher value of STD. There is a very perceptible difference between samples A and C. And even more obvious difference between samples A and D.

The box graphs illustrate the comparison of the average values of length, width and area. The sample with the longest particles is D3-II-A; the same result is in case of width and area.

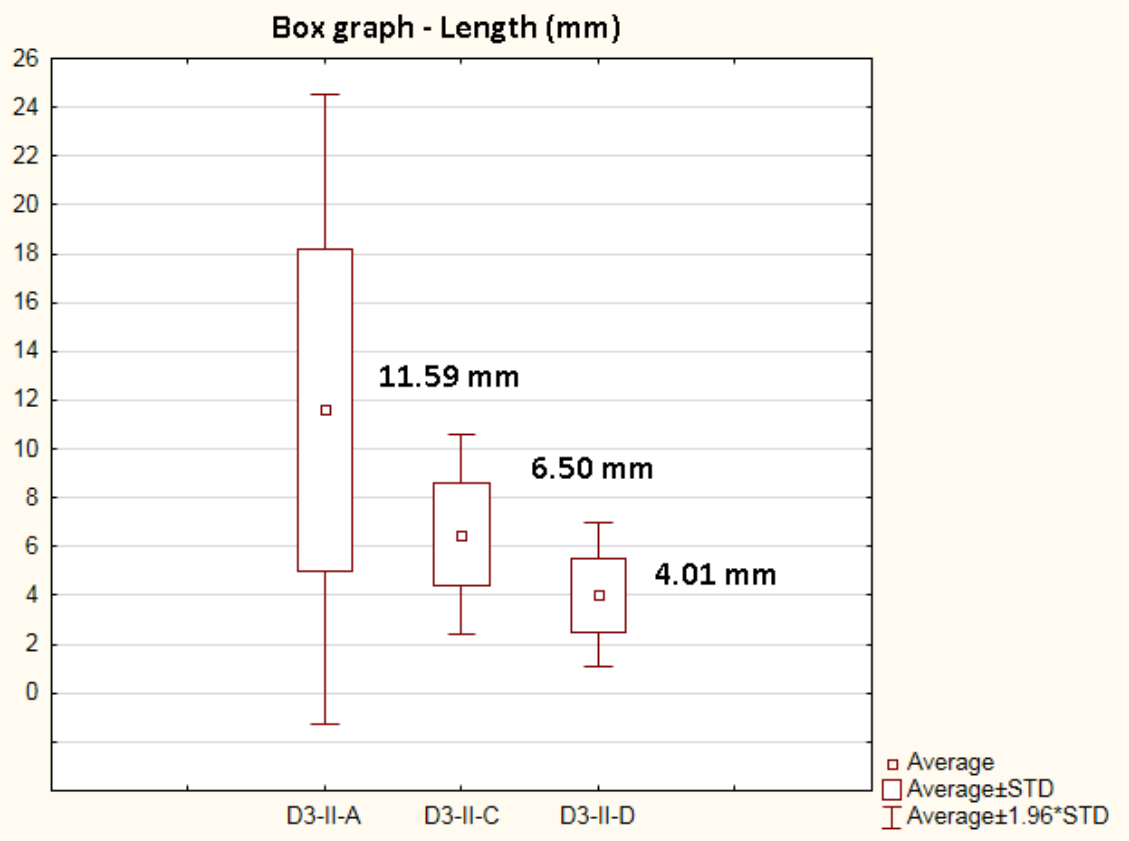

Figure 52: Box plot of length for three samples D3IIA, C, D

The shortest and the smallest particles in every aspect are those in the D3-II-D sample. These results are even listed in the chart-form (see Chart 16) supplemented by the aspect ratio average values.

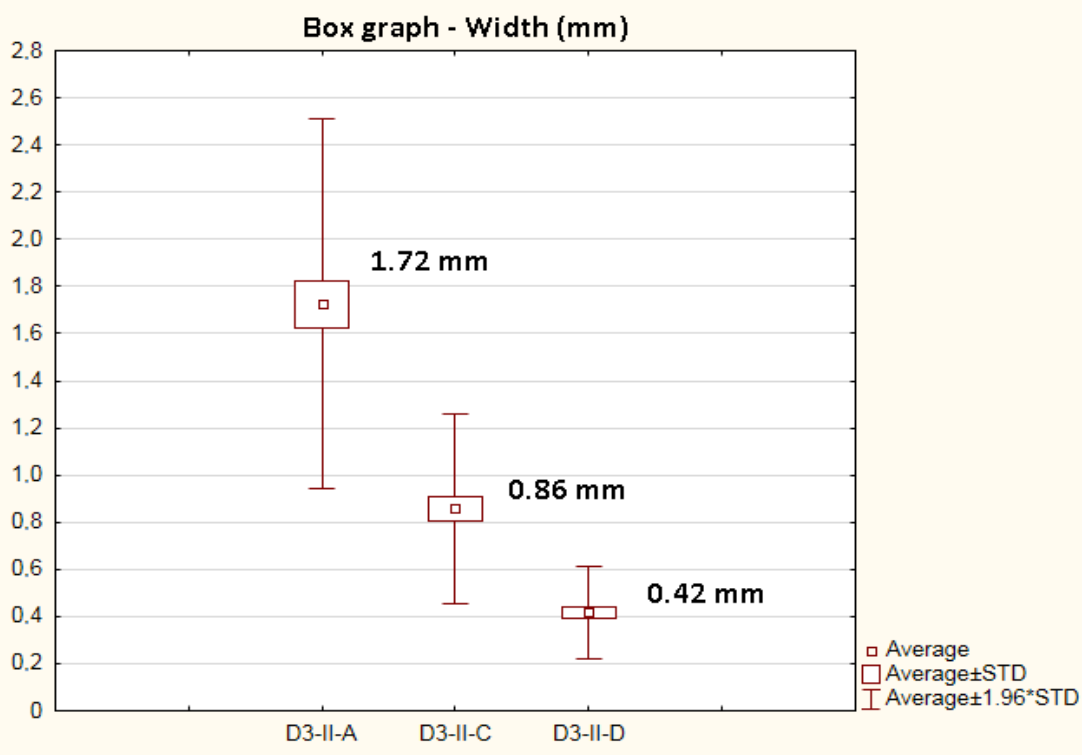

Figure 53: Box plot of length for three samples D3-II-A, C, D

Chart 16: Left – the image analysis shows average values and aspect ratio. Right – sizes of particles according to mesh size.

	LENGTH [mm]	WIDTH [mm]	AVERAGE A
D3-I	-	-	-
D3-II-A	11.6	1.7	6.7
D3-II-C	6.5	0.9	7.6
D3-II-D	4.0	0.4	9.5

SAMPLE	MESH SIZE [mm²]
D3-I	>8.7
D3-II-A	8.7-3.8
D3-II-C	3.8-1.5
D3-II-D	<1.5

The size and shape of the digestate particles affect average density of briquettes toward its higher values (Hann & Stražišar, 2007). The aspect ratio in this study is within the range of 6.7 – 9.5. In the Guo et al, 2012 study, the aspect ratio was in the range of 2 – 9, which refers about the shape. The higher the aspect ratio is, the longer the particle. If we compare approximately the same size fraction, their aspect ratio varies in 3 – 7. This result shows high variability of particle shapes. In our study prevails the shape of higher length dimension - the needle-shaped particles. Particles in sample D2 are also longer and straighter and thus form less compact briquettes, whereas in the D1 briquettes is less space between the individual particles. The influence of particle size and shape also reflects in the value of abrasion.

Conclusion: Upon the basis of the image analysis performed, the compared three samples of digestate matter showed particle distribution in terms of distinguishing according to the dimensions. The longest and the widest particles were present in the D3-II-A sample. However, this data had a higher value of STD (1.50 – 6.60 mm). The average length dimension of the D3-II-A sample was 11.59 mm; this is the longest measured average length for the A size group (3.80 – 8.70 mm sieve mesh). The width dimensions of the same sample were 1.72 mm in average. It may seem illogical as the length of the particle exceeds the sieve mesh aperture size, but particles of longer lengths can go through the sieve mesh when properly axially oriented. As expected, the smallest particles were observed in the D3-II-D sample, having the shortest and the narrowest dimensions.

The image analysis, compared to the sieve analysis, is based on direct measurement of the particle dimensions, which together with the thickness will be more accurate method of particle size distribution assessment. With all dimensions known, the gravimetric measurements won't be necessary due to the possibility to calculate the particle weight from the given dimensions. As per the previous study by Černá & Pecen, 2015, and as it is illustrated in Chart 17 in the "Appendices" chapter for the Miscanthus material, the aspect ratio was calculated to confirm the shape of particles numerically. The higher the A parameter the longer the particle. In this study particles had needle-like shape with prevalent length dimension.

Recommendation: It is desirable to investigate all particle dimensions using different measurement method (this one is too demanding) and automate the process of particle measuring, then compare it with the sieve analysis results.

5.5.3. Others

For calliper measurement, it is important to realize that samples evaluated by this method were particles bigger than 1 mm and one parameter prevailed (e.g. length). For particles smaller than 1 mm, it is necessary to use another method (there is no prevalent dimension). This method is partially outlined in the document: "Dependence of the mean and the confidence interval of oilseed sets on its size and the method of statistical processing" (Pecen et al, 2014). The length, width and thickness of each particle were measured using the calliper. Based on this data the volume and density of each particle was calculated. The mass of each particle was weighted using a balance with a resolution of 0.1 mg. The particle thickness values were used for calculation of volume and density in the applied image analysis method. The D1 digestate sample was used as the model material for detailed particle size analysis,

respectively its size fraction of 1 mm from the sieve analysis. The result mean values are listed in the Appendices, including the calculated differences for area, volume and density.

Conclusion: The calliper measuring is applicable only on particles of a given dimension, in this case it was 1 mm and bigger. This method was very laborious and the accuracy is influenced by human factor. However, the thickness dimension is impossible to measure in this lab method via image analysis for this type of particle shape.
This measurement was the best solution of measuring the thickness.

Thus we recommend finding a method of measuring the thickness dimension of needle-like particles in easier or automated way.

5.6. Water sorption

The briquettes surrounded by soil, are showing consistently very high value of sorption progress, as proven by experiment of Pecen et al, (2013) comparing the sorption properties of other materials as well. The briquette material is the essential aspect for water uptake amount; important factors are also the dimensions of pressed particles and the compression force used as described by Tabil[a] et al, (2011); Chen, et al, (2015). All these factors, including deposition of the briquettes in soil, the technology and conditions of briquette production used, were same for both the digestate and the woodchip materials. Thus there is only one variable - the material. Figure 54 shows that both the digestate samples have similar water uptake. Both the digestate and the woodchip briquettes show similar initial sorption water uptake (Pecen et al, 2015; Černá, 2015; Černá & Pecen, 2015), but after about ten days the water sorption by the briquettes practically stops, reaching different values for different briquette materials. In this final phase, the briquette moisture and soil moisture contents are in balance (Singh, 2004). It should be noted that both the mechanical and physical sorption occurs, which is dependent mainly on the texture of the briquettes. Figure 55 shows that the change of the soil moisture (between the beginning and end of the experiment) is very small compared to the briquette moisture change (Pecen et al, 2015). This pattern of sorption is very similar in repeated tests (Černá, 2015). Therefore, the water sorption data in Chart 6 are expressed as average values. Figure 54 is well illustrating the differences in water sorption between briquettes made of different materials. The woodchip briquettes have lower density and thus accept higher content of water compared to the digestate briquettes of higher density. The graph curve is similar in both D1 and D2, WCH samples. Less difference is in sorption by soil over the time.

According to the Bergeret, 2011 research, the dependency of water absorption on fibre type was observed.

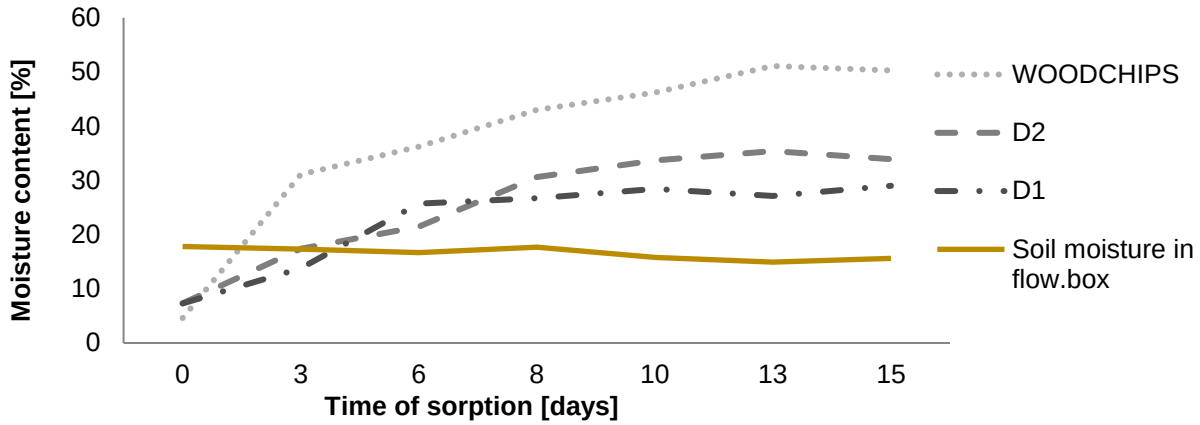

Figure 54: Progression of water sorption by D1, D2 and WOODCHIPS briquettes in soil environment.

In comparison to previous research regarding water adsorption into the briquette mass, the digestate materials showed higher volume of water intake (543 cm^{-3}), the digestate with additives like Zeolites or Lime showed the fastest time to reach the full saturation n 147 – 165 minutes of measuring. The digestate has proven its ability to adsorb liquids while multiplying its mass even five times in open environment (not limited). In a closed environment, such as the soil, the volume of water absorbed increased by 200 ml. The initial moisture content increased from 8 – 10% to 20% (Černá, 2015). In another measuring of Pecen, Piksa & Zabloudilová 2014 the sorption properties of different material briquettes were compared. The briquettes were made of Miscanthus, hemp and digestate and the sorption was studied in fully soil-like closed environment. Over a 15 day period the highest moisture content was measured in the Miscanthus briquettes (62.7%), but in the other materials it was 59-60%. The surrounding soil kept the same level of the moisture as in this study. In the open environment, the sorption was completed during the first 20 minutes.

Conclusion: The digestate as well as other fibrous materials in the briquette form is a very good sorbent agent. As a biofuel it contains high amount of ashes and minerals, so it is nonsense to combust such nutrition-rich material. The briquette can increase its volume even five times by adsorbing sufficient volume of liquid which could be useful in agriculture. However, the Miscanthus material can adsorb higher moisture volume in less time, the digestate, except the sorption potential, contains high volume of fertilising organics and minerals as investigated. Moreover the digestate is a very good material for compression with possibility to add some additives, as conditioners to the soil. This fact supports the idea of

using the digestate briquettes as a fertiliser and a soil additive. Other studies tested the adsorption capacity of the biomass to adsorb heavy metals and other substances (pesticides) from the soil (Mukherjee et al, 2016; Baig et al, 1999). This would have another possible use, not just in the agriculture sector.

Recommendation: It is desirable to perform a long term experiment in the soil to investigate the nutritional, sorption and amendment properties of digestates of variable composition. Laboratory tests could be performed as well to investigate the capacity of the digestate briquettes to adsorb chemical substances.

In the terms of particle size, differences of sorption by briquettes made of different particle size groups (this requires high amount of the matter) can be observed. Also tests for observing the surface areas (N_2 or CO_2) of inner particles can be performed.

6. Resume

The digestate nutritional composition is based on the feedstock input to the AD process. The digestate has high content of nutritious matter with high ratio of fibrous structures but high content of ashes due to which is not suitable as a good fuel source, but thanks to high nitrogen content it is a very valuable fertiliser. Due to high share of organic matter (up to 97%) ash and nitrates, the digestate is used rather in agriculture for fertilising. To avoid issues of high storage space need associated with the liquor digestate, the possibility to compress the dehydrated form makes sense. This research has shown that the digestate is a good matter for compression of exact shapes of high density varying between 0.770 – 0.980 g cm^{-3}, what is a good value for biomass materials. Future experiments should compare more samples of digestate of different feedstock materials having different ratio of animal and plant material contents in terms of particle size distribution and nutritional characteristics influenced by the pre-treatment processes affecting the properties of briquetting and the final product.

The digestate material is a good material for compression. It demonstrates high density values. If considering adding additives, e.g. zeolite and lime, the digestate briquette density value exceeds the water density and will be comparable to wooden briquettes. This could be successfully utilized in agriculture to prevent acidification of soil if considering incorporation into the soil. The average density value calculated from the briquette mass and volume depends mainly on the applied pressure, and the briquette density increases with increasing working pressure. The briquette characteristics are closely related to the feedstock composition, the compression techniques and the settings and the possibility to add some mixtures and additives compliant with the standards. Because the digestate itself has been found a proper material for compression with high density value, it is desirable to exploit the possibilities of compressing more different conditioning additives than the zeolite and lime used. The best particle composition (powders, granules) of the additive should be assessed to support the final structure of briquette improving physical properties, e.g. the density durability, hardness and water sorption.

The durability tests have proven the decreasing tendency of successive abrasion rates. This tendency is caused by sharp initial edges of the briquettes. The influence of the particle size and shape on the briquette durability is demonstrated presuming that the abrasion of the different briquette samples is performed by the same way and at the same device. Thus the durability test performed represents the "coherence" of briquettes. It was proven that the

particle sizes are an important variable in case of abrasion rate (the D1, D2 and D3-II-C, D samples show less abrasion than those with bigger particles such as the D3-I and D3-II-A) and later in text even in case of hardness. This was described as coherence between smaller particles and decreased penetration into the briquette matter. The rate of abrasion of the digestate briquettes depends primarily on material properties of the briquettes. The size and the shape of particles of the uncompressed digestate also have a significant influence on the briquette durability. Particles with one diameter longer (plate particles) are bound in the digestate briquettes with a smaller force between the particles, thus the briquette fragments are readily released. Comparison of abrasion based on the fraction distribution was not investigated and is recommended for further research. The previous research experiences show that the biggest particles of the digestate briquettes have higher rate of abrasion and even sorption capacity and lower stability.

It is recommended to perform this testing on more samples for longer time period on digestate briquettes differentiated by various particle sizes considering the possibility of mixture and additives use. The aim should concentrate on the significance of the particle size influence on the durability and other variables, e.g. moisture content, time, compression procedure, temperatures etc.

The measurement of hardness by the hardness tester using the Shore scale is not typical for briquettes. Anyway, values of hardness are ranging high (89.7 – 98.9). Higher values of Shore hardness test were obtained at points on perimeter (98) that on diameter. Observed relation of particle size and hardness tested was obvious; samples with smaller particles had higher values of hardness than those composed of bigger particles. It could be said that the smaller particles the higher the hardness. This is caused by the process of briquette-making, where the compression force (by the wall of compression chamber) is causing the friction along the perimeter particles, thus increasing the temperature of the briquette as well as the chamber wall temperature. If compressed material contains lignin polymers then lignin serves as the particle binder. That is why the perimeter areas are smooth and harder than the diameter structures. The digestate briquettes, according to the tests, are coherent and relatively hard. The range of these properties is influenced by the particle size used for briquette-making. The particles of sizes < 1.5 mm and between 1.5 – 3.8 mm demonstrated better values. It is advisable to repeat this hardness test with more representative samples and with more different measuring methods. It could reveal the relation between the briquette materials, e.g. digestate

with different feedstock or the digestate enriched with additives. Finally, it the relation between particles size and hardness should be studied.

From the sieve analysis of the digestate solid matter which was evaluated by Rosin-Rammler method, the size group in general was 0.50 – 5.60 mm. Sizes were distributed correspondingly by the sieving process, thus the sample with the smallest particles (D) according to sieve mesh had the most frequent particle size of 0.5 – 1.00 mm. Sample with the biggest particles (A) according to sieving process had particles of 2.50 – 5.60 mm. Due to the pre-treatment of fresh feedstock prior to the AD and due to the digestion process itself, the particles are sized as already mentioned, with negligible amount of fine particles (up to 2.6% only). In terms of the graphic form, the histogram size distribution curve is easier to understand and clearly organized. On the other hand, the RR diagram is used more frequently in different scientific researches and is less laborious. In different samples (D1, D2) the representation of the 0.25 – 5.6 mm sizes of particles was the highest.

This research shows a reasonable approach of analysing the particle size distribution in biomass matter samples such as the digestate. It could be used for analysing the size optimization of additives in the digestate matter intended for compression.

The particle shape was not the main object of testing, thus the aspect ratio was calculated showing prevalence of particles with one dimension parameter bigger – this dimension is length (mm). The aspect ratio varied in range of 6.7 – 9.5, characterizing needle-like shape. The image analysis has shown normal distribution in most samples; however in some cases two dimensions were significantly out of bounds. The most frequent length range was 5 – 10 mm and width 1 – 2 mm. This shows that the length dimension is the quintuple of the width dimension.

The digestate, as well as other fibrous materials in briquette form, is a very good sorbent. As a biofuel it contains high amount of ashes and minerals, so it is inconvenient to combust such nutrition-rich material. The water sorption of briquettes placed into the soil and its speed depends mostly on the material type and partly on the particle size. The woodchip briquettes have been found better water sorbents than the digestate ones, but the difference is only up to 10%. While the initial soil moisture is not decisive for achieving constant moisture of briquettes, which occurs within approximately ten days from putting the briquettes into the soil, the briquettes can increase its volume even five times by adsorbing sufficient volume of the liquid. The briquette moisture content at this stage is always significantly higher than the

surrounding soil moisture content. The Miscanthus material can adsorb more moisture in less time. The digestate, beside its sorption potential, was found to contain high volume of fertilising organics and minerals. Moreover, the digestate is a very suitable material for compression with the possibility to add some additives as enrichment agents to the soil. This facts supports the idea of adding the digestate briquettes into the soil as a fertiliser and conditioning matter. Other studies surveyed the adsorption capacity of the biomass to adsorb heavy metals and other substances (pesticides) from the soil. This could be another possible application, not just for the agriculture sector.

It is desirable to perform a long term experiment with the soil to investigate the nutritional, sorption and amendment properties of the digestates of variable composition. Lab tests could be also performed to investigate the ability of the digestate briquettes to adsorb chemical substances. In terms of particle size, differences of sorption could be observed between briquettes made of different particle size groups (this requires high volume of the matter). Tests observing the surface areas (N_2 or CO_2) of the inner particles can be performed as well.

The facts stated above imply that the results would be implemented rather in practice than in the general scientific knowledge, even though each finding can benefit both sectors. Determining the texture properties in 3-D environment is not a simple issue, and if we could at least partially solve it, this method could be applied elsewhere. Quite a large part of the work deals with the methods of image analysis and the processing of the input image information. This study suggested the method that allows analysing particle size distribution in samples and describes other briquette properties, which can be useful for next research and commercial applications.

7. References

Abubaker, J., K. Risberg and M. Pell, 2012. Biogas residues as fertilisers – Effects on wheat growth and soil microbial activities. *Applied Energy*. vol. **99**, pp. 126 – 134.

Adapa, P.K., Tabil, L.G., Schoenau, G.J., Crerar, B., & Sokhansanj, S. 2002. Compression Characteristics of Fractionated Alfalfa Grinds. *Powder Handling and Processing*, **14**(4), pp. 252 – 259.

ADBA, Anaerobic digestion & biogas association. **2012**. Practical guide to AD-Chapter 7, London, pp. 82 – 90, (in United Kingdom).

Ahlgren, S., Bernesson, S., Nordberg, Å. & Hansson, P-A. 2010. Nitrogen fertiliser production based on biogas – Energy input, environmental impact and land use. *Bioresource Technology* **101**(18), 7181–7184.

Amon, T., Amon, B., Kryvoruchko, V., Zollitsch, W., Mayer, K. & Gruber, L. 2007. Biogas production from maize and dairy cattle manure: Influence of biomass composition on the methane yield. *Agriculture, Ecosystems & Environment* **118**(1 – 4), 173 – 182.

Antognoni, S., Ragazzi, M., Rada, E. C., Plank, R., Aichinger, P., Kuprian, M., & Ebner, C. 2013. Potential effects of mechanical pre-treatments on methane yield from solid waste anaerobically digested. *International Journal of Environmental Bioremediation & Biodegradation*, **1**(1), 20 – 25.

Antwi-Boasiako, C. & Acheampong, B. 2016. Strength properties and calorific values of sawdust-briquettes as wood-residue energy generation source from tropical hardwoods of different densities. *Biomass and Bioenergy*, **85**: 144 – 152.

Ashiya, P., Rai, N., Rathore, D. S., & Jain, S. 2015. Influence of Chemical fertilisers and Organic fertilisers on pH and available Nitrogen content of Vermicompost with earthworm *Eisenia foetida*. *International Journal*, **3**(7), 1030 – 1036.

Baig, T. H., Garcia, A. E., Tiemann, K. J., & Gardea-Torresdey, J. L. 1999. Adsorption of heavy metal ions by the biomass of Solanum elaeagnifolium (Silverleaf night-shade). *In Proceedings of the 1999 Conference on Hazardous Waste Research* (pp. 131-142).

Bergeret, A. 2011. Environmental-friendly biodegradable polymers and composites. *Integrated waste management, 1*.

Bitra, V., Womac, A., Chevanan, N., Miu, P., Igathinathane, C., & Sokhansanj, S. et al 2009. Direct mechanical energy measures of hammer mill comminution of

switchgrass, wheat straw, and corn stover and analysis of their particle size distributions. *Powder Technology*, **193**(1): 32 – 45.

Brezani, I., & Zelenak, F. 2010. Improving the effectivity of work with Rosin-Rammler diagram by using MATLAB (R) GUI tool. *Acta Montanistica Slovaca*, **15**(2), 152 – 157.

Brožek, M. 2013. Study of briquette properties at their long-time storage. *Journal of Forest Science* **59**(3), 101–106.

Brunerová, A., Pecen, J., Brožek, M., & Ivanova, T. 2016. Mechanical durability of briquettes from digestate in different storage conditions. *Agronomy Research*, **14**(2), 327-336.

Canam, T., Town, J., Iroba, K., Tabil, L., & Dumonceaux, T. 2013. Pre – treatment of lignocellulosic biomass using microorganisms: Approaches, Advantages, and Limitations. *Sustainable degradation of lignocellulosic biomass-Techniques, Applications and Commercialization. In Tech publisher. DOI, 10*, 55088.

CCSi. 2006. *Duromatters! Basic Durometer Testing Information*. [Accessed: 20 March 2016] Retrieved at: www.ccsi-inc.com/t-durometer-testing.htm

Černá, I. 2015. *Partially dehydrated digestate from biogas plant*. Saarbrücken: LAP LAMBERT Academic Publishing. ISBN: 978 – 3 – 659 – 69651 – 0.

Cerna, I., & Pecen, J. 2015. DETERMINING MEAN VALUE OF MISSING PARTICLE SIZE FOR WEIGHT CALCULATION. In *14th International Scientific Conference Engineering for Rural Development, Jelgava, Latvia, 20 – 22 May, 2015* (pp. 195 – 201). Latvia University of Agriculture.

ČSN, EN. 14961-1, 2010. Tuhá biopaliva–Specifikace a třídy paliv–Část, 1.

EN ISO 17225-1. Solid biofuels – Fuel specifications and classes – Part 1: General requirements. 2015, pp. 1–64.

Chen, H. 2015. *Lignocellulose biorefinery engineering*. *Principles and Applications*. No. 74. Woodhead Publishing.

Chen, W., Peng, J., & Bi, X. 2015. A state-of-the-art review of biomass torrefaction, densification and applications. *Renewable and Sustainable Energy Reviews*, **44**: 847 – 866.

Ciolkosz, Daniel. 2015. Manufacturing process. *Pellet Process, Wood pellet Production Technology*. [Online] Magel Maschinenhandel GmbH, 2015. [Accessed: 27 April, 2015] Retrieved at: http://www.pelletprocess.de/?page_id=18&lang=en.

Comoglu, T. 2007. An Overview of Compaction Equations. *Journal of Faculty of Pharmacy*, Ankara **36**(2), 123 – 133.

Denny, P. J. 2002. Compaction Equations: A Comparison of the Heckel and KawakitaEquations. *Powder Technology*, **127**, 162 – 172.

DoE, U. S. 2006. Breaking the biological barriers to cellulosic ethanol: a joint research agenda. *US Department of Energy, Washington*.

EBA. **2015**. Biomethane & Biogas Report. *European Biogas Association* [online] [Accessed: 14 March 2016]. Retrieved at:http://european-biogas.eu/2015/12/16/biogasreport2015/

EBTP, **European Biofuels Technology Platform**. **2014**. Production of biogas (biomethane) as a biofuel in Europe. *Biofuelstp.eu* [online] [Accessed: 12 October 2015] Retrieved at: http://biofuelstp.eu/biogas.html.

Eissa, A.H.A. Gamea, G.R., El Saeidy, E.A. & El Sisi, S.F. 2013. Quality characteristics for agriculture residues to produce briquette. In *Trends in agriculture engineering*. Praha: Czech University of Life Sciences, Prague, pp. 156–162.

European Nitrates Directive (91/676/EEC.) [Acessed: 12 January 2016] Retrieved at: http://ec.europa.eu/environment/water/water-nitrates/report.html

Fernlund, J., Zimmerman, R., & Kragic, D. 2007. Influence of volume/mass on grain-size curves and conversion of image-analysis size to sieve size. *Engineering Geology*, **90**(3 – 4): 124 – 137.

FitzPatrick, M., Champagne, P., Cunningham, M.F., Whitney, R.A., 2010. A biorefinery processing perspective: treatment of lignocellulosic materials for the production of value-added products. *Bioresour. Technol*. **101**, 8915–8922.

Fletcher, A.J., 2008. Porosity and sorption behaviour. *Department of Chemical and Process Engineering, University of Strathclyde.* [Online] [Accessed: 20 April, 2013] Retrieved at: http://personal.strath.ac.uk/ashleigh.fletcher/index.htm

Gantenbein, Daniel, Joachim Schoelkopf, G. Peter Matthews and Patrick A.C. Gane, 2011. Determining the size distribution-defined aspect ratio of rod-like particles. *Applied Clay Science*. **53**(4), 538 – 543.

Gao, T. & Li, X. 2011. Using thermophilic anaerobic digestate effluent to replace freshwater for bioethanol production. *Bioresource Technology*, **102**(2): 2126 – 2129.

Gnansounou E., Dauriat A. 2016. Bioethanol [Online] [Accessed 20 May 2016]. Retrieved at: http://bpe.epfl.ch/page-34012-en.html

Grover, P. D., & Mishra, S. K. 1996. *Biomass briquetting: technology and practices*. Food and Agriculture Organization of the United Nations.

Gruszkiewicz, M., Simonson, J., Burchell, T., & Cole, D. 2005. Water adsorption and desorption on microporous solids at elevated temperature. *J Therm Anal Calorim*, **81**(3): 609 – 615.

GTOS. 2009. Biomass. *Assessment of the status of the development of the standards for the Terrestrial Essential Climate Variables.* Rome: FAO.

Guo, Q., Chen, X., & Liu, H. 2012. Experimental research on shape and size distribution of biomass particle. *Fuel*, **94**: 551 – 555.

Hakeem, K., Jawaid, M., & Alothman, O. 2015. *Agricultural biomass based potential materials*. Springer International Publishing, p. 505. ISBN 978-3-319-13847-3

Hann, D. & Stražišar, J. 2007. Influence of Particle Size Distribution, Moisture Content, and Particle Shape on the Flow Properties of Bulk Solids. *Instrumentation Science & Technology*, **35**(5): 571 – 584.

Hills, D. & Roberts, D. 1981. Anaerobic digestion of dairy manure and field crop residues. *Agricultural Wastes*, **3**(3): 179 – 189.

Himmel, M., Ding, S., Johnson, D., Adney, W., Nimlos, M., & Brady, J. et al 2007. Biomass Recalcitrance: Engineering Plants and Enzymes for Biofuels Production. *Science*, **315**(5813): 804 – 807.

Ivanova, T. Kolaříková, M., Havrland, B. & Hutla, P. 2014. Mechanical and chemical properties of briquettes made of waste hemp (*Cannabis sativa* var. Finola) biomass. *Agritech Science* **8**(2), 1–4.

Kaliyan[a], N. & Morey, V. R. 2009. Factors affecting strength and durability of densified biomass products. *Biomass and Bioenergy*, **33**(3): 337 – 359.

Kaliyan[b], N. & Morey, R. V., 2009. Densification Characteristics of Corn Stover and Switchgrass. *Transactions of the ASABE*, **52**(3): 907 – 920.

Kaneko, K. 1994. Determination of pore size and pore size distribution. *Journal of Membrane Science*, **96**(1 – 2): 59 – 89.

Karkania, V., Fanara, E., & Zabaniotou, A. 2012. Review of sustainable biomass pellets production – A study for agricultural residues pellets' market in Greece. *Renewable and Sustainable Energy Reviews*, **16**(3): 1426 – 1436.

Kashaninejad, M. & Tabil, L. 2011. Effect of microwave–chemical pre-treatment on compression characteristics of biomass grinds. *Biosystems Engineering*, **108**(1): 36 – 45.

Kashaninejad, M., Tabil, L., & Knox, R. 2014. Effect of compressive load and particle size on compression characteristics of selected varieties of wheat straw grinds. *Biomass and Bioenergy*, **60**, 1 – 7.

Kaválek, M., Bohumil, H., & Josef, P. 2012. Analysis of Usability of shells from Processing of Palm Nuts to Palm Oil as Solid Fuel. In 11th International Scientific Conference: Engineering for rural development, Jelgava, Latvia, 24-25 May, 2012. Latvia University of Agriculture.

Koyama, M., Yamamoto, S., Ishikawa, K., Ban, S., & Toda, T. 2015. Enhancing anaerobic digestibility of lignin-rich submerged macrophyte using thermochemical pre-treatment. *Biochemical Engineering Journal*, **99**: 124 – 130.

Kratzeisen, M., Starcevic, N., Martinov, M., Maurer, C., & Müller, J. 2010. Applicability of biogas digestate as solid fuel. *Fuel*, **89**(9), 2544-2548.

Kurchania, A. 2012. Biomass Energy. *Biomass Conversion*, 91 – 122.

Li, Y., Park, S., & Zhu, J. 2011. Solid-state anaerobic digestion for methane production from organic waste. *Renewable and Sustainable Energy Reviews*, **15**(1): 821 – 826.

Liedl, B., Bombardiere, J., & Chatfield, J. 2006. Fertiliser potential of liquid and solid effluent from thermophilic anaerobic digestion of poultry waste. *Water Science and Technology*, **53**(8): 69 – 79.

Lindley, J. A., & Vossoughi, M. 1989. Physical properties of biomass briquets. *Transactions of the ASAE*, **32**(2), 361 – 0366.

Macías-García, A., Cuerda-Correa, E., & Díaz-Díez, M. 2004. Application of the Rosin–Rammler and Gates–Gaudin–Schuhmann models to the particle size distribution analysis of agglomerated cork. *Materials Characterization*, **52**(2): 159 – 164.

MacLellan, J., Chen, R., Kraemer, R., Zhong, Y., Liu, Y., & Liao, W. 2013. Anaerobic treatment of lignocellulosic material to co-produce methane and digested fiber for ethanol biorefining. *Bioresource Technology*, **130**: 418 – 423.

Makádi, M., Tomócsik, A., & Orosz, V. 2012. Digestate: a new nutrient source–review. *Energy*, **4**(7.5), 8 – 7.

Mangwandi, C., JiangTao, L., Albadarin, A., Allen, S., & Walker, G. 2013. The variability in nutrient composition of Anaerobic Digestate granules produced from high shear granulation. *Waste Management*, **33**(1): 33 – 42.

Mani, S., Tabil, L.G. & Sokhansanj, S. 2004. Evaluation of compaction equations applied to four biomass species. *Canadian Biosystems Engineering*, **46**(3), pp. 55 – 61.

Mankowski, J. & Kolodziej, J. 2008. Increasing Heat of Combustion of Briquettes Made of Hemp Shives. *International Conference on Flax and Other Bast Plants*. 344 – 352. ISBN 978-0-9809664-0-4.

Manyi-Loh, C., Mamphweli, S., Meyer, E., Okoh, A., Makaka, G., & Simon, M. 2013. Microbial Anaerobic Digestion (Bio-Digesters) as an Approach to the Decontamination of Animal Wastes in Pollution Control and the Generation of Renewable Energy. *International Journal of Environmental Research and Public Health*, **10**(9): 4390 – 4417.

Menind, A., Križan, P., Šooš, Ľ., Matúš, M., & Kers, J. 2012. Optimal conditions for valuation of wood waste by briquetting. *Cellulose*, **45**(43.2), 39 – 2.

Miao, Z., Phillips, J., Grift, T., & Mathanker, S. 2014. Measurement of Mechanical Compressive Properties and Densification Energy Requirement of Miscanthus × giganteus and Switchgrass. *BioEnergy Research*, **8**(1): 152 – 164.

Michael G., 2013. Cells & tissues. *STUDYBLUE University of Queensland* [online] [Accessed. 8. March 2016]. *Renewable and Sustainable Energy Reviews*. 2012. pp. 1426 – 1436. Retrieved at: https://www.studyblue.com/notes/note/n/chapter-4-cells-tissues/deck/6524943?blurry=e&ads=true

Miroljub, M., & Savi, R. A. 2013. Cooling of wood briquettes. *Thermal Science*, **17**(3), 833 – 838.

Mitchual, S. J., Frimpong-Mensah, K., & Darkwa, N. A. 2013. Effect of species, particle size and compacting pressure on relaxed density and compressive strength of fuel briquettes. *International Journal of Energy and Environmental Engineering*, **4**(1), 1 – 6.

Möller, K., Stinner, W., Deuker, A., & Leithold, G. 2008. Effects of different manuring systems with and without biogas digestion on nitrogen cycle and crop yield in mixed organic dairy farming systems. *Nutrient Cycling in Agroecosystems*, **82**(3): 209 – 232.

Monlau, F., Barakat, A., Trably, E., Dumas, C., Steyer, J., & Carrère, H. 2013. Lignocellulosic Materials Into Biohydrogen and Biomethane: Impact of Structural Features and Pre-treatment. *Critical Reviews in Environmental Science and Technology*, **43**(3): 260 – 322.

Moreno, A., Font, R., & Conesa, J. 2016. Physical and chemical evaluation of furniture waste briquettes. *Waste Management*, **49**: 245 – 252.

Mukherjee, S., Weihermüller, L., Tappe, W., Hofmann, D., Köppchen, S., Laabs, V., ... & Burauel, P. 2016. Sorption–desorption behaviour of bentazone, boscalid and

pyrimethanil in biochar and digestate based soil mixtures for biopurification systems. *Science of the Total Environment*, **559**, 63-73.

Naik, S., Goud, V., Rout, P., & Dalai, A. 2010. Production of first and second generation biofuels: A comprehensive review. *Renewable and Sustainable Energy Reviews*, **14**(2): 578 – 597.

Nikon Instruments, 2016. Učit se a zkoumat - Microscopes and Imaging Systems. *Nikoninstruments.com*. [online] [Accessed. 20. February 2016]. Retrieved at https://www.nikoninstruments.com/cz_CZ/Ucit-se-a-zkoumat

Obernberger, I. & Thek, G. 2004. Physical characterisation and chemical composition of densified biomass fuels with regard to their combustion behaviour. *Biomass and Bioenergy*, **27**(6): 653 – 669.

Olson, E. 2011. Particle shape factors and their use in image analysis-part 1: Theory. *Journal of GXP Compliance*, **15**(3), 85.

ÖNORM M 7135, Preßlinge aus naturbelassenem Holz und naturbelassender Rinde Pellets und Briketts -Anforderungen und Prüfbestimmungen.

Onuegbu, T. U., Ogbu, I. M., & Ejikeme, C. 2012. Comparative analyses of densities and calorific values of wood and briquettes samples prepared at moderate pressure and ambient temperature. *International Journal of Plant, Animal and Environmental Sciences*, **2**(1), 40 – 45.

Pecen, J., Černá, I. and Zabloudilová, P. 2015. Závislost střední hodnoty a intervalu spolehlivosti souboru řepky na jeho velikosti a způsob u statistického zpracování. Conference proceedings, "Prosperující plodiny", ČZU Praha, 11.12.12. pp. 98 – 101, ISBN-978-80-213-2517-3.

Pecen, J., Piksa, Z., & Zabloudilová, P. 2014. Alternative Use of a Compressed Component of a Digestate from Agricultural BGSs (Biogas Stations). *Journal of Energy and Power Engineering*, **8**(4).

Pechoušek, J. 2010. Měření plochy povrchu pevných látek a určování jejich porozity metodou sorpce. Olomouc: Univerzita Palackého v Olomouci, p.19

Peng, J., Wang, J., Bi, X. T., Lim, C. J., Sokhansanj, S., Peng, H., & Jia, D. 2015. Effects of thermal treatment on energy density and hardness of torrefied wood pellets. *Fuel Processing Technology*, **129**, 168 – 173.

Pognani, M., D'Imporzano, G., Scaglia, B., & Adani, F. 2009. Substituting energy crops with organic fraction of municipal solid waste for biogas production at farm level: A full-scale plant study. *Process Biochemistry*, **44**(8): 817 – 821.

Pulvirenti, A., Ronga, D., Zaghi, M., Tomasselli, A., Mannella, L., & Pecchioni, N. 2015. Pelleting is a successful method to eliminate the presence of Clostridium spp. from the digestate of biogas plants. *Biomass and Bioenergy*, **81**: 479 – 482.

Qi, H. J., Joyce, K., & Boyce, M. C. 2003. Durometer hardness and the stress-strain behavior of elastomeric materials. *Rubber chemistry and technology*, **76**(2), 419 – 435.

Rajkumar, D. & Venkatachalam, P. 2013. Physical properties of agro residual briquettes produced from Cotton, Soybean and Pigeon pea stalks. *International Journal on Power Engineering and Energy* **4**(4), 414–417.

Rawle, A. 2003. Basic of principles of particle-size analysis. *Surface coatings international. Part A, Coatings journal*, **86**(2), 58 – 65.

Reeb, J. 1995. *Wood and moisture relationships*. [Corvallis, Or.]: Oregon State University Extension Service.

Rouquerol, J., Avnir, D., Fairbridge, C., Everett, D., Haynes, J., & Pernicone, N. et al 1994. Recommendations for the characterization of porous solids (Technical Report). *Pure and Applied Chemistry*, **66**(8).

Rynkiewicz, M., Trávníček, P., Krčálová, E., & Mareček, J. 2013. Influence of annealing temperature of straw briquettes on their density and hardness. *Acta Universitatis Agriculturae et Silviculturae Mendelianae Brunensis*, **61**(5), 1377-1382.

Sawatdeenarunat, C., Surendra, K., Takara, D., Oechsner, H., & Khanal, S. 2015. Anaerobic digestion of lignocellulosic biomass: Challenges and opportunities. *Bioresource Technology*, **178**: 178 – 186.

Schleiss, K., & Barth, J. 2008. Use of compost and digestate: choosing the product depending on utilisation, strategy and aim. *Compost and digestate: sustainability, benefits, impacts for the environment and for plant production*, **27**, 29th. 199 – 208.

Scientific, H. 2012. A guidebook to particle size analysis. *Horiba Instruments, Inc*, 1 – 29.

Singh, R. 2004. Equilibrium moisture content of biomass briquettes. *Biomass and Bioenergy*, **26**(3): 251 – 253.

Stinner, W., Möller, K., & Leithold, G. 2008. Effects of biogas digestion of clover/grass-leys, cover crops and crop residues on nitrogen cycle and crop yield in organic stockless farming systems. *European Journal of Agronomy*, **29**(2 – 3): 125 – 134.

Tabil Jr, L., & Sokhansanj, S. 1996. Process conditions affecting the physical quality of alfalfa pellets. *Applied Engineering in Agriculture*, **12**(3), 345 – 350.

Tabil[a], L., Kashaninejad, M., & Adapa, P. 2011. *Biomass feedstock pre-processing-part 1: pre-treatment*. INTECH Open Access Publisher. pp. 412 – 438.

Tabil[b], L., Adapa, P., & Kashaninejad, M. 2011. Biomass feedstock pre-processing-part 2: densification. *Biofuel's Engineering Process Technology*, **19**, 439 – 446.

Takara, D. & Khanal, S. 2011. Green processing of tropical banagrass into biofuel and biobased products: An innovative biorefinery approach. *Bioresource Technology*, **102**(2): 1587 – 1592.

Tambone, F., Scaglia, B., D'Imporzano, G., Schievano, A., Orzi, V., & Salati, S. et al 2010. Assessing amendment and fertilizing properties of digestates from anaerobic digestion through a comparative study with digested sludge and compost. *Chemosphere*, **81**(5): 577 – 583.

Tumuluru, J., Wright, C., Hess, J., & Kenney, K. 2011. A review of biomass densification systems to develop uniform feedstock commodities for bioenergy application. *Biofuels, Bioprod. Bioref.* **5**(6): 683 – 707.

Vandenbossche, V., Brault, J., Vilarem, G., Hernández-Meléndez, O., Vivaldo-Lima, E., & Hernández-Luna, M. et al 2014. A new lignocellulosic biomass deconstruction process combining thermo-mechano chemical action and bio-catalytic enzymatic hydrolysis in a twin-screw extruder. *Industrial Crops and Products*, **55**: 258 – 266.

VŠCHT. 2008. Stanovení hustoty slitin - návod. [Online] Vysoká škola chemicko-technologická v Praze, 2008. [Cited: April 25, 2015.] http://www.vscht.cz/met/stranky/vyuka/labcv/labor/fm_termicka_analyza/hustota.htm.

Weiland, P. 2010. Biogas production: current state and perspectives. *Appl Microbiol Biotechnol*, **85**(4): 849 – 860.

Wilkinson, K. G. 2011. Development of On-Farm Anaerobic Digestion, Integrated Waste Management - Volume I, Mr. Sunil Kumar (Ed.), *InTech*.

WRAP, 2012. Enhancement and treatment of digestates from anaerobic digestion [online]. UK: *The Old Academy*. [Accessed 3 April 2016]. OMK006 – 002. Available from: http://www.wrap.org.uk

Yank, A., Ngadi, M., & Kok, R. 2016. Physical properties of rice husk and bran briquettes under low pressure densification for rural applications. *Biomass and Bioenergy*, **84**: 22 – 30.

Zhang, J. & Guo, Y. 2014. Physical properties of solid fuel briquettes made from Caragana korshinskii Kom. *Powder Technology*, **256**: 293 – 299.

8. Appendices

Chart 17: Crushed plant (Miscanthus Giganteus, MG) particles dimensions including volume V_o and density ρ_o and dimensions chart.

	$A_o \cdot 10^2$	$m_o \cdot 10^3$	h_o	h	Δh	$V_o \cdot 10^3$	$V \cdot 10^3$	$\Delta V \cdot 10^3$	ρ_o	ρ
	cm^2	g	cm	cm	cm	cm^3	cm^3	cm^3	$kg.m^{-3}$	$kg.m^{-3}$
	2	**3**	**4**	**5**	**6**	**7**	**8**	**9**	**10**	**11**
1	0.093	0.56	0.027	0.038	-0.011	2.4806	3.52	-1.394	225.7	252.9
2	0.078	0.38	0.015	0.038	-0.023	1.1474	2.96	-1.813	331.2	252.9
3	0.082	0.33	0.010	0.038	-0.028	0.7878	3.09	-2.302	418.9	252.9
4	0.064	1.31	0.012	0.038	-0.026	0.7670	2.42	-1.653	1707.9	252.9
5	0.126	0.77	0.015	0.038	-0.023	1.8530	4.79	-2.937	415.5	252.9
6	0.151	0.87	0.020	0.038	-0.018	3.0244	5.73	-2.706	287.7	252.9
7	0.106	0.63	0.075	0.038	0.037	7.9470	4.03	3.917	79.3	252.9
8	0.107	1.28	0.060	0.038	0.022	6.3739	4.05	2.324	200.8	252.9
9	0.016	1.41	0.031	0.038	-0.007	4.9170	0.60	4.317	286.8	252.9
10	0.079	1.11	0.062	0.038	0.024	4.9058	3.00	1.906	226.3	252.9
Σ	**0.902**	**8.65**	**0.327**	0.038	**-0.052**	**34.204**	**34.19**	**-0.341**	**4180.1**	**252.9**
11	0.068	0.67	0.059	0.041	0.018	3.9916	2.81	1.182	167.9	322.0
12	0.099	1.05	0.042	0.041	0.001	4.1044	4.07	0.034	255.8	322.0
13	0.088	0.80	0.031	0.041	-0.010	2.7119	3.61	-0.898	295.0	322.0
14	0.022	0.41	0.037	0.041	-0.004	0.8527	0.94	-0.087	480.8	322.0
15	0.101	0.84	0.037	0.041	-0.004	3.7790	4.18	-0.401	222.3	322.0
16	0.023	0.28	0.036	0.041	-0.005	0.8338	0.97	-0.136	335.8.	322.0
17	0.030	0.57	0.035	0.041	-0.006	1.0373	1.22	-0.183	549.5	322.0
18	0.087	0.46	0.025	0.041	-0.016	2.1467	3.59	-1.443	214.3	322.0
19	0.079	2.89	0.072	0.041	0.031	5.6534	3.26	2.393	511.2	322.0
20	0.077	1.09	0.039	0.041	-0.002	3.0213	3.17	-0.149	360.8	322.0
Σ	**0.674**	**9.06**	**0.413**	**0.041**	**0**	**28.132**	**27.82**	**0.312**	**3393.3**	**322.0**
21	0.089	1.66	0.050	0.041	0.009	4.4814	3.65	0.831	370.4	400
22	0.094	0.62	0.030	0.041	-0.011	2.8307	3.87	-1.039	219.0	400
23	0.069	0.38	0.013	0.041	-0.028	0.8701	2.82	-1.950	436.7	400
24	0.107	3.47	0.048	0.041	0.007	5.1838	4.40	0.784	669.4	400
25	0.056	0.30	0.010	0.041	-0.031	0.5756	2.28	-1.704	521.2	400
26	0.133	2.59	0.051	0.041	0.010	6.7140	5.43	1.284	385.8	400
27	0.039	1.11	0.046	0.041	0.005	1.8040	1.61	0.194	615.3	400
28	0.074	0.60	0.045	0.041	0.004	3.3398	3.02	0.320	179.7	400
29	0.042	1.03	0.068	0.041	0.027	2.8718	1.74	1.132	358.7	400
30	0.073	1.12	0.048	0.041	0.007	3.4895	3.00	0.490	321.0	400
Σ	**0.776**	**12.9**	**0.409**	**0.041**	**-0.001**	**32.161**	**31.82**	**0.341**	**4077**	**400**
ΣΣ	**2.352**	**30.6**	**1.149**	**0.041**	**-0.053**	**94.497**	**93.83**	**0.312**	**11,651**	**323.7**

where:

A_o – measured area of particle

m_o – measured particle weight

h_o – measured particle height

V_o – particle volume calculated from measured values

ρ_o – particle density calculated from measured values and measured weight of each particle

h – calculated particle height

V – particle volume calculated from particle height in the measured area

ρ – average density of the particle sample calculated from $m_{\circ}$ and $V_{\circ}$

$\Delta h = h_{\circ} - h$

$\Delta V = V_{\circ} - V$

$\Delta \rho = \rho_{\circ} - \rho$

Chart 18: Statistics of image analysis

D3-II-A

VARIABLE	**Mean**	**STD**	**Min**	**Max**
Area	19.97	14.36	5.59	84.30
Equivalent diameter	4.79	1.57	2.67	10.36
Length	11.59	6.53	4.90	40.25
Width	1.73	0.78	0.56	4.80
Circularity	0.38	0.15	0.12	0.77
Average intensity	59.96	14.78	33.18	103.76

D3-II-C

VARIABLE	**Mean**	**STD**	**Min**	**Max**
Area	5.46	2.99	0.98	15.15
Equivalent diameter	2.54	0.71	1.12	4.39
Length	6.5	2.08	2.60	13.25
Width	0.86	0.40	0.12	2.01
Circularity	0.33	0.14	0.04	0.70
Average intensity	20.74	5.23	11.47	46.40

D3-II-D

VARIABLE	**Mean**	**STD**	**Min**	**Max**
Area	1.61	0.93	0.34	5.74
Equivalent diameter	1.38	0.37	0.65	2.70
Length	4.01	1.50	1.86	8.33
Width	0.42	0.19	0.08	0.99
Circularity	0.28	0.14	0.06	0.69
Average intensity	29.99	7.26	16.63	64.23

Chart 19: Sieve analysis of the D1 and D2 samples.

	Size of sieve mesh [mm]								
	bowl	0.1	0.25	0.50	1.00	2.50	5.60	10.00	Σ
	1	2	3	4	5	6	7	8	
D1									
[g]	0.55	1.02	2.38	3.12	10.96	17.25	10.74	19.14	65.31
[%]	0.86	1.56	3.65	4.79	16.84	26.42	16.50	29.40	100.0
STD1	0.11	0.19	0.46	0.74	1.00	1.15	1.09	3.60	
D2									
[g]	0.98	1.54	3.44	9.00	22.82	27.59	22.64	14.14	102.15
[%]	0.96	1.50	3.36	8.81	22.34	27.03	22.16	13.84	100.0
STD2	0.08	0.28	0.57	2.03	3.20	1.67	2.30	8.97	

*STD – standard deviation

Chart 20: Briquette sorption

Order of sampling		1	2	3	4	5	6	7
Total sorption time	[days]	0	3	6	8	10	13	15
Sampling interval	[days]	0	3	3	2	2	3	2
BRIQUETTES FROM D1								
briquette diameter	[cm]	6.70	7.00	7.30	7.50	7.50	7.40	7.2
briquette moisture	[%]	7.30	13.80	25.70	26.70	28.40	27.10	29.0
soil moisture in box	[%]	17.80	17.30	16.70	17.10	15.80	14.90	15.1
BRIQUETTES FROM D2								
briquette diameter	[cm]	6.70	7.10	7.20	7.40	7.50	7.50	7.4
briquette moisture	[%]	7.50	17.40	21.50	30.60	33.70	35.40	33.9
soil moisture in box	[%]	17.80	17.30	16.70	17.10	15.80	14.90	15.1
BRIQUETTES FROM WOODCHIPS								
briquette diameter	[cm]	6.50	7.70	7.90	8.30	8.50	8.70	8.6
briquette moisture	[%]	4.60	31.10	36.20	43.00	46.20	51.10	50.3
soil moisture in box	[%]	17.80	17.30	16.70	17.10	15.80	14.90	15.1

Chart 21: D1 particles' dimensions measured by calliper.

Calliper measuring							
Parameter	Length	Width	Height	Area $L_0 \cdot B_0$	Volume	Density	Weight
Abb.	L_0	B_0	Y_0	S_0	V_0	ρ_0	M
Unit	mm	mm	mm	mm^2	mm^3	$g \cdot cm^{-3}$	g
No.	1	2	3	4	5	6	7
$MEAN_A$	3.94	0.98	0.27	3.78	1.11	0.5573	0.0005
MAX	8.25	1.68	0.55	9.49	4.26	5.4681	0.0017
MIN	1.13	0.27	0.04	1.30	0.05	0.1899	0.0001
STD	1.63	0.28	0.13	1.78	0.90	0.6667	0.0003

*****Area $S_0=L_0 \bullet B_0$| Volume $V_0=L_0 \bullet B_0 \bullet Y_0$

Chart 22: D1 particles' dimensions measured by image analysis.

Image analysis measuring							
Parameter	Length	Width	Height	Area $L_1 \cdot B_1$	Volume $S_1 \cdot Y_1$	Density	Weight
Abb.	L_1	B_1	Y_1	S_1	V_1	ρ_1	M
Unit	mm	mm	mm	mm^2	mm^3	$g \cdot cm^{-3}$	g
No.	8	9	10	11	12	13	14
$MEAN_A$	4.03	0.84	0.27	3.37	0.88	0.6977	0.0005
MAX	8.79	1.44	0.55	9.98	4.09	5.7596	0.0017
MIN	1.19	0.27	0.04	0.76	0.05	0.2059	0.0001
STD	0.15	0.26	0.13	1.75	0.78	0.8197	0.0003

***** Area $S_1=L_1 \bullet B_1$ | Volume $V_1=S_1 \bullet Y_1$

Chart 23: Differences between calliper and image analysis measurements.

Difference			
Parameter	Area	Volume	Density
Abb.	ΔS	ΔV	$\Delta\rho$
$MEAN_A$	-0.9215	-0.2151	0.0330
MAX	4.2538	0.9770	2.1222
MIN	-6.1280	-2.4484	-0.7101
STD	1.9365	0.5426	0.3828

***** $\Delta S = S_1 - S_0 \mid \Delta V = V_1 - V_0 \mid \Delta\rho = \rho_1 - \rho_0$

The uncertainty of a calipper measuring is in the order of few percent (0.1mm); in case of the image analysis it is lower (0.01mm).

Chart 24: Measured durability test results, with the AR and SIndex results. Samples D3-I, n=13.

	Weight of sample (g)		Weight of sample		Weight of sample		Weight of sample		Weight of sample		Weight of sample	
Sample	Before	After	Before	After	Before	After	Before	After	Before	After	Before	After
D3-I	Round 1		Round 2		Round 3		Round 4		Round 5		Round 6	
1	162.48	161.68	161.68	161.10	161.10	160.30	160.30	159.87	159.87	159.43	159.43	159.04
2	152.60	151.62	151.62	150.99	150.99	150.10	150.10	149.64	149.64	149.29	149.29	148.94
3	158.56	157.72	157.72	156.88	156.88	156.17	156.17	155.71	155.71	155.28	155.28	154.81
4	147.67	146.76	146.76	146.09	146.09	145.48	145.48	144.93	144.93	144.23	144.23	143.86
5	154.24	153.50	153.50	152.69	152.69	151.68	151.68	151.27	151.27	150.89	150.89	150.61
6	129.04	128.29	128.29	127.42	127.42	126.75	126.75	126.27	126.27	125.43	125.43	124.52
7	160.25	159.45	159.45	158.61	158.61	157.93	157.93	157.47	157.47	157.14	157.14	156.77
8	167.75	166.99	166.99	166.23	166.23	165.48	165.48	164.97	164.97	164.45	164.45	163.86
9	160.54	159.78	159.78	159.25	159.25	158.51	158.51	157.90	157.90	157.22	157.22	156.72
10	148.36	147.54	147.54	146.95	146.95	146.35	146.35	145.69	145.69	145.33	145.33	144.98
11	164.56	163.66	163.66	162.60	162.60	161.90	161.90	161.19	161.19	160.66	160.66	159.97
12	156.91	156.09	156.09	155.43	155.43	154.87	154.87	154.23	154.23	153.73	153.73	153.08
13	150.10	149.24	149.24	148.27	148.27	147.08	147.08	147.14	147.14	146.67	146.67	146.16
AR (g)	8.22		10.54		11.01		5.21		6.55		4.97	
S_{index}	99.5%		99.5%		99.5%		99.7%		99.7%		99.7%	

Chart 25: Measured, with the AR and SIndex results. Samples D3-II-A, n=12.

	Weight of sample (g)		Weight of sample		Weight of sample		Weight of sample		Weight of sample		Weight of sample	
Sample	Before	After	Before	After	Before	After	Before	After	Before	After	Before	After
D3-II-A	Round 1		Round 2		Round 3		Round 4		Round 5		Round 6	
1	140.29	139.31	139.31	138.60	138.60	137.84	137.84	137.23	137.23	136.57	136.57	136.10
2	131.36	130.41	130.41	129.79	129.79	129.41	129.41	128.93	128.93	128.53	128.53	127.94
3	135.44	134.47	134.47	133.47	133.47	132.54	132.54	131.98	131.98	131.54	131.54	131.14
4	155.67	154.62	154.62	135.77	135.77	153.15	153.15	152.57	152.57	151.31	151.31	150.79
5	172.32	170.96	170.96	170.25	170.25	169.51	169.51	169.19	169.19	168.42	168.42	168.01
6	126.07	125.07	125.07	124.20	124.20	123.24	123.24	122.55	122.55	122.02	122.02	121.31
7	139.77	138.94	138.94	138.18	138.18	137.52	137.52	136.89	136.89	135.98	135.98	135.54
8	144.78	143.35	143.35	142.53	142.53	141.63	141.63	141.18	141.18	140.69	140.69	140.16
9	136.96	136.11	136.11	135.25	135.25	134.34	134.34	133.79	133.79	133.37	133.37	133.00
10	183.43	182.14	182.14	181.01	181.01	180.35	180.35	179.80	179.80	179.32	179.32	178.79
11	139.14	137.92	137.92	137.02	137.02	136.29	136.29	135.39	135.39	134.86	134.86	134.28
12	175.76	174.92	174.92	174.10	174.10	173.33	173.33	172.63	172.63	171.72	171.72	171.06
AR (g)	11.78		8.26		8.07		6.64		6.27		4.86	
S_{index}	99.3%		98.4%		100.5%		99.6%		99.6%		99.6%	

Chart 26: Measured durability test values, with the AR and SIndex results. Samples D3-II-C, n=5.

	Weight of sample (g)		Weight of sample		Weight of sample		Weight of sample		Weight of sample		Weight of sample	
Sample	Before	After	Before	After	Before	After	Before	After	Before	After	Before	After
D3-II-C	Round 1		Round 2		Round 3		Round 4		Round 5		Round 6	
1	151.39	150.39	150.39	149.25	149.25	148.69	148.69	148.20	148.20	147.81	147.81	147.29
2	197.10	196.00	196.00	195.20	195.20	194.46	194.46	193.59	193.59	193.20	193.20	192.66
3	139.58	138.89	138.89	137.92	137.92	134.43	134.43	137.00	137.00	136.47	136.47	136.00
4	75.01	71.87	71.87	71.38	71.38	70.92	70.92	70.32	70.32	69.90	69.90	69.48
5	75.96	74.68	74.68	45.27	45.27	44.80	44.80	44.51	44.51	44.17	44.17	43.87
AR (g)	7.21		5.81		4.16		3.83		2.84		3.25	
S_{index}	98.5%		90.0%		99.0%		99.9%		99.6%		99.5%	

Chart 27: Measured durability test values, with the AR and SIndex results. Samples D3-II-D, n=5.

	Weight of sample (g)		Weight of sample		Weight of sample		Weight of sample		Weight of sample		Weight of sample	
Sample	Before	After	Before	After	Before	After	Before	After	Before	After	Before	After
D3-II-D	Round 1		Round 2		Round 3		Round 4		Round 5		Round 6	
1	216.25	213.64	213.64	212.40	212.40	207.89	207.89	206.76	206.76	206.00	206.00	204.89
2	185.49	183.41	183.41	181.55	181.55	179.60	179.60	178.27	178.27	177.26	177.26	176.69
3	210.95	209.13	209.13	207.59	207.59	206.33	206.33	205.40	205.40	204.72	204.72	204.14
4	184.94	183.18	183.18	181.39	181.39	180.55	180.55	179.50	179.50	178.70	178.70	178.02
5	147.78	146.31	146.31	145.11	145.11	144.37	144.37	143.35	143.35	142.56	142.56	141.85
AR (g)	8.31		6.31		7.51		6.16		3.31		3.31	
S_{index}	99.0%		99.2%		99.0%		99.4%		99.5%		99.6%	